Baroclinic Instabilities

Laurent Joly

P. Chassaing, V. Chapin, J.N. Reinaud, J. Micallef,
J. Suarez, L. Bretonnet, J. Fontane

ENSICA - Département de Mécanique des Fluides

Variable Density Turbulent Flows – Villanova i la Geltru - Septembre 2003

Outline of the talk

- Introduction - Illustrative examples from experiments and simulations
- The baroclinic torque in high Froude number flows, its organization, scale and order of magnitude
- Stability of the inhomogeneous mixing-layer

...Break...

4. Transition of the inhomogeneous mixing-layer and the 2D secondary baroclinic instability
5. The strain field of 2D light jets
6. Transition to three-dimensionality in light jets and the question of side-jets
7. Baroclinic instability of heavy vortices and some elements on vortex interaction in inhomogeneous 2D turbulence

Inhomogeneous flows submitted to external versus internal acceleration

Buoyancy dominated flows — Inhomogeneous medium in a gravity field

Accelerated Inhomogeneous flows — Inhomogeneous medium in an external acceleration field

High Froude number flows — Mixing inhomogeneous streams

Stratified medium in a gravity field (type I)

Tilted tank experiments : « A method of producing a shear flow in a stratified fluid »
S.A. Thorpe JFM32 1968

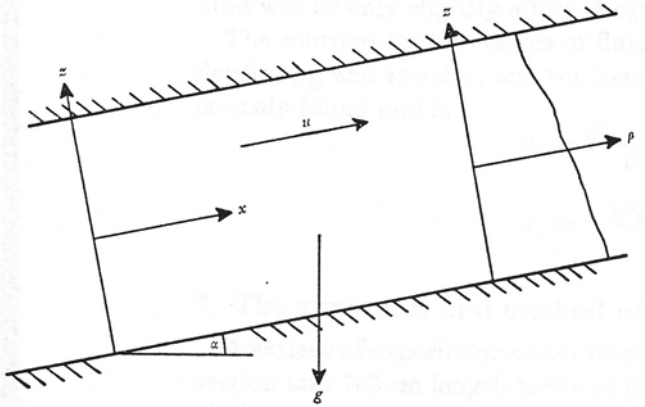

FIGURE 1. Notation.

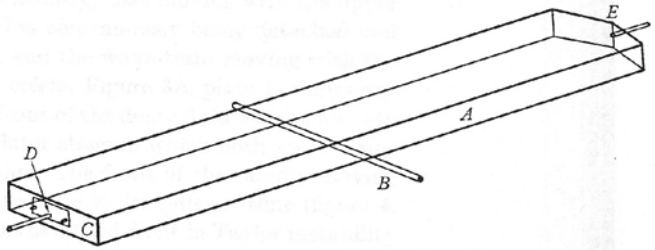

FIGURE 2. The apparatus.

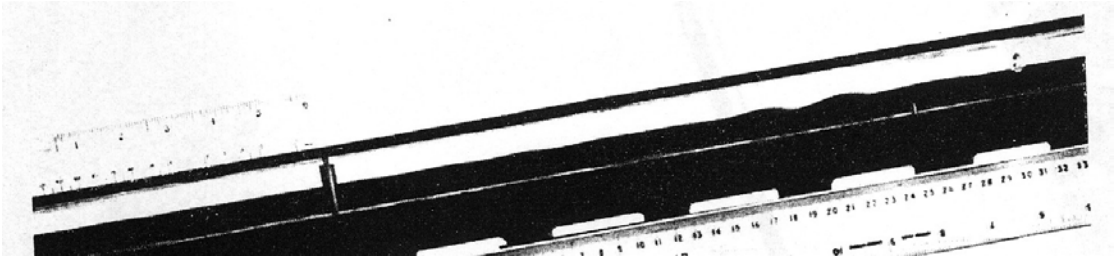

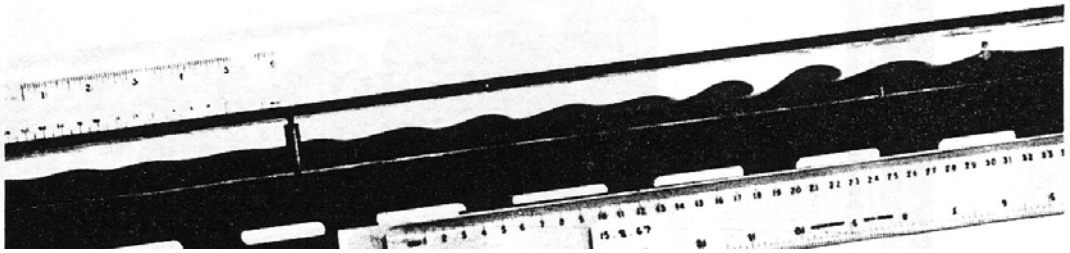

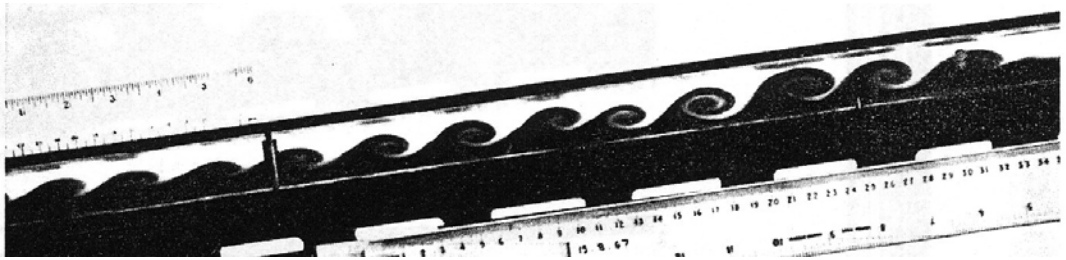

Two-dimensionnal Stratified Mixing Layer (vertical shear)

Klaassen and Peltier JFM227 (1991)

Re=300

$$Ri = g\frac{\Delta\rho}{\bar{\rho}}\frac{\delta_\omega}{\Delta U^2} = \frac{1}{Fr^2}$$

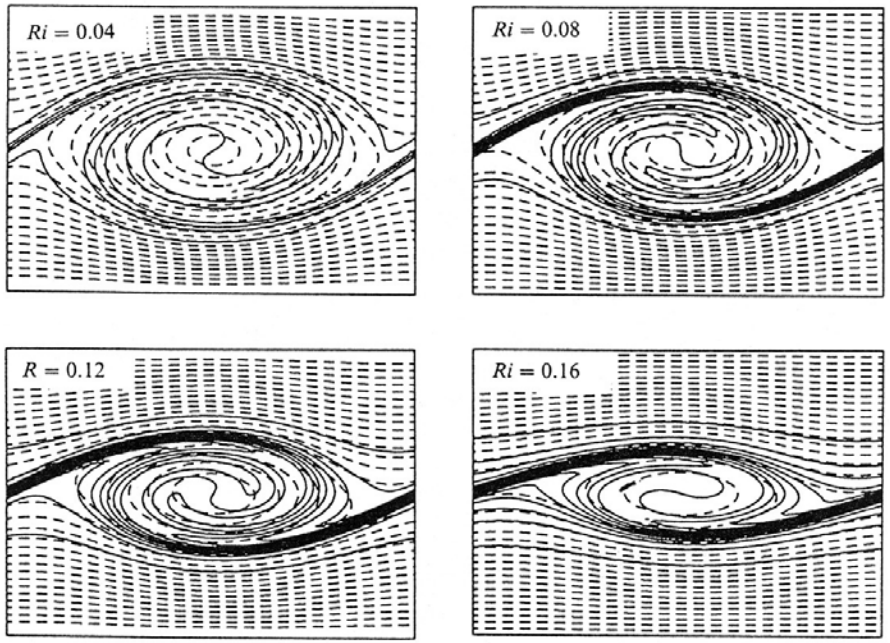

FIGURE 2. Stream function (dashed contours) and potential temperature field (solid contours) for stratified Kelvin–Helmholtz billows at various Richardson numbers Ri and $Re = 300$, $Pr = 1$. The waves are shown at the times of maximum kinetic energy, which are $t = 26$ ($Ri = 0$), 30 ($Ri = 0.04$), 34 ($Ri = 0.08$), 42 ($Ri = 0.12$) and 52 ($Ri = 0.16$). Contour intervals are the same for each wave. The horizontal period is $14h$ and the domain height is $10h$.

Staquet JFM296 (1995)

Re=2000 – Ri = 0.167

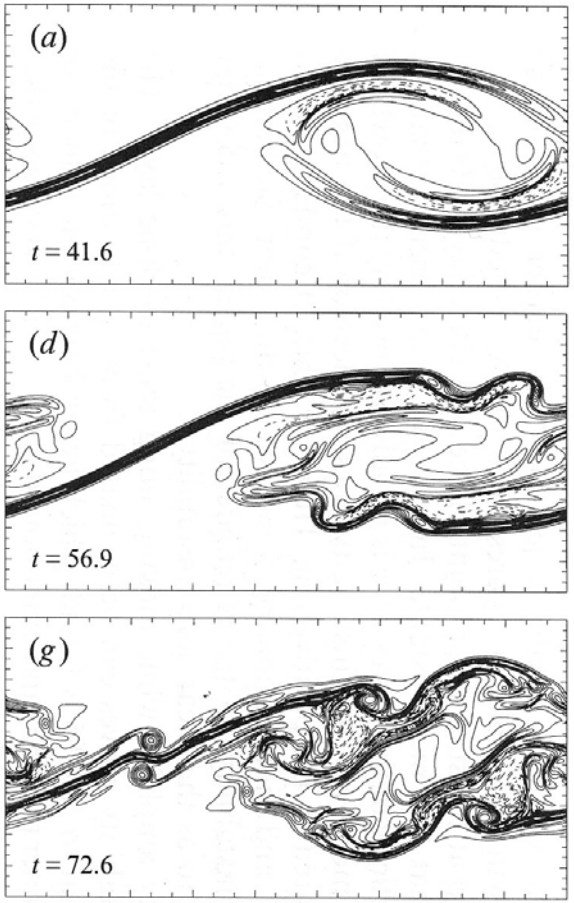

*Three-dimensionnal **homogeneous** Mixing Layer*

Bernal and Roshko JFM170 (1986)

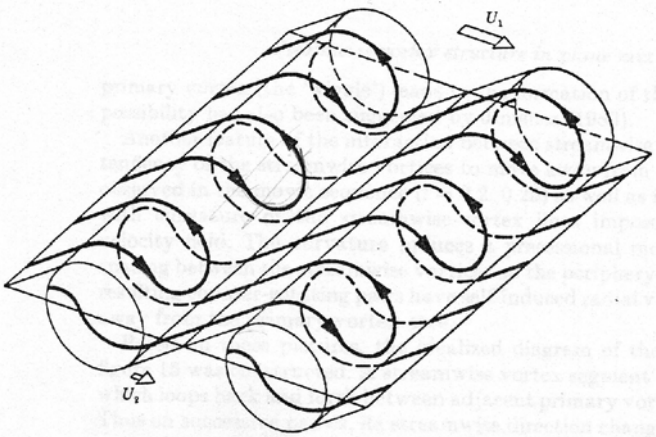

FIGURE 15. Topology of streamwise vortex lines.

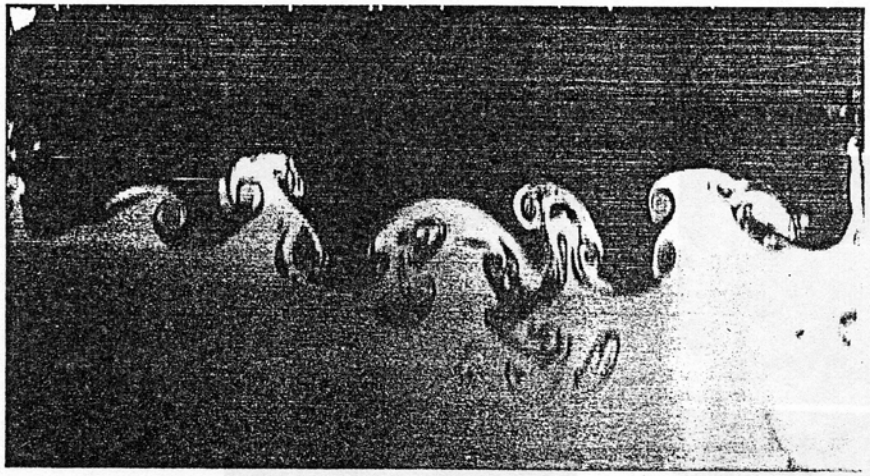

FIGURE 12. Laser-induced fluorescence (y,z) cross-section through the braid. $U_1 = 29$ cm/s, $U_2 = 10$ cm/s. The entire channel span (11 cm) is shown.

Rogers and Moser JFM243 (1992)

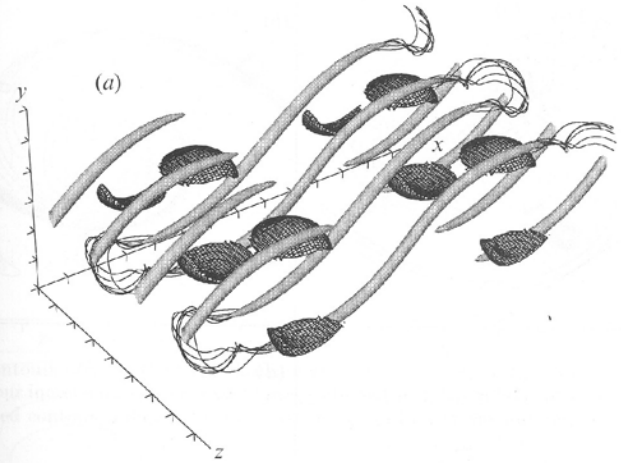

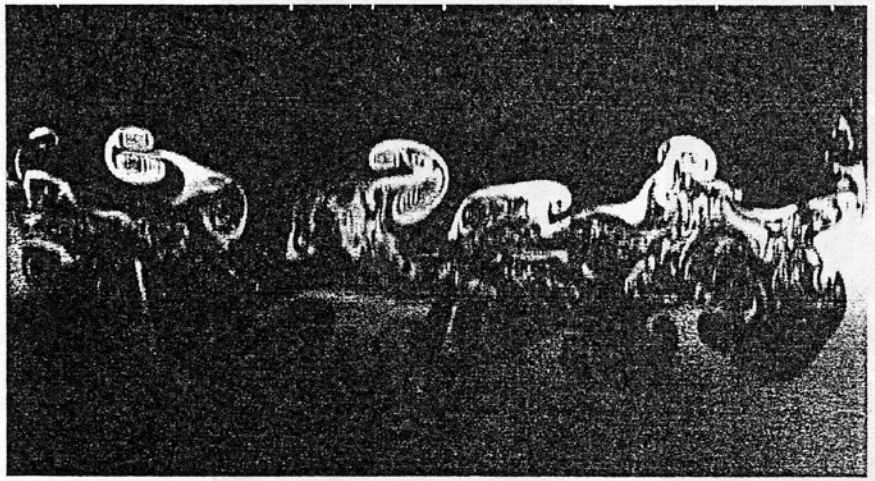

FIGURE 13. Laser-induced fluorescence (y,z) cross-section through the core. $U_1 = 20$ cm/s, $U_2 = 8$ cm/s. The entire channel span (11 cm) is shown.

Three-dimensionnal stratified Mixing Layer

Schowalter, Van Atta and Lasheras JFM281 (1994)

Ri=0.06

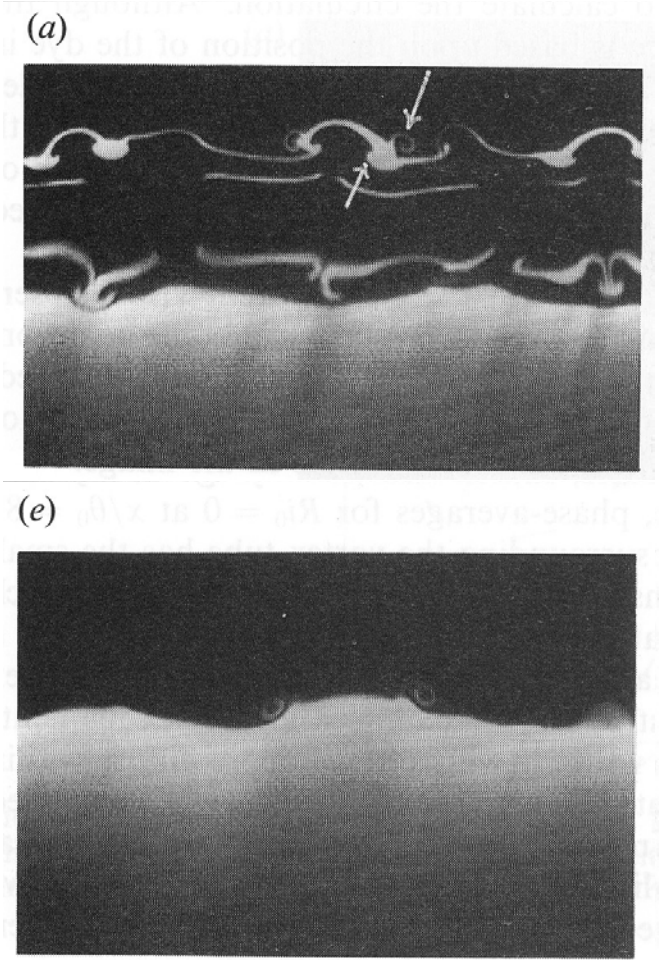

Klaassen and Peltier JFM227 (1991)

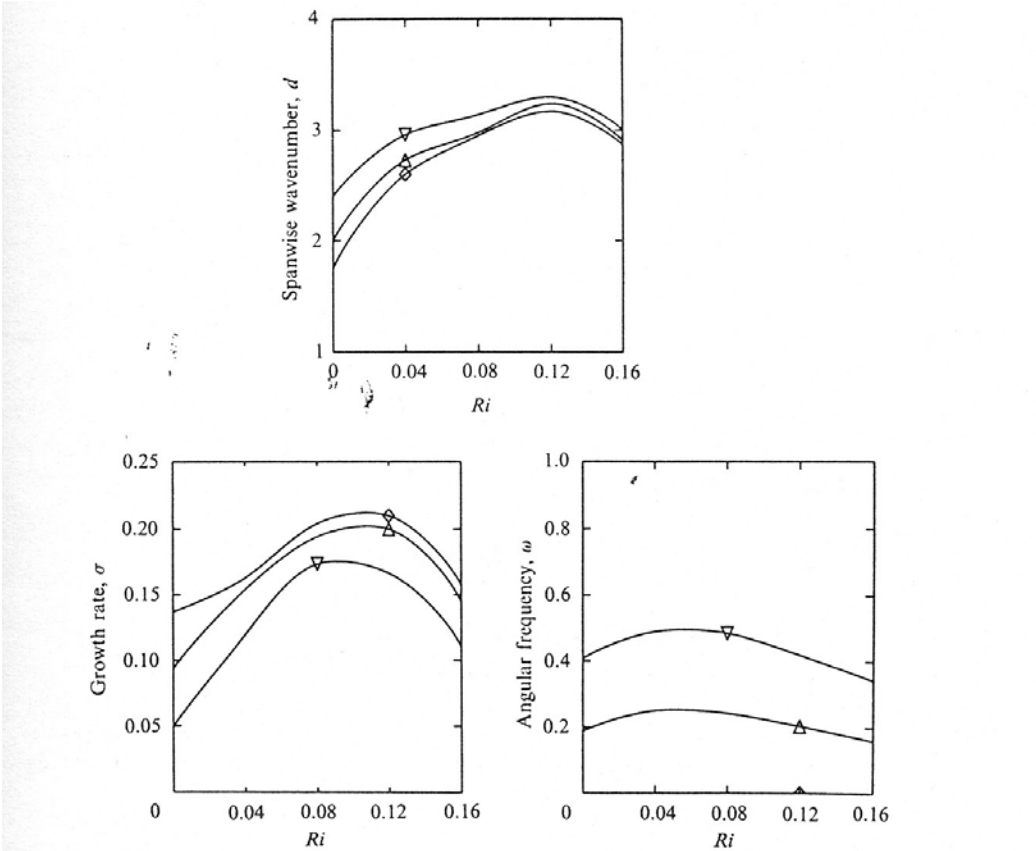

FIGURE 22. The effect of bulk Richardson number Ri on the most unstable ω_0 ($\diamond$), Ω_1 ($\triangle$), and ω_2 (∇) modes of the maximum amplitude KH wave state. For Floquet parameter $b = 0$.

Mixing of a pocket of light fluid in a shaker

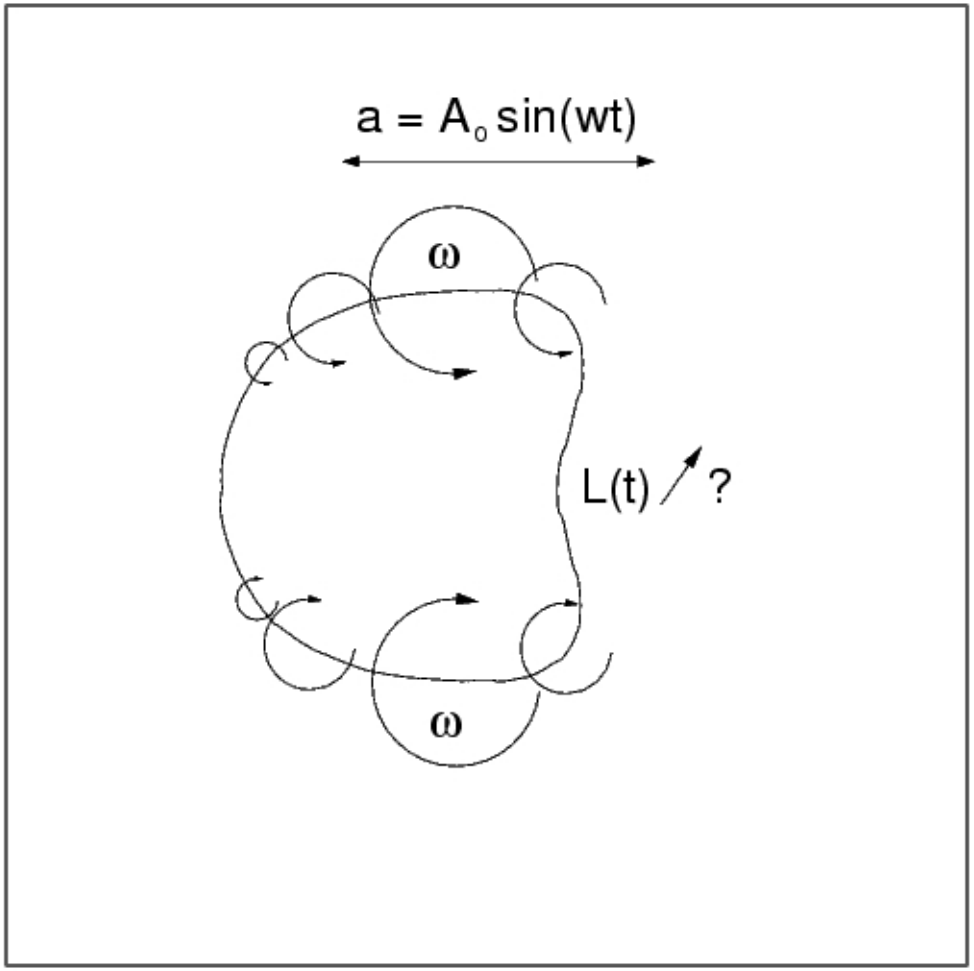

Brown and Roshko, « On density effects and large structure in turbulent mixing layers », JFM 64, 1974

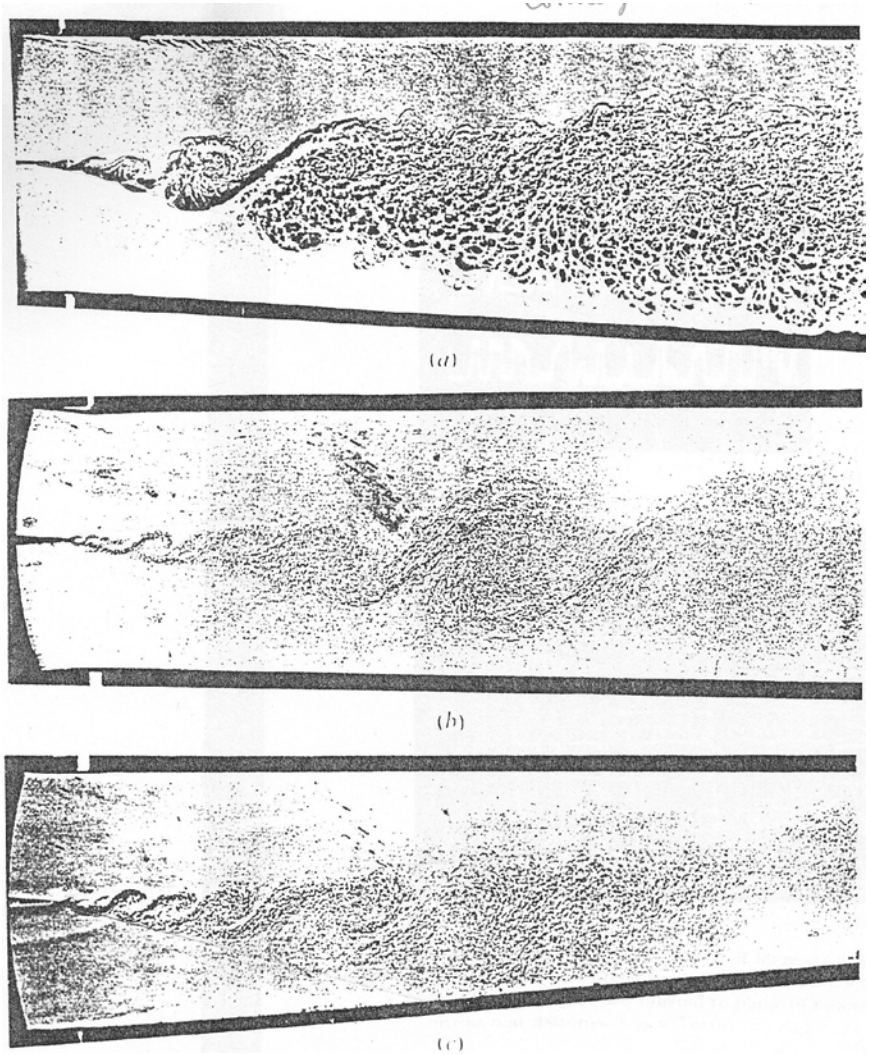

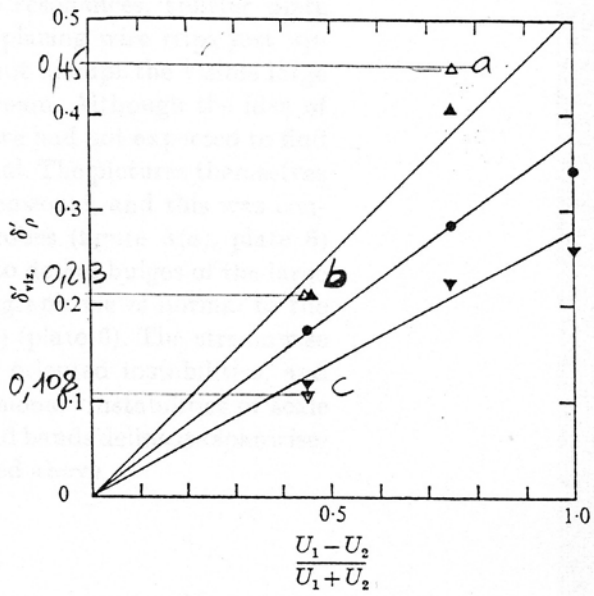

FIGURE 7. Visual growth rates.

δ'_ρ	δ'_{viz}	ρ_2/ρ_1
△	▲	7
	●	1
▽	▼	$\frac{1}{7}$

Mixing inhomogeneous streams : baroclinic instability

Two-dimensionnal secondary baroclinic instability : Reinaud, Joly and Chassaing, PoF vol 12(10), pp 2489-2505, 2000

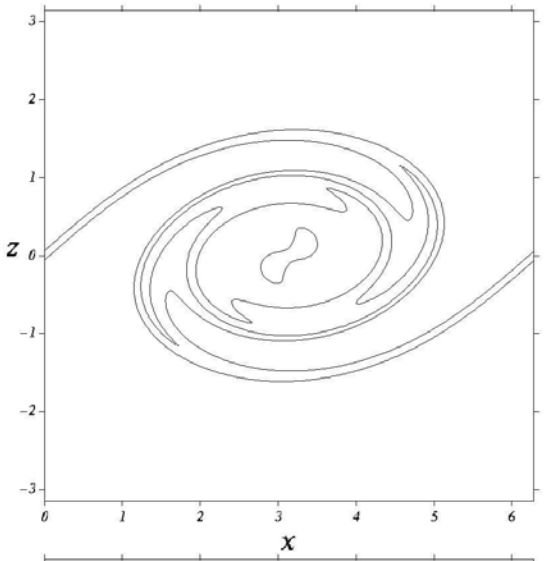

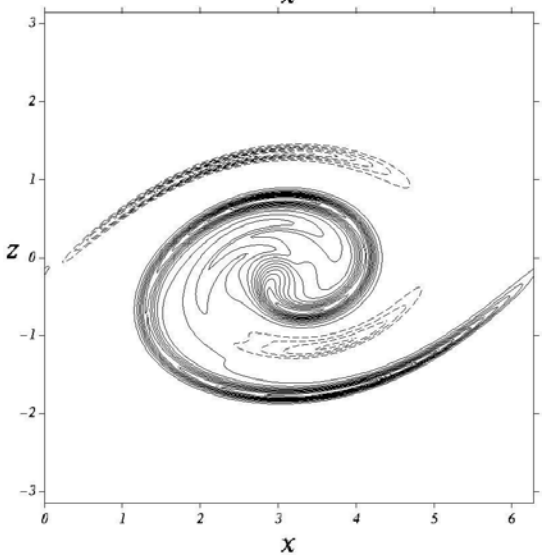

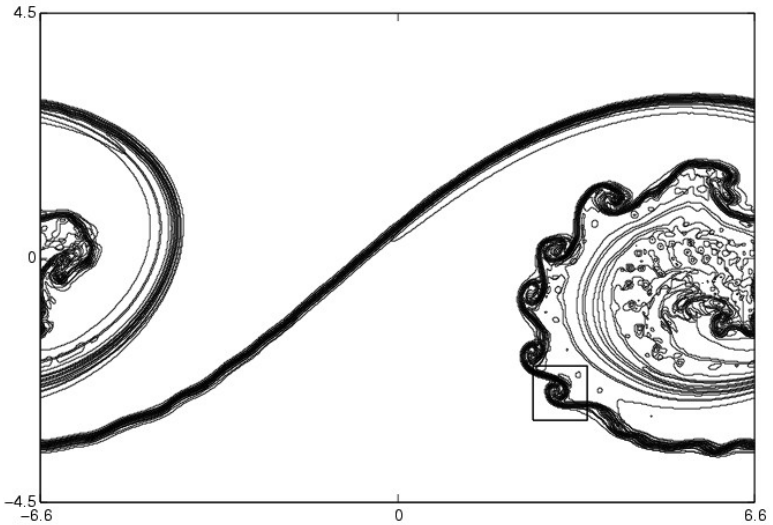

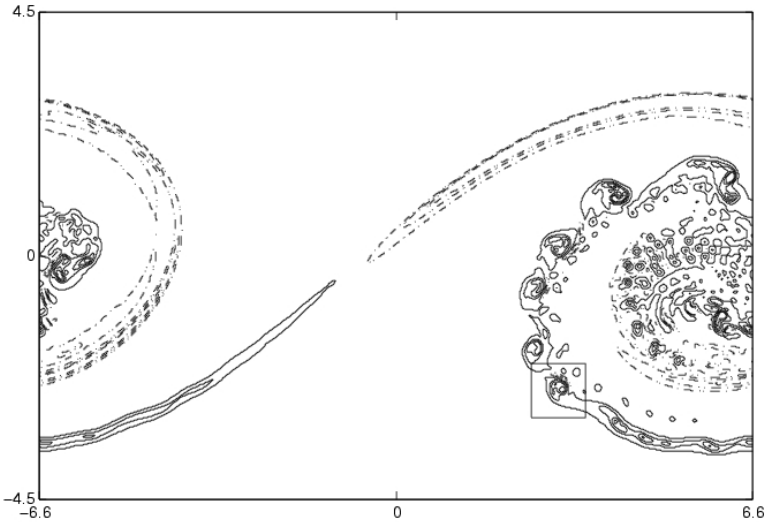

Self-excited oscillations and mixing in a hot jet : Monkewitz and Bechert, PoF Gallery of fluid motion, 1988

S=0,47

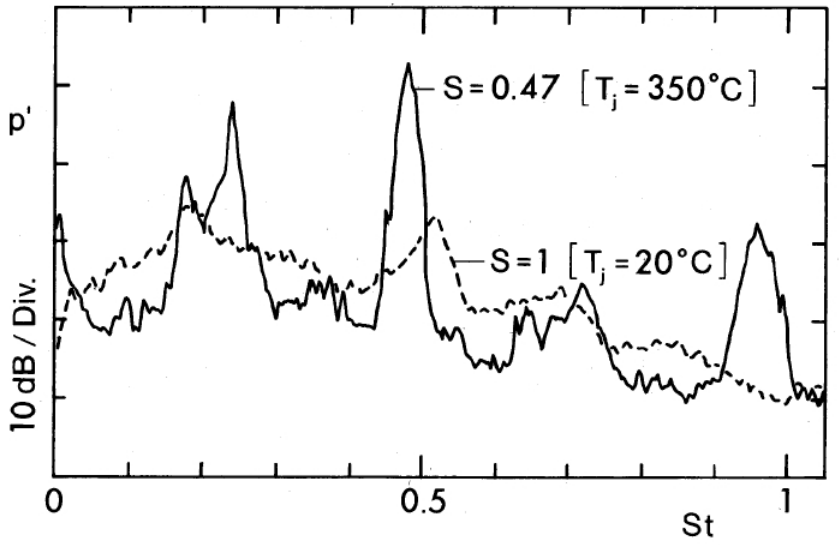

Figure 3. Pressure spectra (B&K $\frac{1}{4}$ in. microphone located at $x/D = 0.2$, $r/D = 1$) for the hot jet of Fig. 2 and a cold jet of equal dynamic head $q = 135$ Pa.

Mixing inhomogeneous streams : Side ejections in light jets

Side ejections in a round laminar helium-jet S=0,14 : Hermouche, 1996 IMFT PhD supervised by P. Chassaing

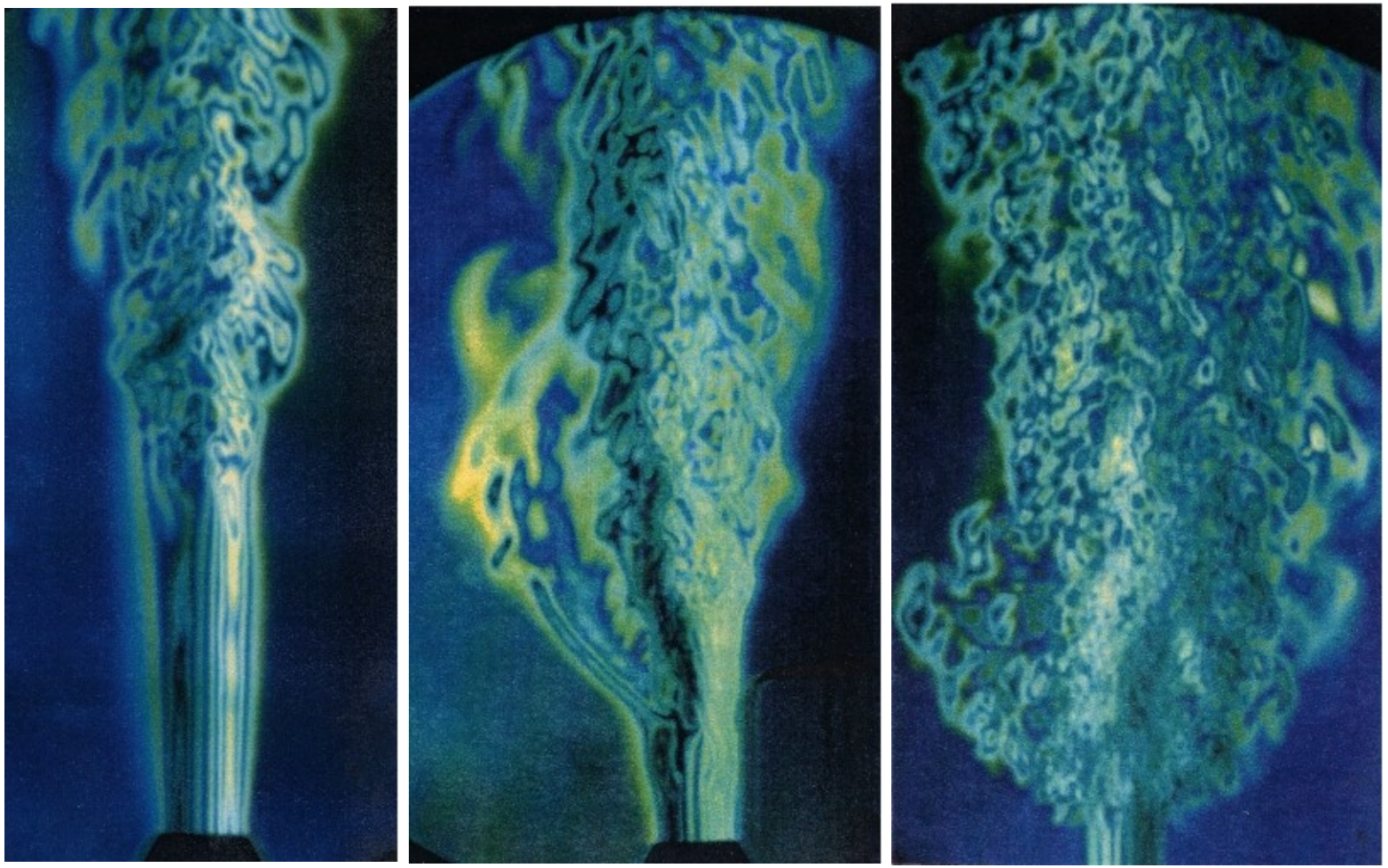

Re = 750 Re = 1000 Re = 2600

Outline of the talk

- Introduction - Illustrative examples from experiments and simulations

  non-barotropic flows exhibit deviations from their homogeneous or barotropic equivalent

- The baroclinic torque in high Froude number flows, its nature, order of magnitude and organization
- Stability of the inhomogeneous mixing-layer

...Break...

4. Transition of the inhomogeneous mixing-layer and the 2D secondary baroclinic instability
5. The strain field of 2D light jets
6. Transition to three-dimensionality in light jets and the question of side-jets
7. Baroclinic instability of heavy vortices and some elements on vortex interaction in inhomogeneous 2D turbulence

Focus : Incompressible mixing at infinite Froude numbers

$$\mathrm{d}_t \varrho = a\Delta\varrho = -d \qquad \varrho = \ln\rho\,, \quad d = \boldsymbol{\nabla}\cdot\mathbf{u}$$

$$\mathrm{d}_t\mathbf{u} = -\boldsymbol{\nabla}\pi - \pi\boldsymbol{\nabla}\varrho + \nu\Delta\mathbf{u} \qquad \pi = p/\rho$$

$$\mathrm{d}_t\boldsymbol{\omega} = (\boldsymbol{\omega}\cdot\boldsymbol{\nabla})\mathbf{u} - d\,\boldsymbol{\omega} - \boldsymbol{\nabla}\pi\times\boldsymbol{\nabla}\varrho + \nu\Delta\boldsymbol{\omega}$$

$$\frac{\mathrm{d}\boldsymbol{\omega}}{\mathrm{d}t} = (\boldsymbol{\omega}\cdot\boldsymbol{\nabla})\mathbf{u} - \frac{1}{\rho^2}\boldsymbol{\nabla}P\times\boldsymbol{\nabla}\rho - d\,\boldsymbol{\omega} + \nu\Delta\boldsymbol{\omega}$$

Inviscid incompressible inhomogeneous flows

$$\mathrm{d}_t \rho = 0$$

$$\mathrm{d}_t \mathbf{u} = -g' \mathbf{i}_z - \dot{\mathbf{u}}_r - \frac{1}{\rho} \boldsymbol{\nabla} p$$

$$g' = \frac{g}{\rho_0}(\rho - \rho_{\mathrm{hydro}}) = g \frac{\rho'}{\rho_0} \sim \mathcal{O}(g C_\rho)$$

$$\mathbf{a} = \underbrace{\mathrm{d}_t \mathbf{u}}_{\mathrm{II}} + \underbrace{g' \mathbf{i}_z + \dot{\mathbf{u}}_r}_{\mathrm{I}} = -\frac{1}{\rho} \boldsymbol{\nabla} p$$

$$\mathrm{Ba}: \quad -\frac{1}{\rho} \boldsymbol{\nabla} p \times \boldsymbol{\nabla} \varrho \equiv \mathbf{a} \times \boldsymbol{\nabla} \varrho$$

A set of scales

$$\mathbf{u} \sim u, \quad x, y, z \sim \ell, \quad \pi \sim u^2 \qquad \rho \sim \rho_0, \quad \mathrm{d}\rho \sim \Delta\rho$$

$$\underbrace{\mathrm{d}_t \mathbf{u}}_{\frac{u^2}{\ell}} = -\underbrace{\boldsymbol{\nabla}\pi}_{\frac{u^2}{\ell}} - \underbrace{\pi \boldsymbol{\nabla}\varrho}_{\frac{u^2}{\ell}\frac{\Delta\rho}{\rho_0}} + \underbrace{\nu \Delta \mathbf{u}}_{\nu\frac{u}{\ell^2}}$$

$$\underbrace{\mathrm{d}_t \boldsymbol{\omega}}_{\frac{u^2}{\ell^2}} = \underbrace{(\boldsymbol{\omega}\cdot\boldsymbol{\nabla})\mathbf{u}}_{\frac{u^2}{\ell^2}} - \underbrace{d\boldsymbol{\omega}}_{Ma^2\frac{u^2}{\ell}} - \underbrace{\boldsymbol{\nabla}\pi \times \boldsymbol{\nabla}\varrho}_{\frac{u^2}{\ell^2}\frac{\Delta\rho}{\rho_0}} + \underbrace{\nu \Delta \boldsymbol{\omega}}_{\frac{u}{\ell^3}}$$

$$\mathrm{d}_t \varrho = \frac{1}{ReSc}\Delta\varrho = -\frac{1}{C_\rho} d$$

$$\mathrm{d}_t \mathbf{u} = -\boldsymbol{\nabla}\pi - C_\rho \pi \boldsymbol{\nabla}\varrho + \frac{1}{Re}\Delta\mathbf{u}$$

$$C_\rho = \frac{\Delta\rho}{\rho_{\mathrm{mean}}} = \frac{\rho'}{\bar{\rho}}$$

$$s = \rho_2/\rho_1$$

$$C_\rho = \frac{\rho_2 - \rho_1}{\rho_2 + \rho_1}$$

$$C_\rho = (s-1)/(1+s)$$

Condition : $2\rho_m - \Delta\rho > 0$

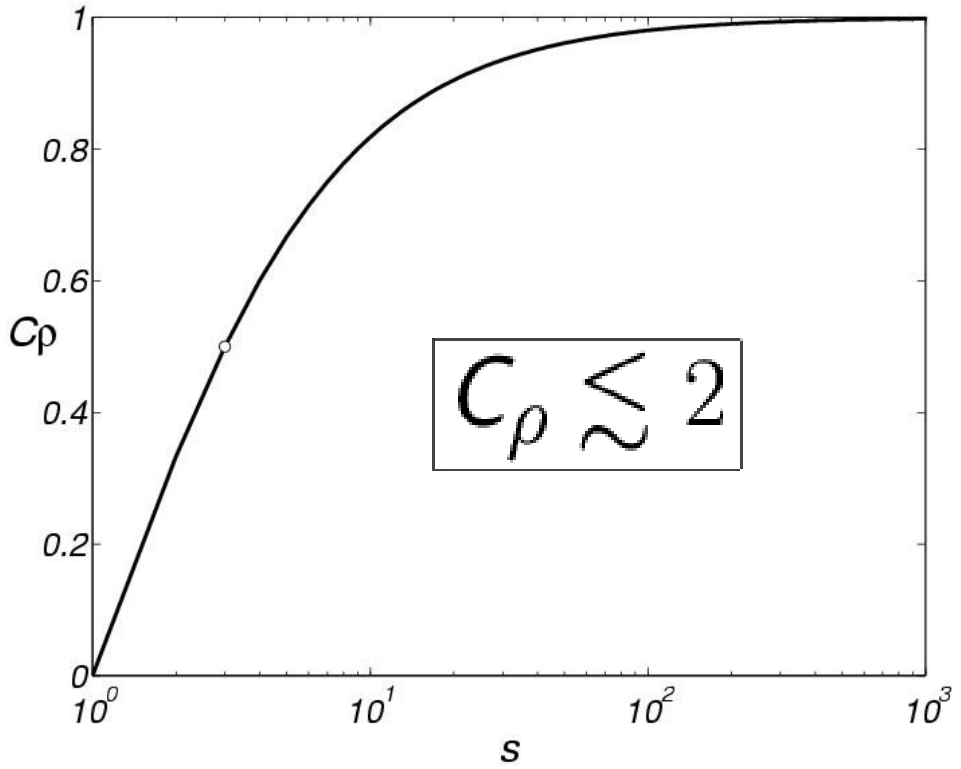

$$\mathrm{d}_t \varrho = \frac{1}{ReSc}\Delta\varrho = -\frac{1}{C_\rho}d$$

$$\mathrm{d}_t \mathbf{u} = -\boldsymbol{\nabla}\pi - C_\rho \pi \boldsymbol{\nabla}\varrho + \frac{1}{Re}\Delta\mathbf{u}$$

$$\mathrm{d}_t\boldsymbol{\omega} = \underline{(\boldsymbol{\omega}\cdot\boldsymbol{\nabla})\mathbf{u}} - d\,\boldsymbol{\omega} - \underline{\boldsymbol{\nabla}\pi\times\boldsymbol{\nabla}\varrho} + \nu\Delta\boldsymbol{\omega}$$

$$\mathrm{Vs} \qquad (\boldsymbol{\omega}\cdot\boldsymbol{\nabla})\mathbf{u} \sim \mathcal{O}(\frac{u^2}{\lambda^2})$$

$$\mathrm{Ba} \qquad \boldsymbol{\nabla}\pi\times\boldsymbol{\nabla}\varrho \sim \mathcal{O}(\frac{u^2}{\ell}\,\frac{C_\rho}{\lambda_\rho})$$

$$\frac{\mathrm{Ba}}{\mathrm{Vs}} \sim C_\rho\cdot\frac{\lambda}{\lambda_\rho}\cdot\frac{\lambda}{\ell}$$

$$\mathrm{d}_t\boldsymbol{\omega} = \underline{(\boldsymbol{\omega}\cdot\boldsymbol{\nabla})\mathbf{u}} - d\,\boldsymbol{\omega} - \underline{\boldsymbol{\nabla}\pi\times\boldsymbol{\nabla}\varrho} + \nu\Delta\boldsymbol{\omega}$$

$$\text{Vs} \qquad (\boldsymbol{\omega}\cdot\boldsymbol{\nabla})\mathbf{u} \sim \mathcal{O}(\frac{u^2}{\lambda^2})$$

$$\text{Ba} \qquad \boldsymbol{\nabla}\pi\times\boldsymbol{\nabla}\varrho \sim \mathcal{O}(g\,\frac{C_\rho}{\lambda})$$

$$\frac{\text{Ba}}{\text{Vs}} \sim g\cdot C_\rho\cdot\frac{\lambda}{u^2} \sim Ri$$

$$\frac{\mathrm{Ba}}{\mathrm{Vs}} \sim C_\rho \cdot \frac{\lambda}{\lambda_\rho} \cdot \frac{\lambda}{\ell}$$

- Fully developped 3D turbulence $\quad \frac{\mathrm{Ba}}{\mathrm{Vs}} \sim \frac{\lambda}{\lambda_\rho} \cdot \frac{C_\rho}{Re_\lambda}$

High Reynolds number turbulence insensitive to density variations

- Two-dimensional flows : no vortex stretching $\quad \boldsymbol{\omega} \perp \boldsymbol{\nabla} \mathbf{u}$

No vortex stretching, baroclinic torque only source/sink of vorticity

- Transition flows $\quad \frac{\lambda}{\ell} \sim \mathcal{O}(1)$

The baroclinic torque may bias the transition

Kelvin-Helmholtz instability s=3, Re = Uδ/ν = 1500

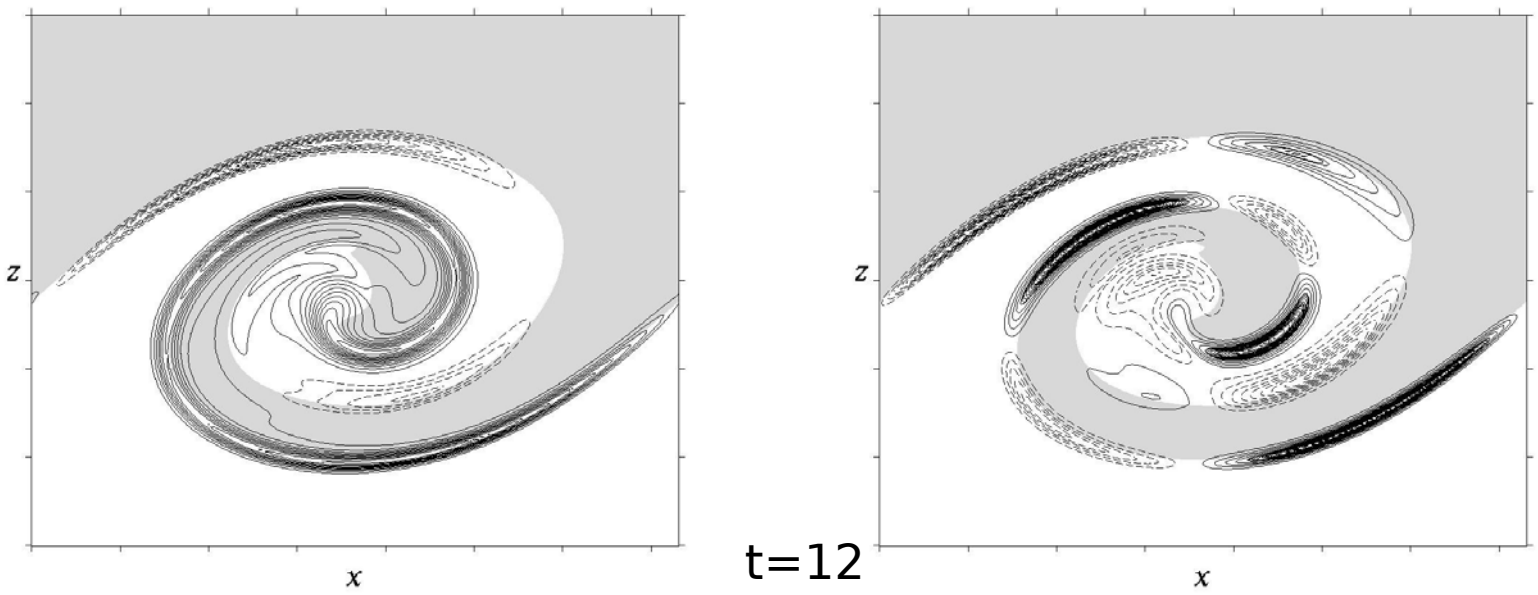

Vorticity

Baroclinic torque

Spatial structure of the variable density mixing layer : length scales

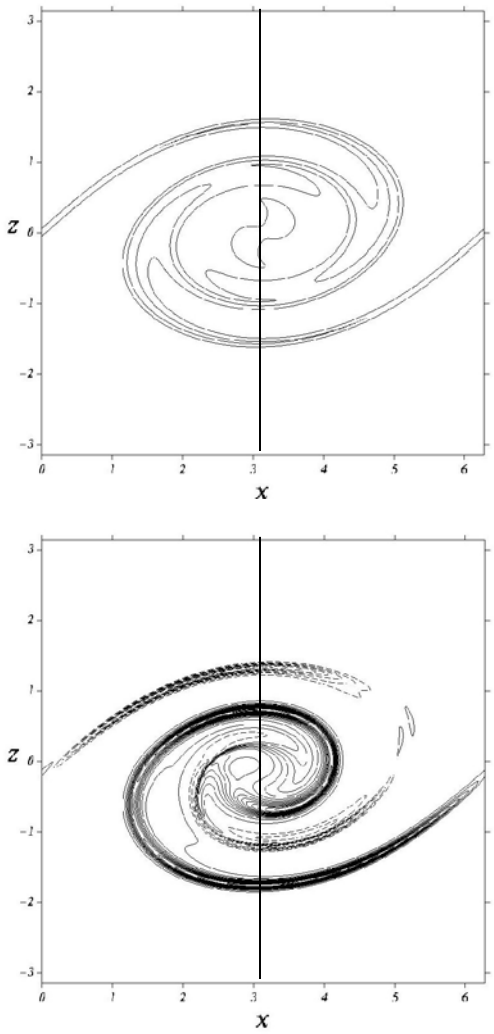

Mixing layer s = 1 or 3 , Re = 3000, t=12

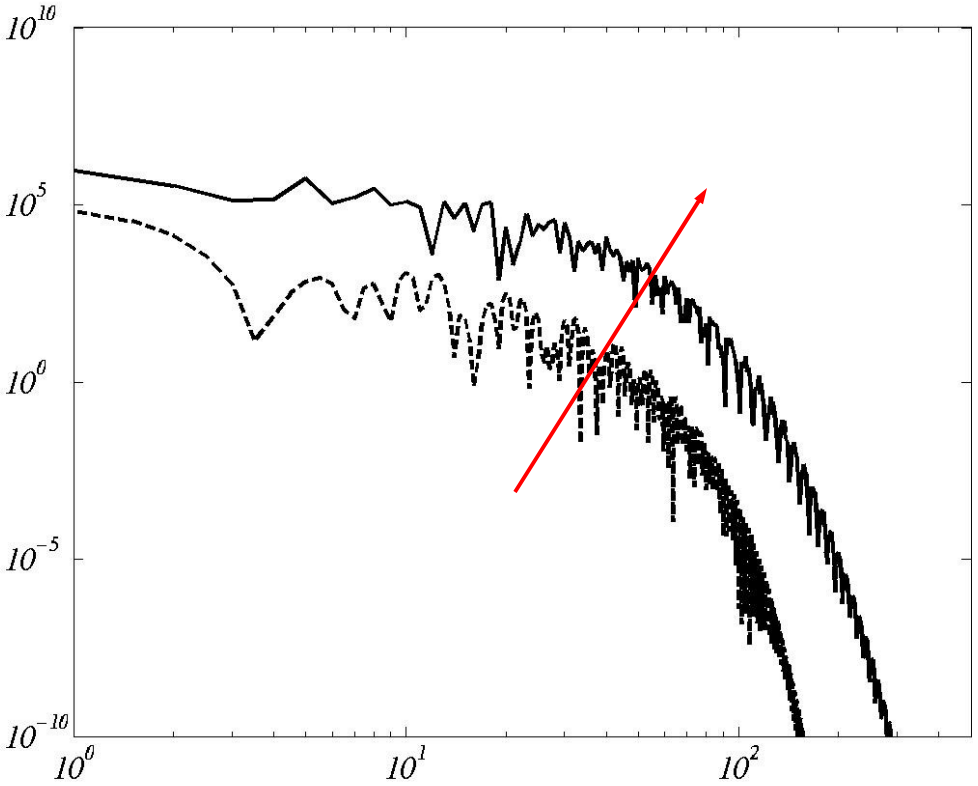

Temporal mixing layer s=3, Re = Uδ/ν = 500,1500,3000

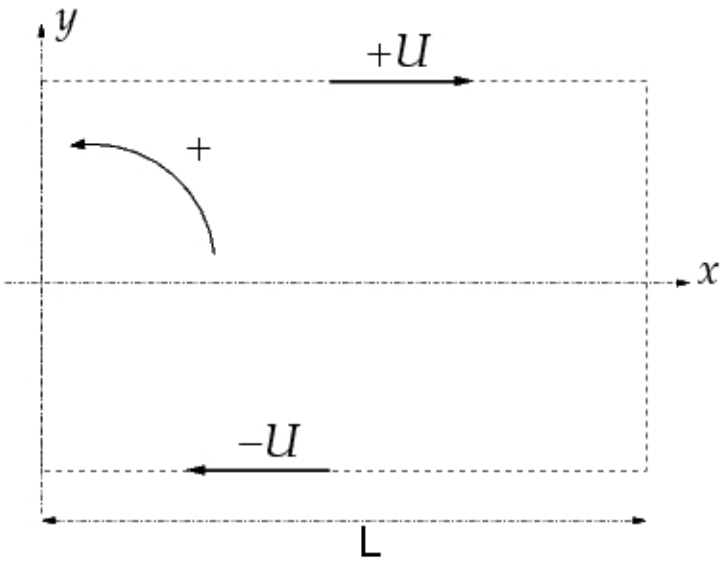

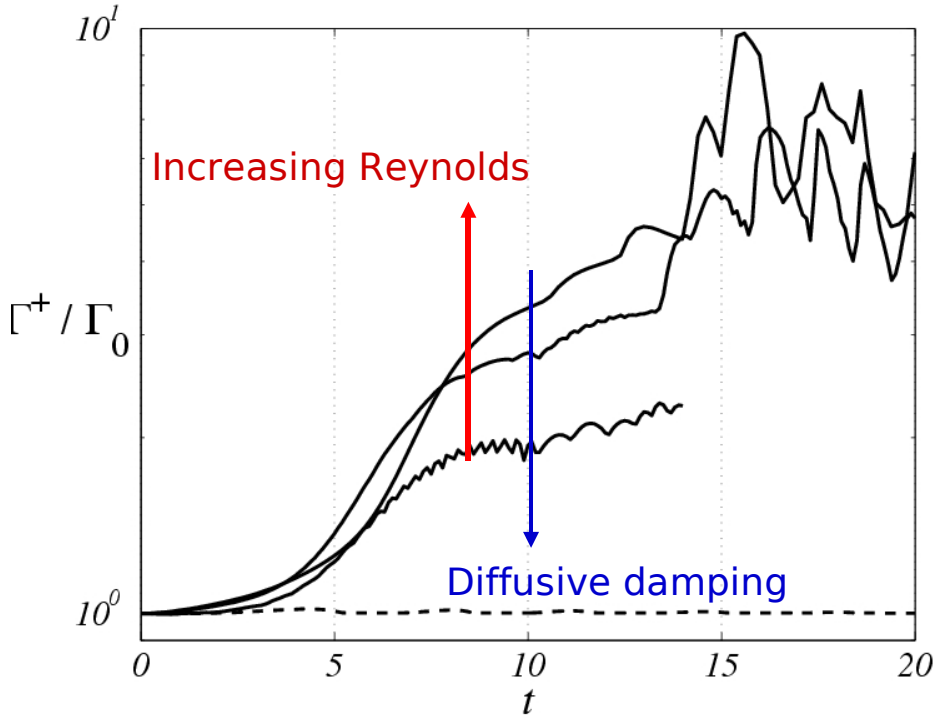

$$\Gamma_0 = -2UL$$

$$\Gamma^+ = \int_{\text{period}} (\omega < 0) \mathrm{d}\sigma$$

Outline of the talk

- *Introduction*
- *The baroclinic torque*

  - *Scales with the bounded density contrast*
  - *Inertial nature : accelerated inhomogeneous medium*
  - *Competes with vortex stretching in transition flows and 3D flows*
  - *Recasts the enstrophy spectrum toward higher wavenumbers*
  - *Intense local source/sink of vorticity but a weak net effect*
  - *Significantly damped by diffusion, enhanced by isopycnal stretching*

4. *Stability of the inhomogeneous shear-flows*

   ...Break...

5. *Transition of the inhomogeneous mixing-layer and the 2D secondary baroclinic instability*

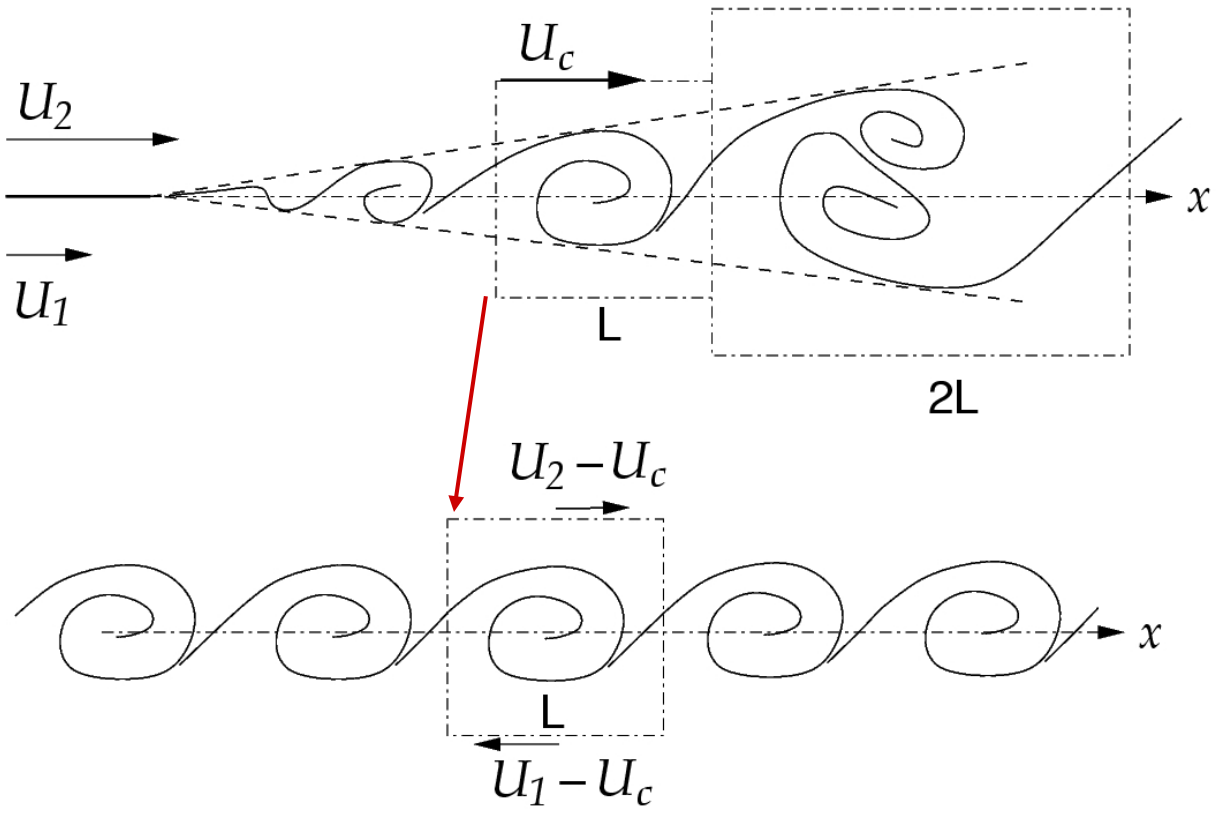

The real flow : the spatially developing mixing-layer

The temporally developing mixing-layer

The temporal approximation :

- The frame of reference is moving with the convection velocity of the large structures
- The flow is considered parallel
- The choosen subharmonic of the primary mode is periodized in the streamwise direction

Due to the temporal approximation, the difference between cogradient and countergradient situations is lost

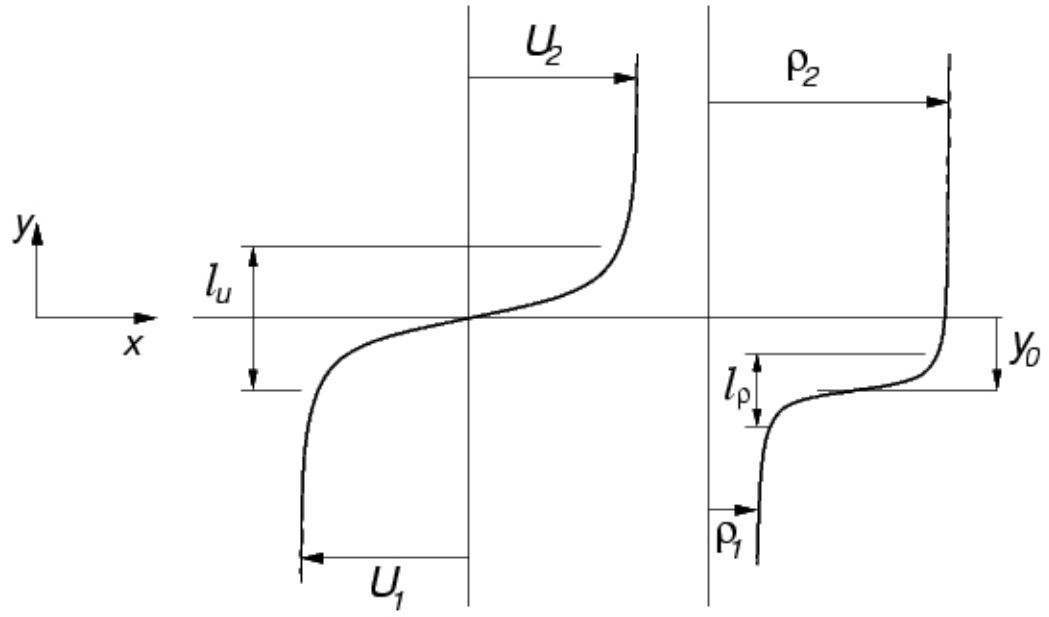

$$U(y) = U\tanh(y/\ell_u) \qquad R(y) = \rho_m + \frac{\Delta\rho}{2} f\left(\frac{y - y_0}{\ell_\rho}\right)$$

- Decomposition of flow variables

$$\mathbf{u}(\mathbf{x},t) = U(y)\mathbf{e}_x + \hat{\mathbf{u}}(\mathbf{x},t)$$

$$\rho(\mathbf{x},t) = R(y) + \hat{\rho}(\mathbf{x},t)$$

- Linearization of the Euler equations : perturbation equations

$$\begin{aligned} \mathrm{D}_t\hat{\rho} + \hat{v}\,R' &= 0 \\ R\mathrm{D}_t\hat{\mathbf{u}} + RU'\,\hat{v}\,\mathbf{e}_x &= -\boldsymbol{\nabla}\hat{p} \\ \boldsymbol{\nabla}\cdot\hat{\mathbf{u}} &= 0 \end{aligned}$$

- The Rayleigh equation for the crosswise perturbation velocity

$$\left[R\mathrm{D}_t\boldsymbol{\nabla}^2 - (RU')'\partial_x + R'\mathrm{D}_t\partial_y\right]\hat{v} = 0$$

- Perturbations are given the 2D wavelike form

$$\begin{aligned} [\hat{\mathbf{u}},\hat{\rho},\hat{p}](\mathbf{x},t) &= [\tilde{\mathbf{u}},\tilde{\rho},\tilde{p}](y)\mathrm{e}^{i(\alpha x - \alpha c t)} \\ &= [\tilde{\mathbf{u}},\tilde{\rho},\tilde{p}](y)\mathrm{e}^{\alpha c_i t}\mathrm{e}^{i\alpha(x-c_r t)} \end{aligned}$$

- α Streamwise wavenumber
- $\sigma = \alpha c_i$ Growth rate
- c_r Phase velocity

- Decomposition of the vorticity field

$$\boldsymbol{\omega}(\mathbf{x},t) = -U'(y)\mathbf{e}_z + \hat{\boldsymbol{\omega}}(\mathbf{x},t)$$

$$\hat{\boldsymbol{\omega}} = (\hat{\xi},\hat{\eta},\hat{\zeta})$$

- Linearized equation for the normal vorticity perturbation (2D)

$$\mathrm{D}_t\hat{\zeta} = U''\hat{v} - U'\partial_z\hat{w} - \frac{R'}{R^2}\partial_x\hat{p}$$

The linearized baroclinic torque is responsible for the differences between the stability of the variable-density and the homogeneous shear flows.

$$\hat{a}_x = \frac{1}{R}\partial_x\hat{p} \qquad \hat{b} = -\frac{R'}{R}\hat{a}_x$$

Effect of the density contrast – same thickness zero offset

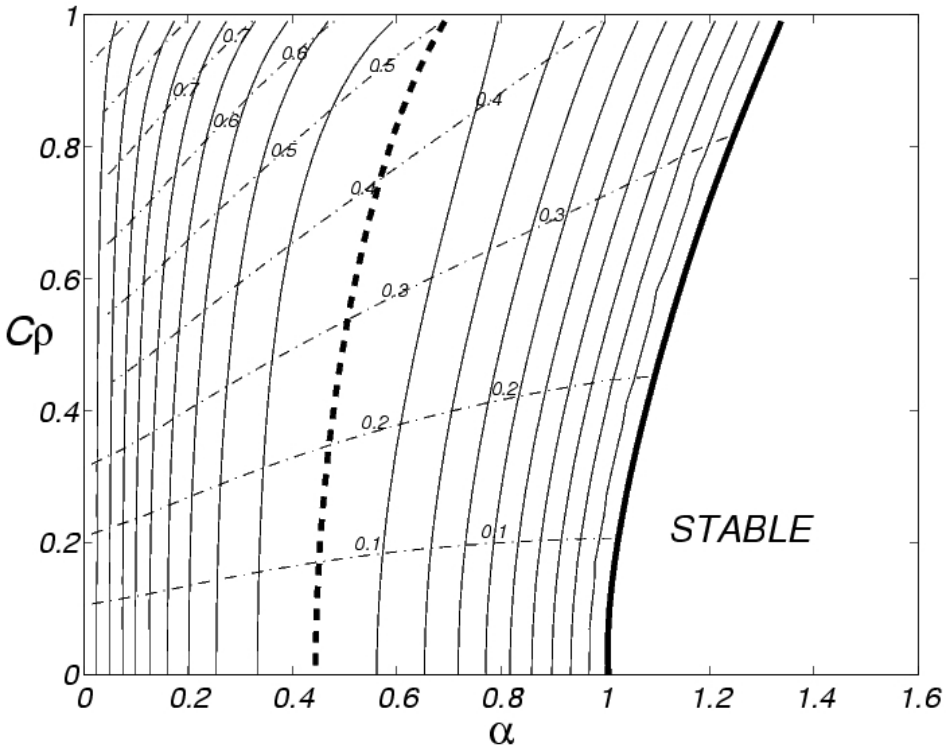

comments

Influence of the thickness ratio $\varepsilon = \ell_u / \ell_\rho$

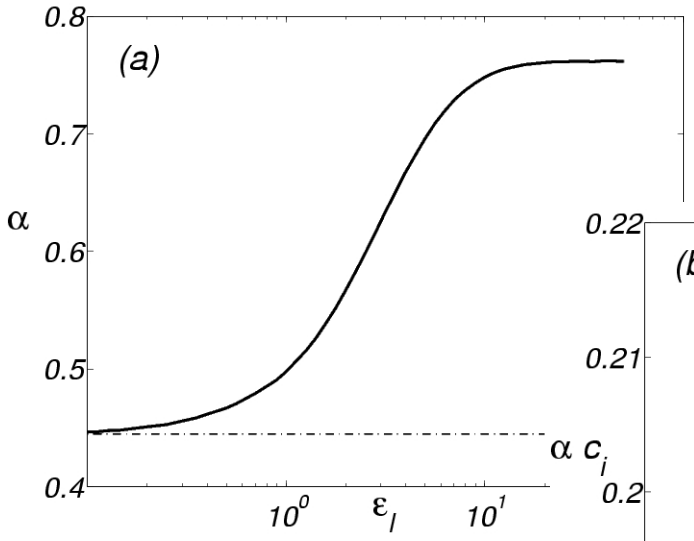

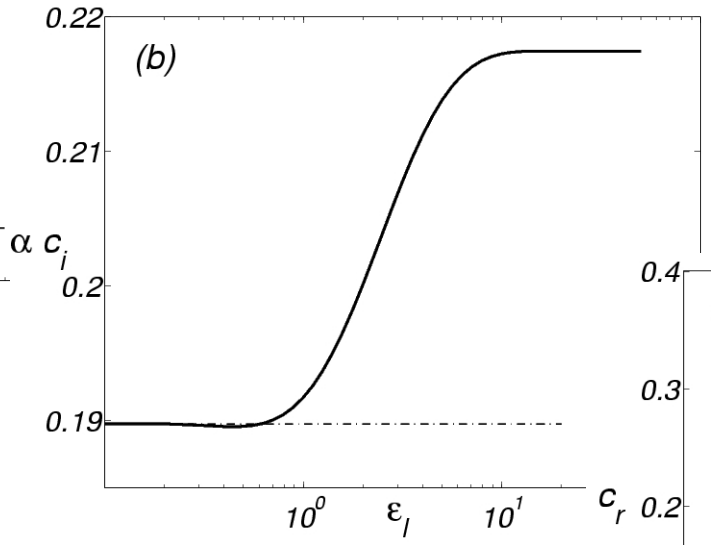

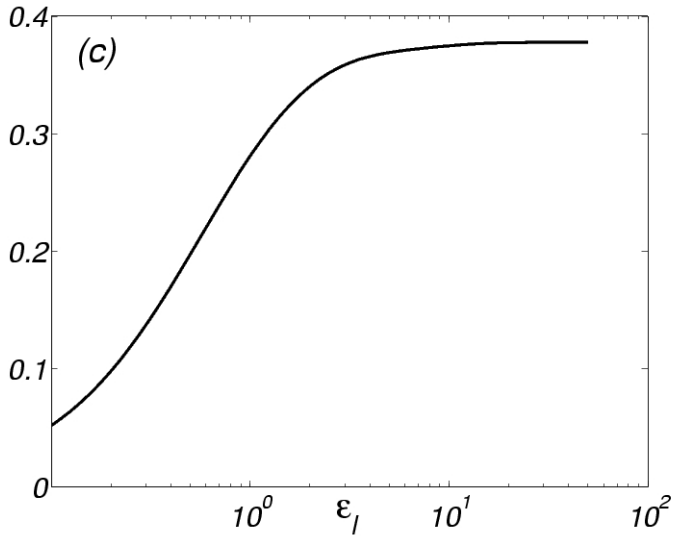

comments

Influence of the crosswise offset

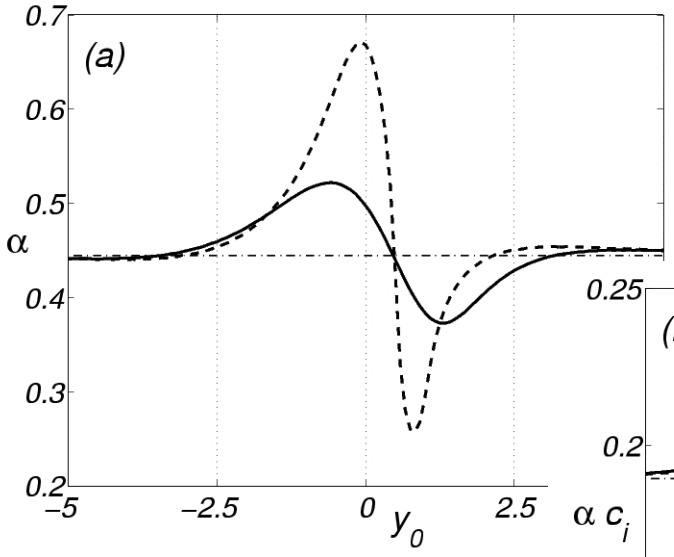

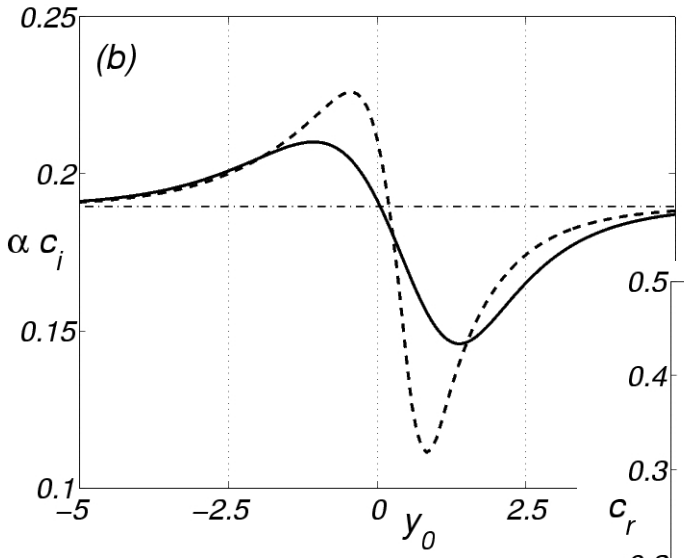

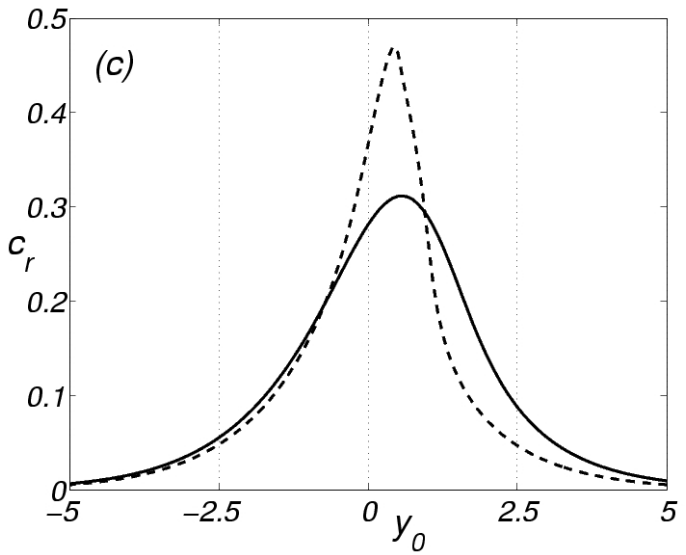

comments

Combined effects of the thickness ratio and the crosswise offset

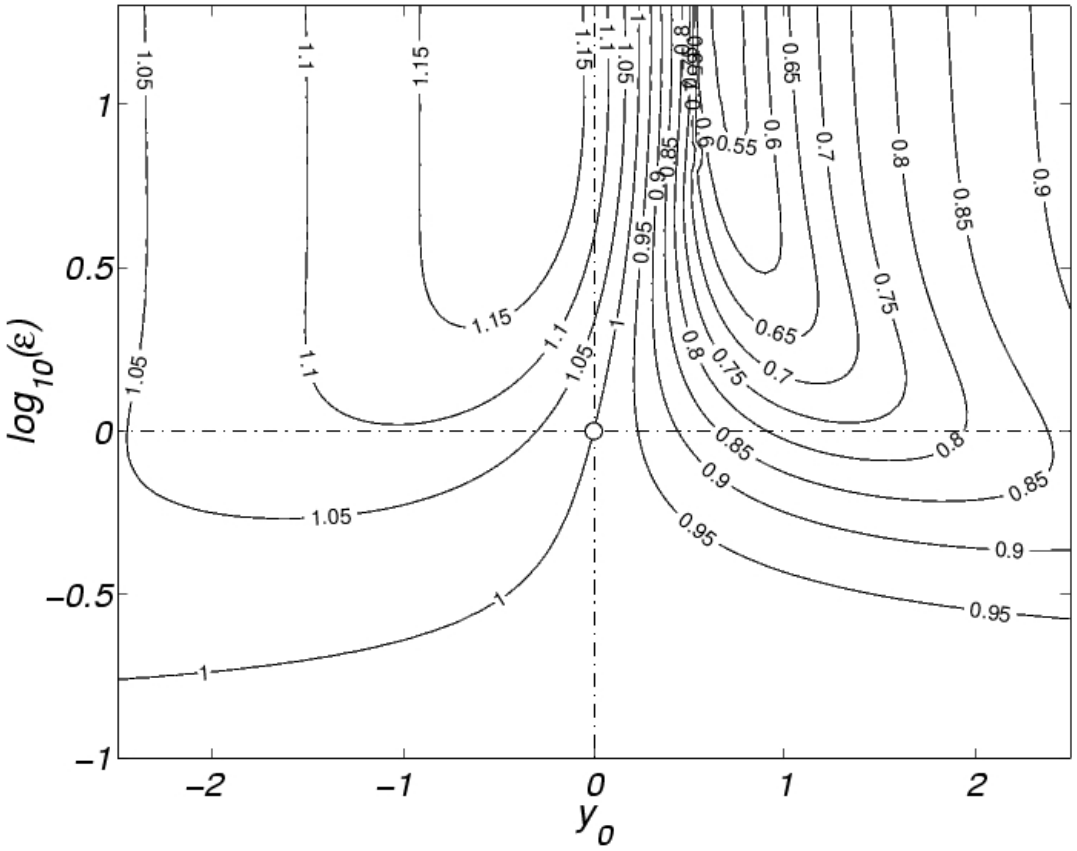

comments

From the impulse response of a system to a perturbation located somewhere

Oscillator behavior, intrinseque behavior with a well defined response

ABSOLUTE INSTABILITY

Amplificator behavior, broad band sensitivity to external perturbations

CONVECTIVE INSTABILITY

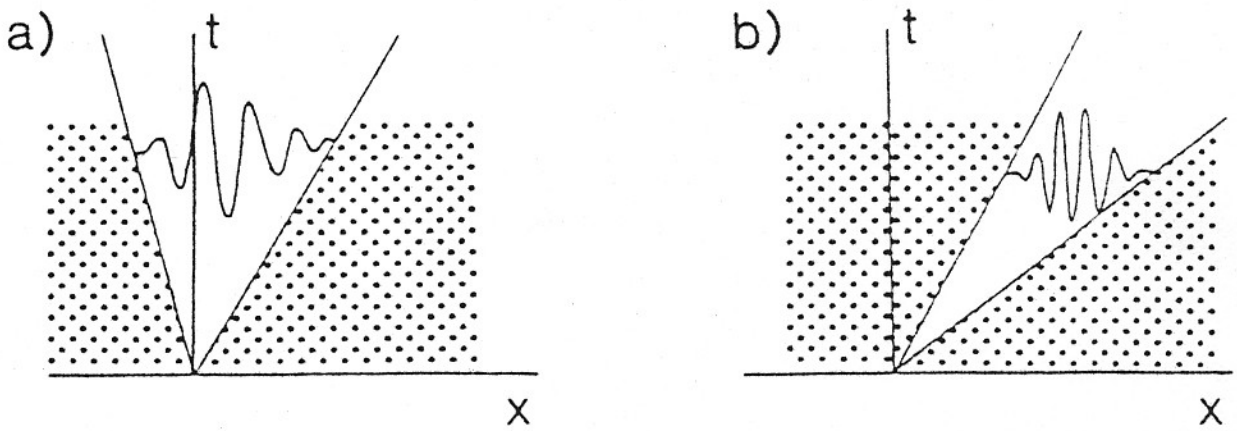

Fig. 3 Sketch of a typical impulse response: a) absolutely unstable flow; b) convectively unstable flow (shaded areas are regions with $\sigma_i < 0$).

Wake of a bluff body, homogeneous jet with a negative coflow, light jet

Boundary layer flow, homogeneous jet

The linearized baroclinic torque is responsible for the differences between the stability of the variable-density and the homogeneous shear flows.

$$\mathrm{D}_t\hat{\zeta} = U''\hat{v} - U'\partial_z\hat{w} - \frac{R'}{R^2}\partial_x\hat{p}$$

S=0,79

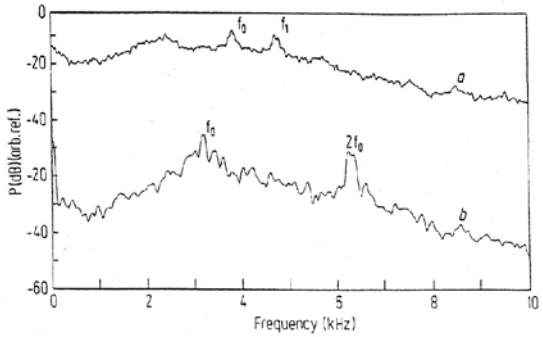

Fig. 2. Two typical power spectral densities in the near field of cold air jets illustrating two different behaviours; the helical mode marked f_1 in the upper figure is absent in the lower figure, where a harmonic appears; x/D in both cases is approximately 2

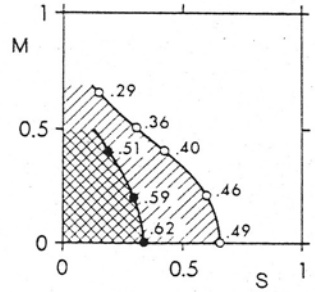

Fig. 4 Absolute instability boundaries for the $m=0$ mode (○) and the $m=1$ mode (●), with $N=\infty$ and $R=1$. The hatched areas are the absolutely unstable regions. The parameter along the curves is the branch point Strouhal number.

S=0,47

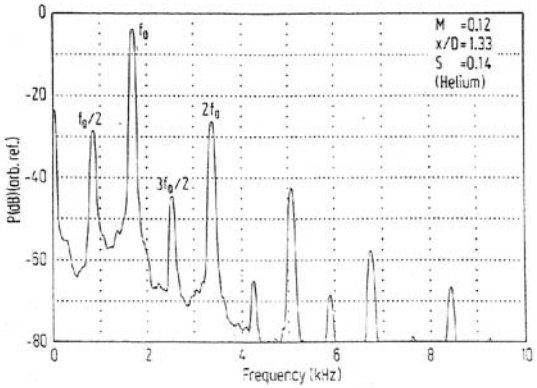

Fig. 3. Power spectral density in helium jet, showing large peaks at f_0, and its harmonics and subharmonic; note the qualitative resemblance to Fig. 1 a

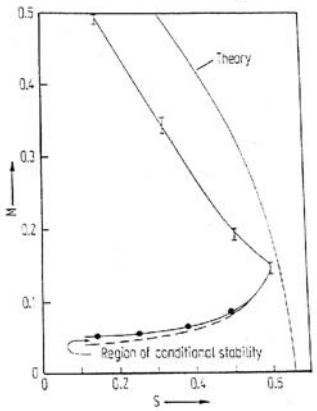

Fig. 4. The region of absolute instability in the Mach number (M)-density ratio (S) plane, compared with the Monkewitz-Sohn theory for a cylindrical vortex sheet; the uncertainty in experimentally marking the boundary is shown: the region of conditional instability is shown at the bottom of the diagram

Critical density ratio for 2D and round light jets

Sc	Plane Jet		Round Jet	
Heated Jet	Measure and Theory Yu & Monkewitz Sc = 0.92		Measure and Theory Monkewitz & Sohn Sc = 0.73	
Light Fluid Jet	Measure Favre-Marinet Sc = 0.8	Stability Favre-Marinet 0.94	Measure Kyle & Sreenivasan Sc = 0.61	Theory 0.72

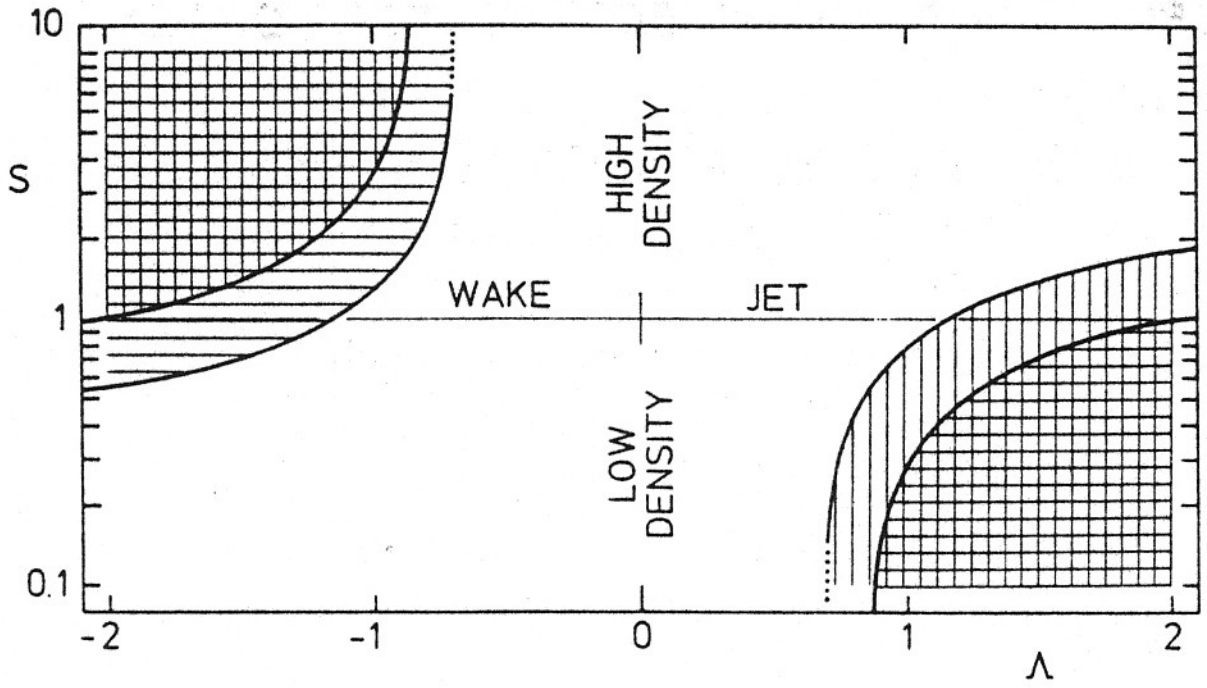

FIG. 2. Stability properties of the two-vortex-sheet model as a function of density ratio $S = \bar{\rho}_c/\bar{\rho}_\infty$ and velocity ratio $\Lambda = (\bar{u}_c - \bar{u}_\infty)/(\bar{u}_c + \bar{u}_\infty)$. Horizontal hatching: absolute instability of the sinuous mode; vertical hatching: absolute instability of the varicose mode.

Outline of the talk

- *Introduction*
- *The baroclinic torque*
- *Stability of the inhomogeneous shear flows*

  - *Linearized baroclinic vorticity generation turns convective instability of jets into absolute instability*
  - *Stability characteristics very sensitive to thckness ratio and relative offset between velocity and density profiles*

...Break...

5. *Transition of the inhomogeneous mixing-layer and the 2D secondary baroclinic instability*

Outline of the talk

- *Introduction*
- *The baroclinic torque*
- *Stability of the inhomogeneous mixing-layer*

  … Break …
- *The 2D mixing-layer in the nonlinear regime and the secondary baroclinic instability*
- *The strain field of 2D light jets*
- *Transition to three-dimensionality in light jets and the question of side-jets*
- *Baroclinic instability of heavy vortices and some elements on vortex interaction in inhomogeneous 2D turbulence*

Kelvin-Helmholtz instability s=3, Re = Uδ/ν = 1500

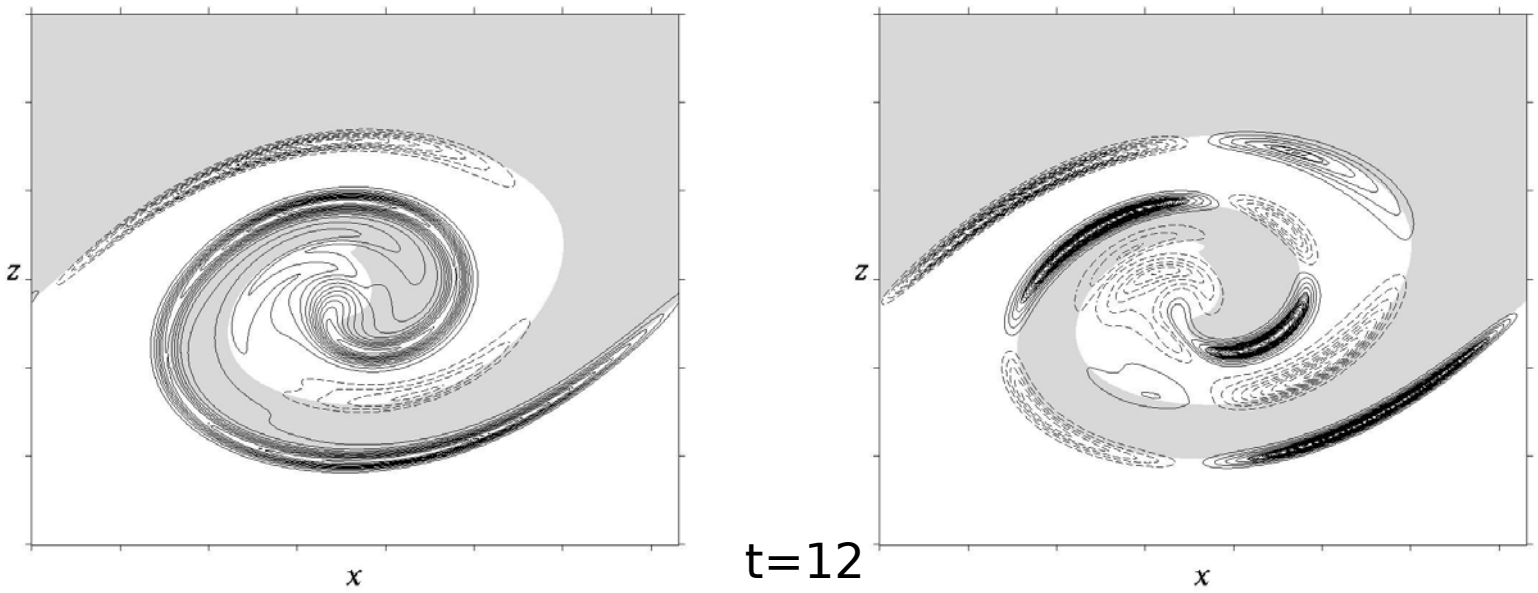

Vorticity

Baroclinic torque

Spatial structure of the variable density mixing layer

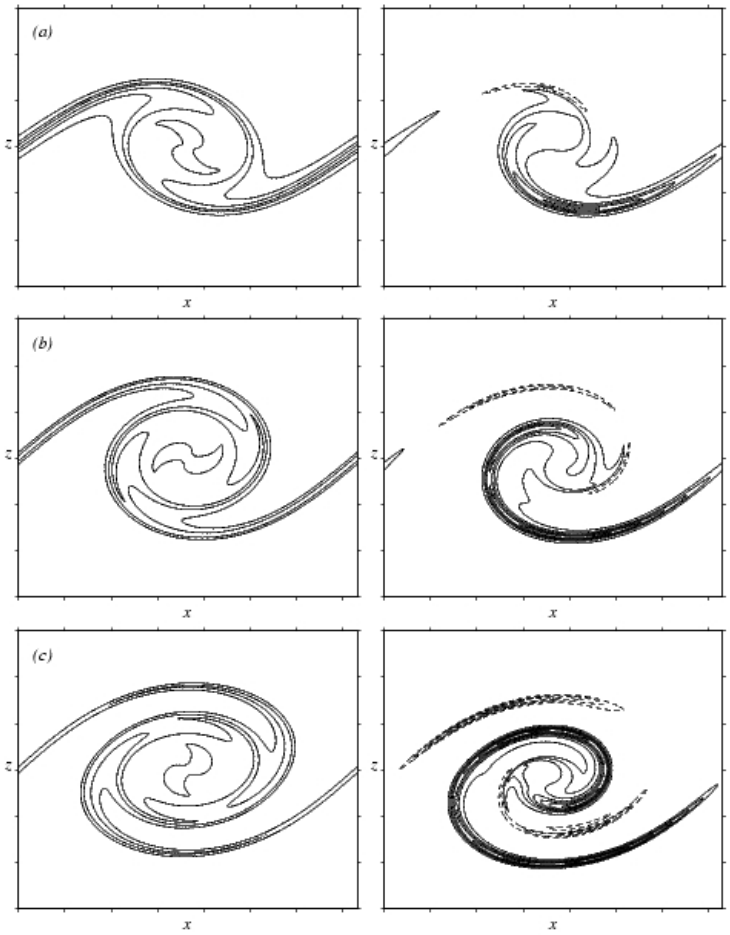

Figure 3.2: Vorticity ω_y contours of the two-dimensional variable density mixing-layer at $Re = 3000$. Left column : passive-scalar case, right column : variable-density situation with density ratio of $S_\rho = 3$. The time normalized by τ, is (a) $t = 8$, (b) $t = 10$, (c) $t = 12$. Contour increment is $1/2\tau$ for the passive-scalar case and twice that value for the variable-density case. The negative contours are drawn with dashed lines; tic marks along x and z coordinates are every δ_ω^0.

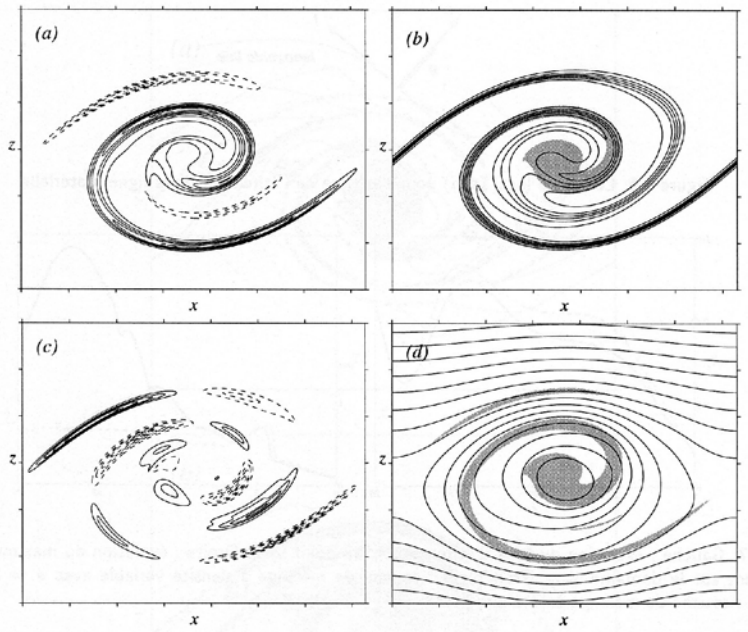

Figure 3.5: Description de la couche de mélange à densité variable à $s = 3$, $Re = 1500$ à l'instant $t = 12$. (a) contours iso-vorticité (incrément U/δ_ω^0), (b) contours iso-densité (incrément $\Delta_\rho/6$), (c) barocline couple (incrément $0.5\delta_\omega^{0\,2}$), (d) lignes de courant. Les contours négatifs sont en pointillés ; dans les figures (b) et (d), la région grisée correspond à des niveaux de vorticité au-delà de $2U/\delta_\omega^0$; les axes sont gradués tous les δ_ω^0.

Normalized vorticity along the central material line

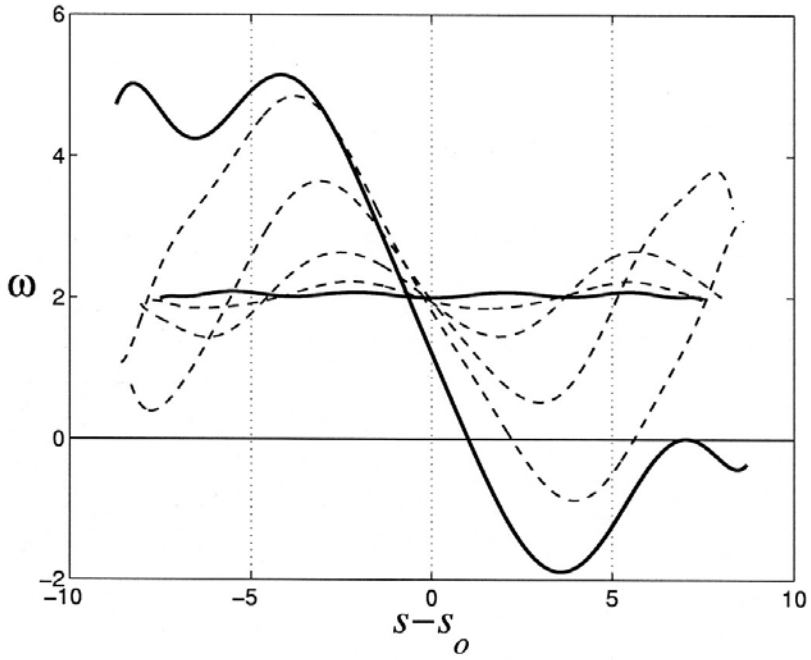

Figure 3.3: Normalized vorticity $\omega \times \tau$ along the central material line (where $\rho = (\rho_{\text{upper}} + \rho_{\text{lower}})/2$) of the variable density mixing layer with $Re = 1500$ and density ratio $S_\rho = 3$. The solid curves are the initial vorticity level and the one at t=10. Dashed lines are every $\Delta t = 2$ and the dot-dashed line marks the zero threshold. The abscissa is given along the normalized curvilinear coordinate s/δ^0_ω associated to the material line, s_o being the origin at the saddle point.

The stretched vorticity filament, Dritschel et al. JFM 230 (1991)

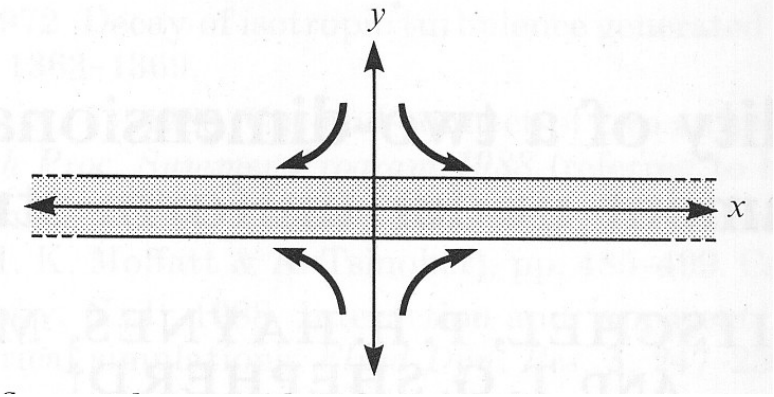

The strain rate has a twofold stabilizing effect :

2. Compresses disturbances in the transverse direction
3. Cause the disturbance wavelength to increase with time

Transient growth before inevitable decay depending on the ratio of strain rate to vorticity

A criterion based on γ/ω :

- more than 0.25 supresses amplification
- Around 0.065 allows for transient growth rate of three,

(passive behaviour of vorticity filaments in 2D turbulence)

Dynamics of unstable stratified mixing layers, Corcos et Sherman JFM 73 (1976),

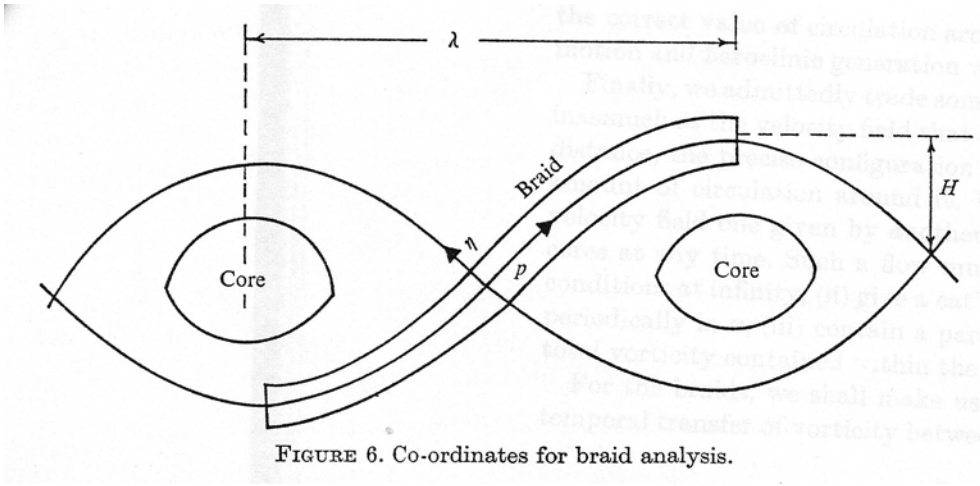

FIGURE 6. Co-ordinates for braid analysis.

Staquet JFM 296 (1995)

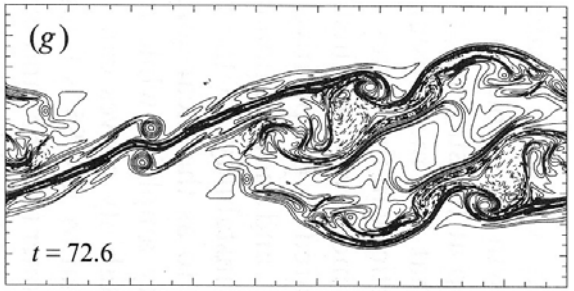

The stretched density-gradient and vorticity filament,

Reinaud, Joly et Chassaing PoF (2002)

$$\mathbf{u} = (\gamma x, -\gamma y) \qquad \mathbf{g} = (0, g_y)$$

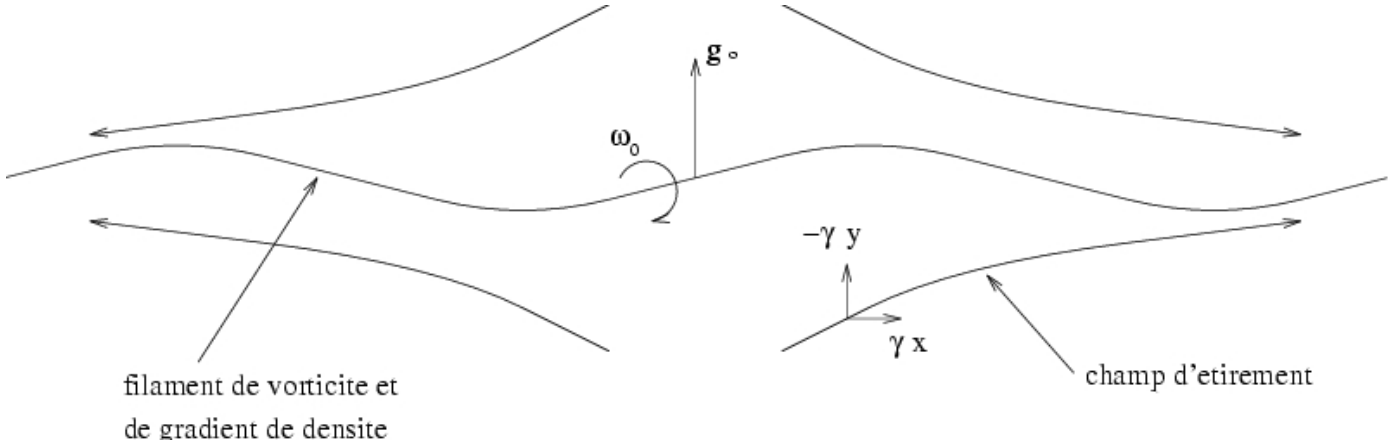

$$\mathrm{d}_t g_y = \gamma g_y \quad \rightarrow \quad g_y(x,t) = g_0 \exp(\gamma t)$$

$$\mathrm{d}_t \omega = \mathrm{d}_t u \frac{g_y}{\rho_0} = \gamma^2 x \frac{g_0}{\rho_0} \exp(\gamma t) \quad \rightarrow \quad \omega(x,t) = \gamma x \frac{g_0}{\rho_0} \sinh(\gamma t) + \omega_0$$

$$\frac{\omega(x,t)}{\gamma} = -\frac{g_0}{\rho_0} x \, \sinh(\gamma t) + \frac{\omega_0}{\gamma}$$

Twodimensional Baroclinic instability of a stretched vorticity sheet

The stretched density-gradient and vorticity filament,
Reinaud, Joly et Chassaing PoF (2002)

$$\frac{\omega(x,t)}{\gamma} = -\frac{g_0}{\rho_0}\, x\, \sinh(\gamma t) + \frac{\omega_0}{\gamma}$$

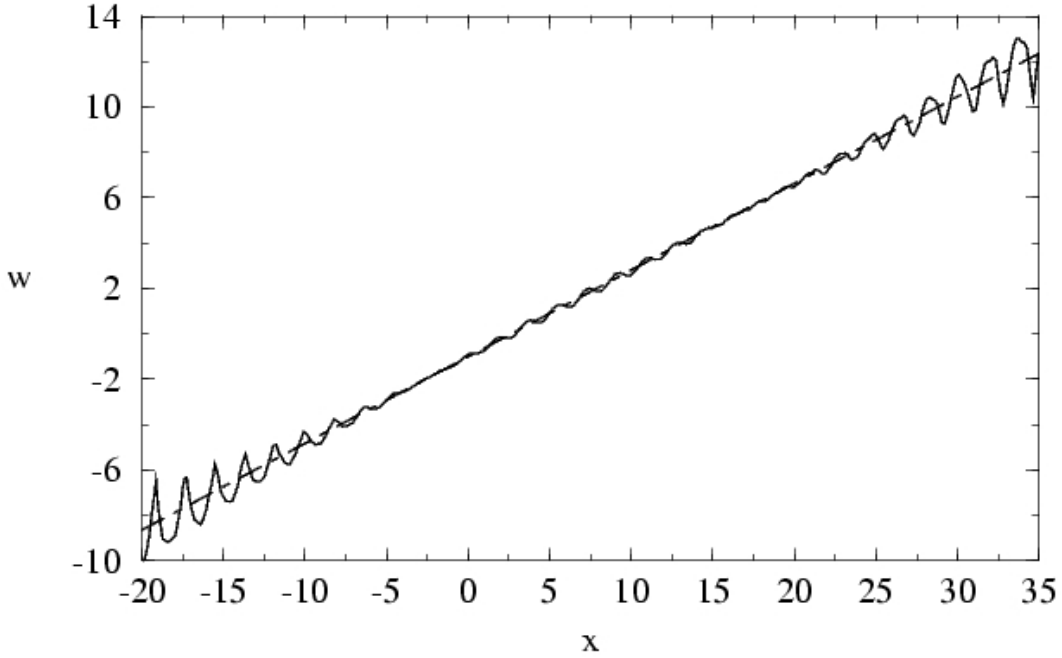

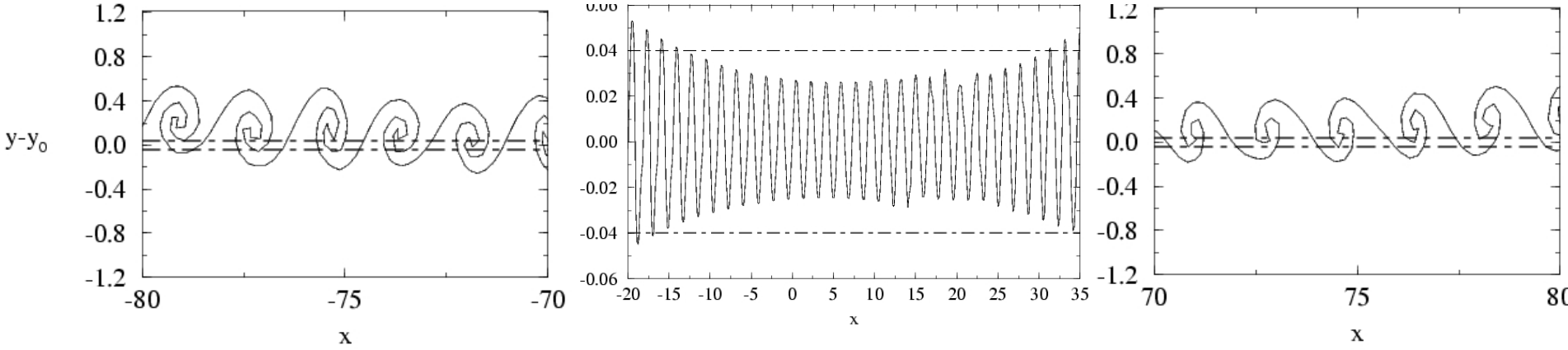

A fascinating breakup into smaller scale vortices

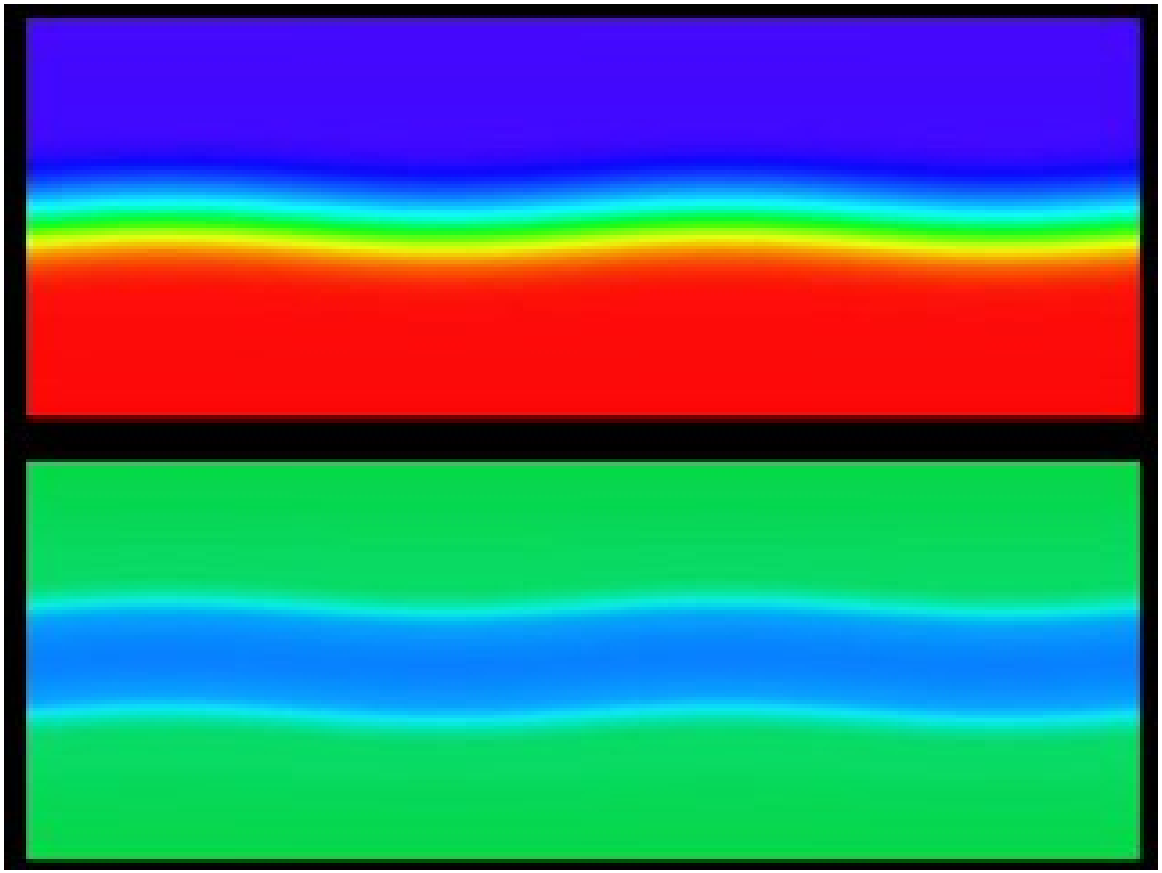

The secondary instability : scale invariance

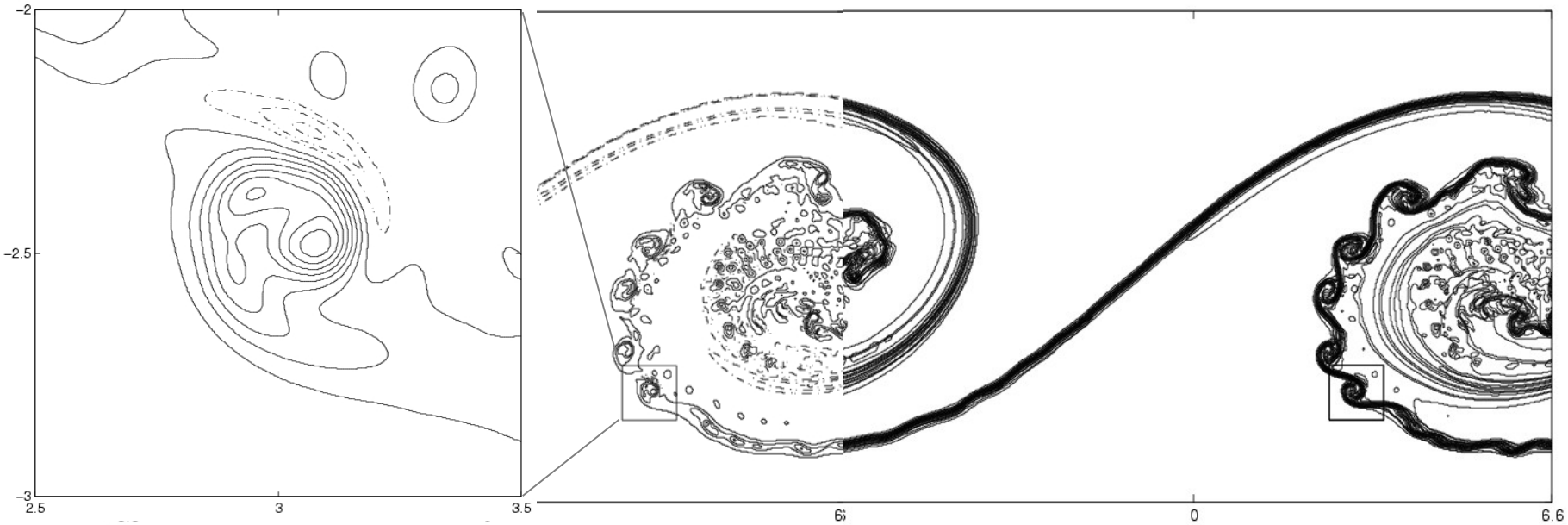

- A specific transition mécanism of the inhomogeneous shear flow;
- Twodimensional secondary mode;
- The vorticity pattern is repeated in second generation structures, and so on untill viscity prevents baroclinic vorticity generation.

Forced spatially developing mixing-layer (simulations with a variable density vortex method)

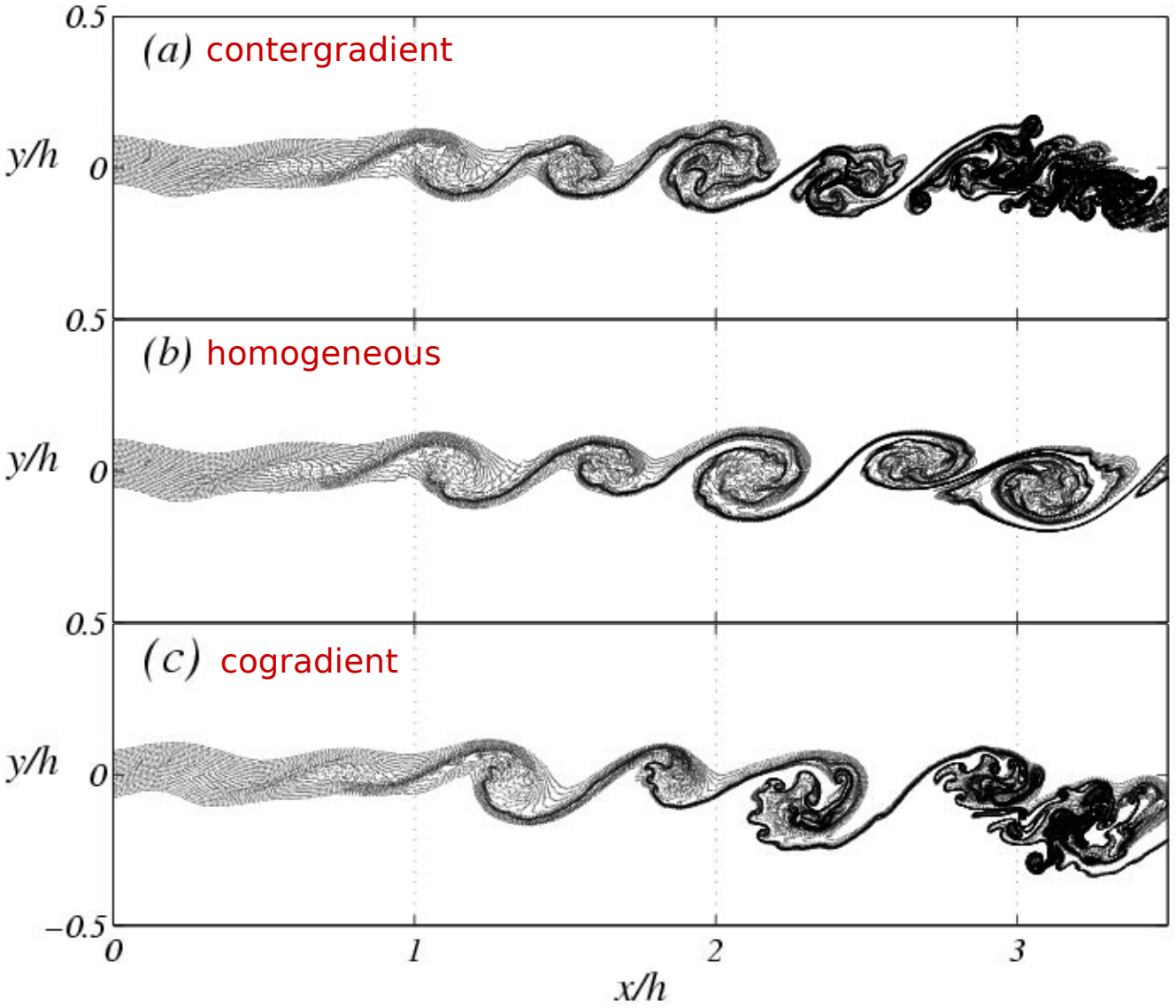

Can you see any secondary generation structures ?

contergradient

homogeneous

cogradient

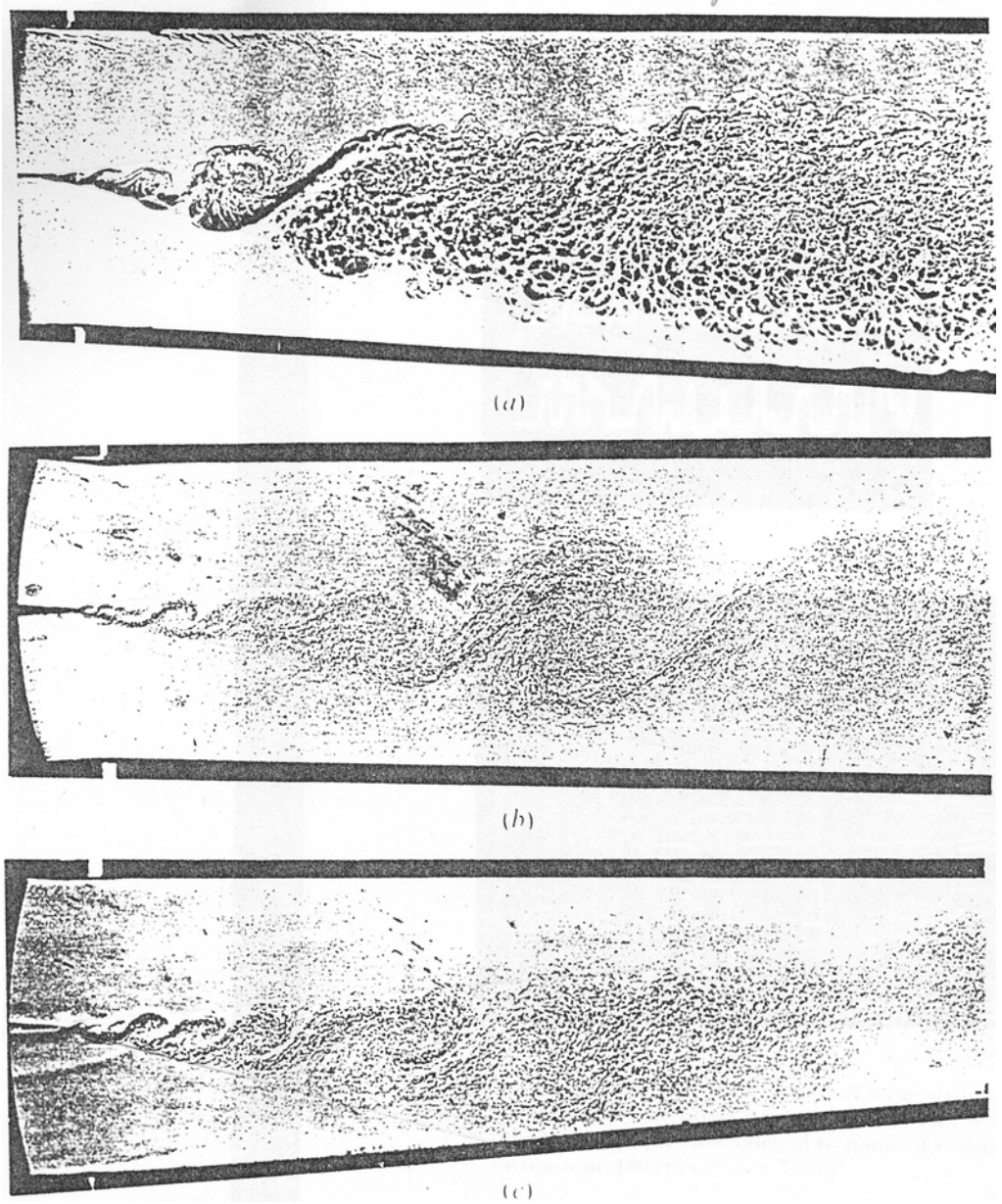

Brown & Roshko (1974)

Outline of the talk

1. *The 2D mixing-layer in the nonlinear regime and the secondary baroclinic instability*

   - *The non-linear stage ends in a rather asymmetric vorticity distribution due to alternate positive and negative baroclinic contributions;*
   - *From the vorticity field the structure is not a standard KH smooth (gentle) roller;*
   - *A secondary baroclinic instability developes on the light side of the KH billow;*
   - *Not observed so far at Reynolds numbers up to 3000 nor in experimental realizations of high Reynolds number flows;*
   - *Provides a 2D bypass route to turbulence under high Reynolds number conditions.*

- *The strain field of 2D light jets*
- *Transition to three-dimensionality in light jets and the question of side-jets*
- *Baroclinic instability of heavy vortices and some elements on vortex interaction in inhomogeneous 2D turbulence*

The strain rate and the shear rate are measured along some relevant line

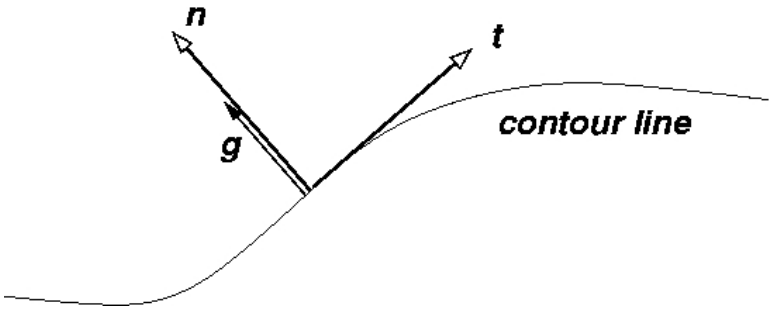

$$\lambda = \frac{\partial u_t}{\partial n} \quad , \quad \gamma = \frac{\partial u_t}{\partial t}$$

$$\lambda = \mathbf{n} \cdot \boldsymbol{\nabla} \mathbf{u} \cdot \mathbf{t} \quad , \quad \gamma = \mathbf{t} \cdot \boldsymbol{\nabla} \mathbf{u} \cdot \mathbf{t}$$

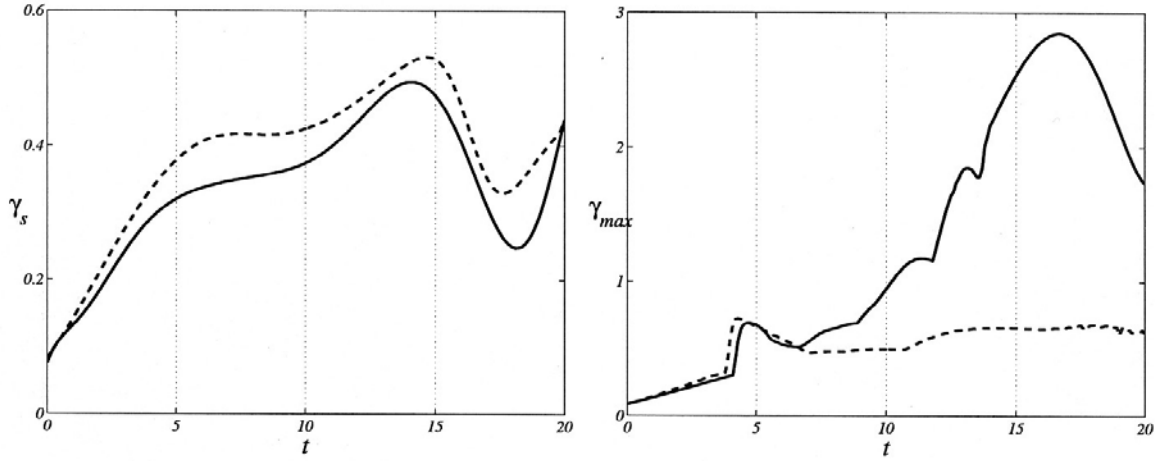

Figure 3.7: Left : the evolution of the strain rate γ_s normal to the density gradient at the saddle point between the main 2D structures. Right : evolution of the overall maximum of the strain rate $\gamma_{\max}$. Solid line : variable density mixing-layer at $S_\rho = 3$; dashed line : passive scalar mixing-layer.

The strain field of the mixing layer

Homogeneous

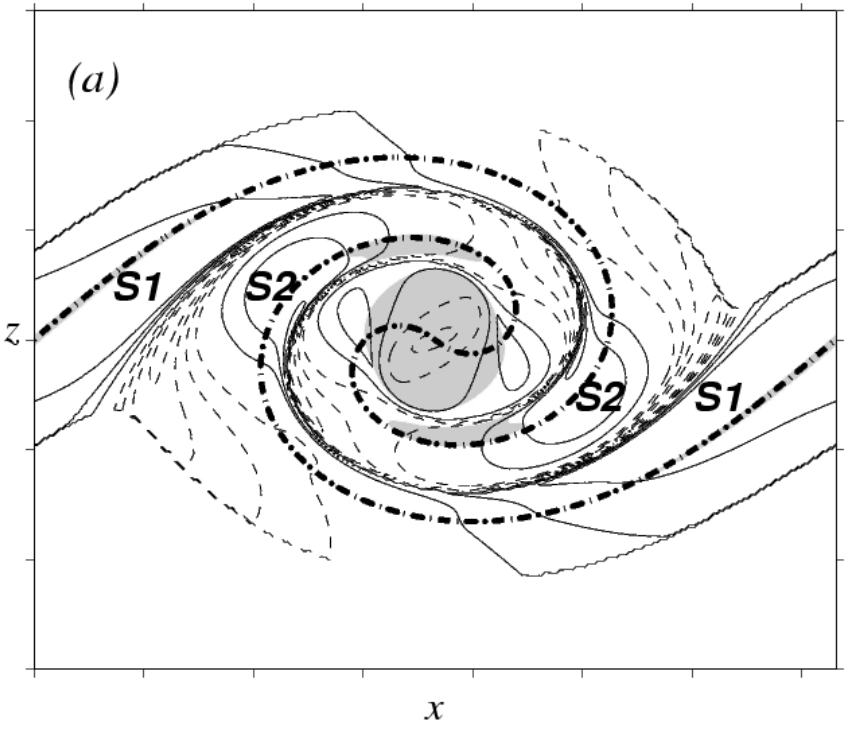

Inhomogeneous, s = 3

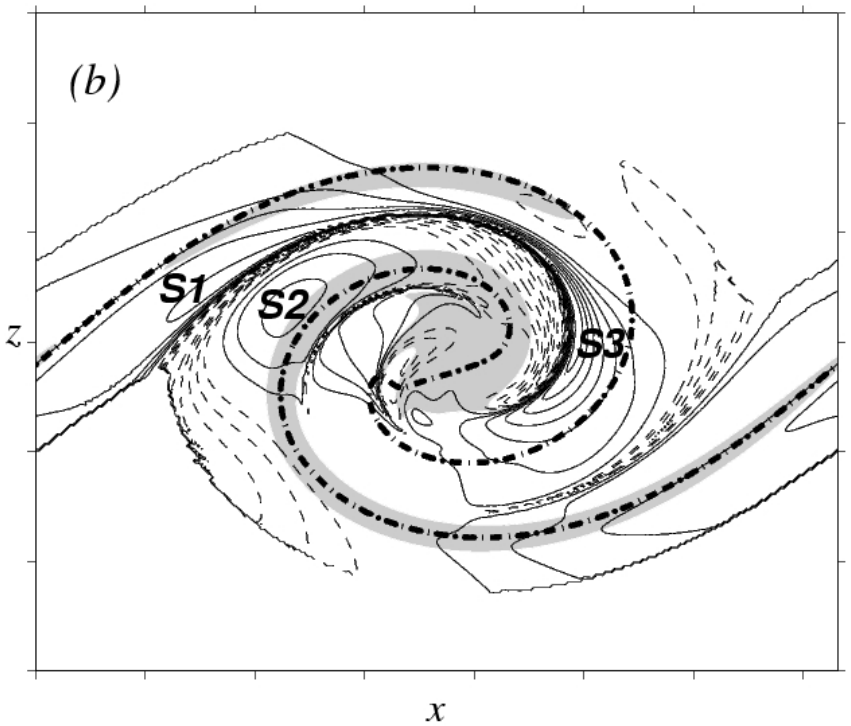

Gray shading where shear rate above $1/\tau = U/\delta\omega$

The model of the braid region according to Caulfield and Kerswell (PoF vol 12, 2000)

Model flow with strain rate γ *and rotation rate* $r = \dfrac{\omega}{2}$

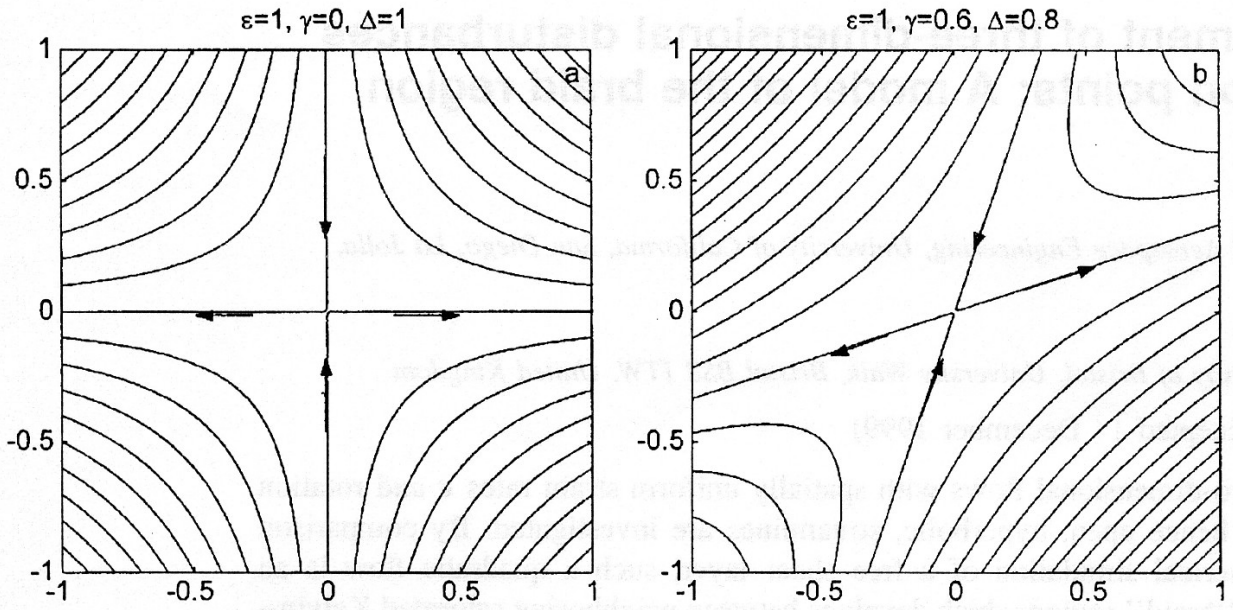

FIG. 1. (a) Contours of streamlines for a pure strain flow. Note the principal directions are perpendicular. (b) Contours of streamlines for a flow with $\epsilon = 1$, $\gamma = 0.6$, and hence $\Delta = 0.8$. Note the principal directions are no longer perpendicular.

$$\mathbf{u} = \begin{pmatrix} \gamma & -r \\ r & -\gamma \end{pmatrix} \begin{pmatrix} x \\ y \end{pmatrix} \equiv \mathbf{A} \cdot \mathbf{x}$$

$$\Delta^2 = \gamma^2 - r^2 = -\det \mathbf{A}$$

$|\gamma| > |r|$, Δ real — *Hyperbolic region*

$|\gamma| < |r|$, Δ imaginary — *Elliptic region*

The model of the braid region according to Caulfield and Kerswell (PoF vol 12, 2000)

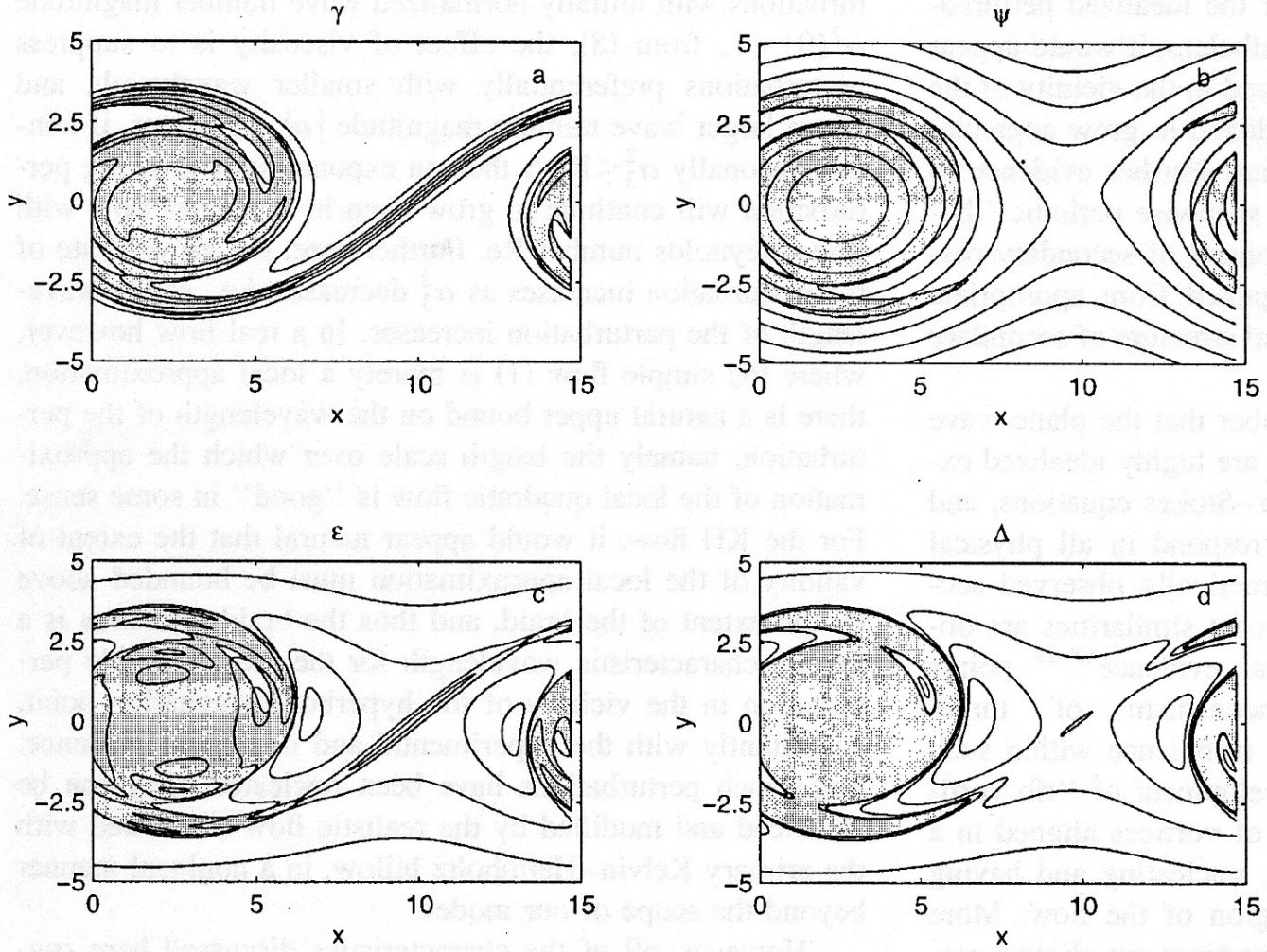

FIG. 3. Contours of (a) rotation rate γ; (b) stream function ψ; (c) strain rate ϵ; and (d) Δ in a mixing layer flow, when the primary KH billow has attained maximal amplitude. Shading denotes regions where $\gamma^2 > \epsilon^2$.

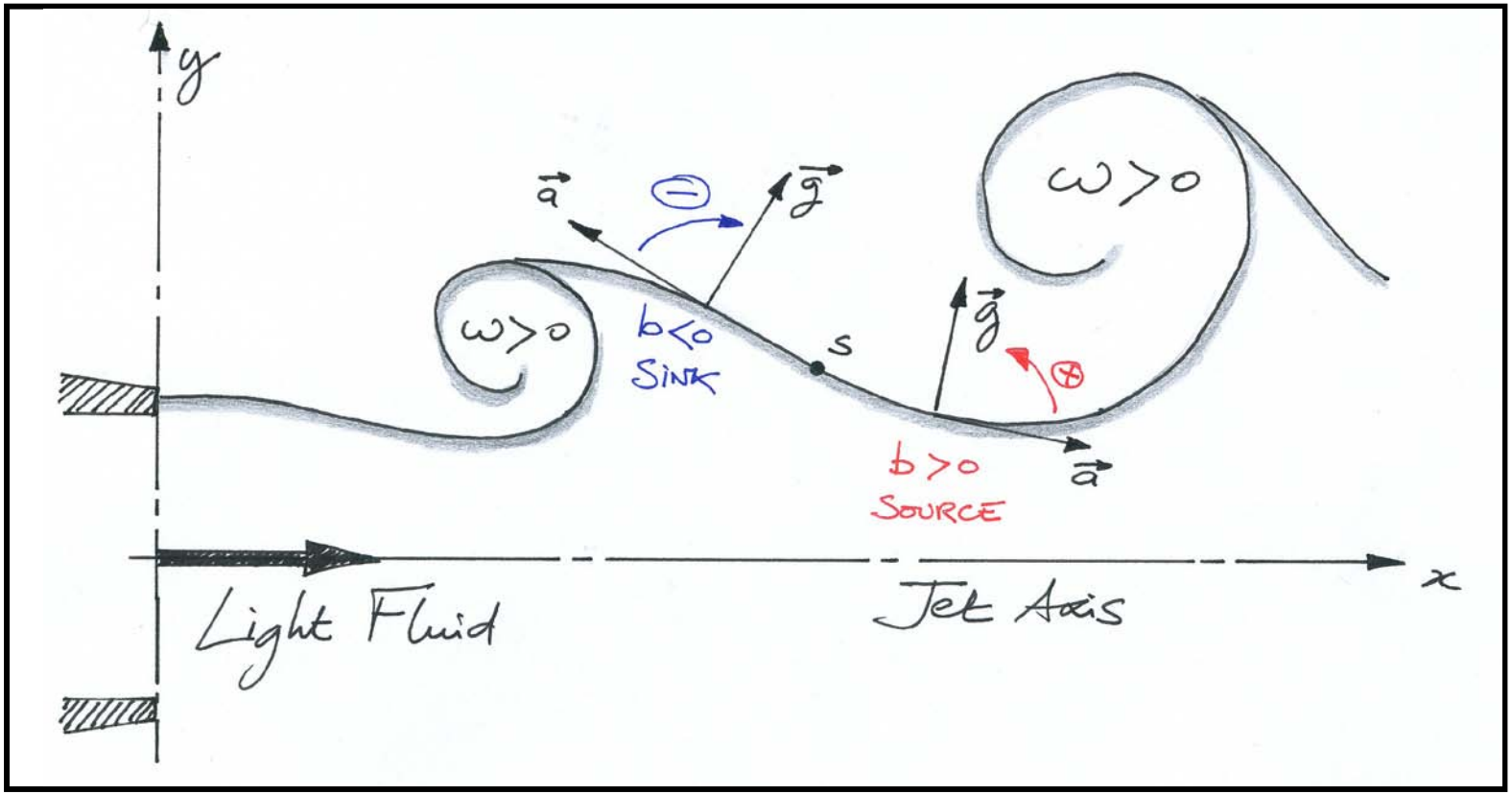

We switch from the spatially developping jet to the temporally developping jet

Temporal jet s=1/3, Re = UD/ν = 2500

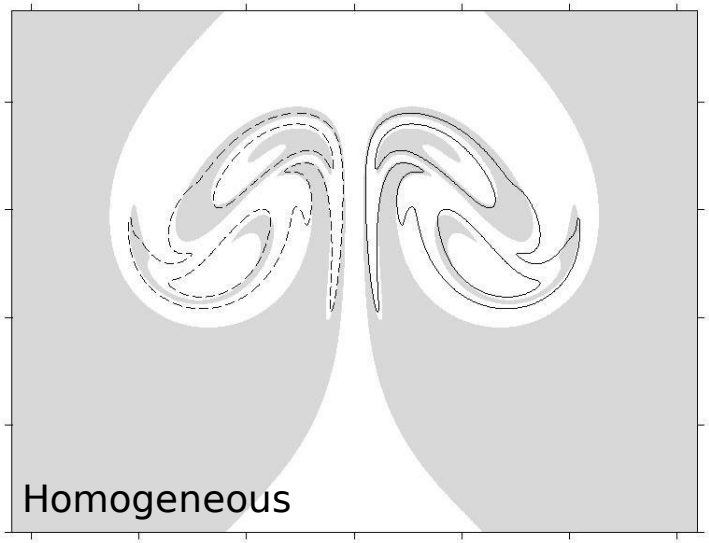

Vorticity

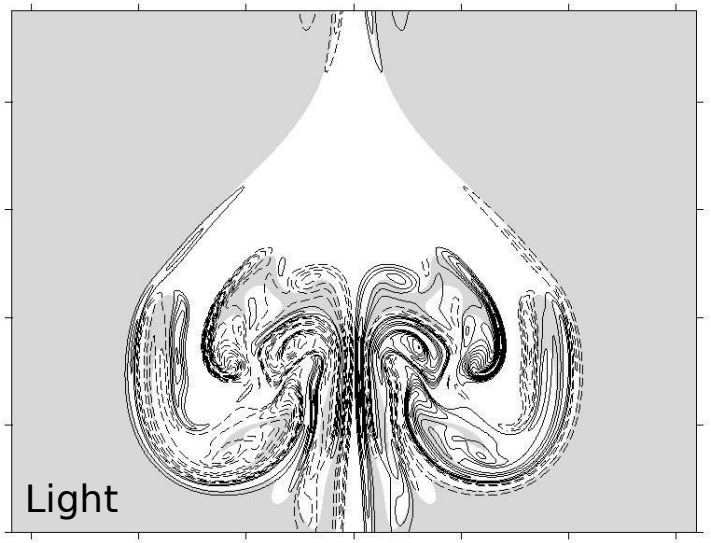

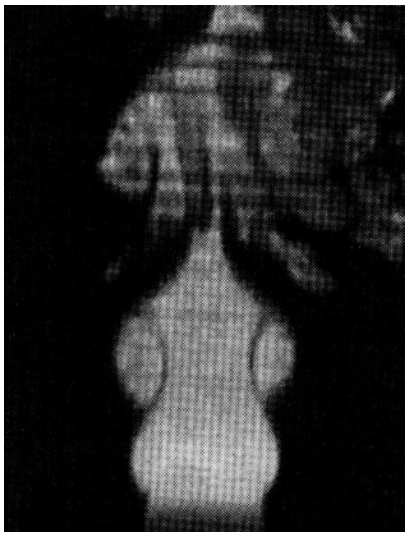

Kyle et Sreenivasan JFM 249 (1993)

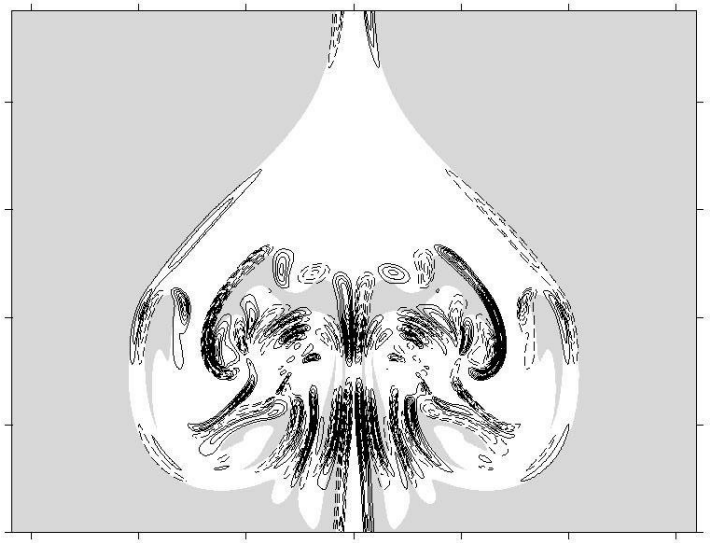

Baroclinic Torque

Temporal jet s=1/3, Re = UD/ν = 2500

Red : positive **γ** (***stretching***) – Blue : negative **γ** (***compression***) – Shaded : above same positive level

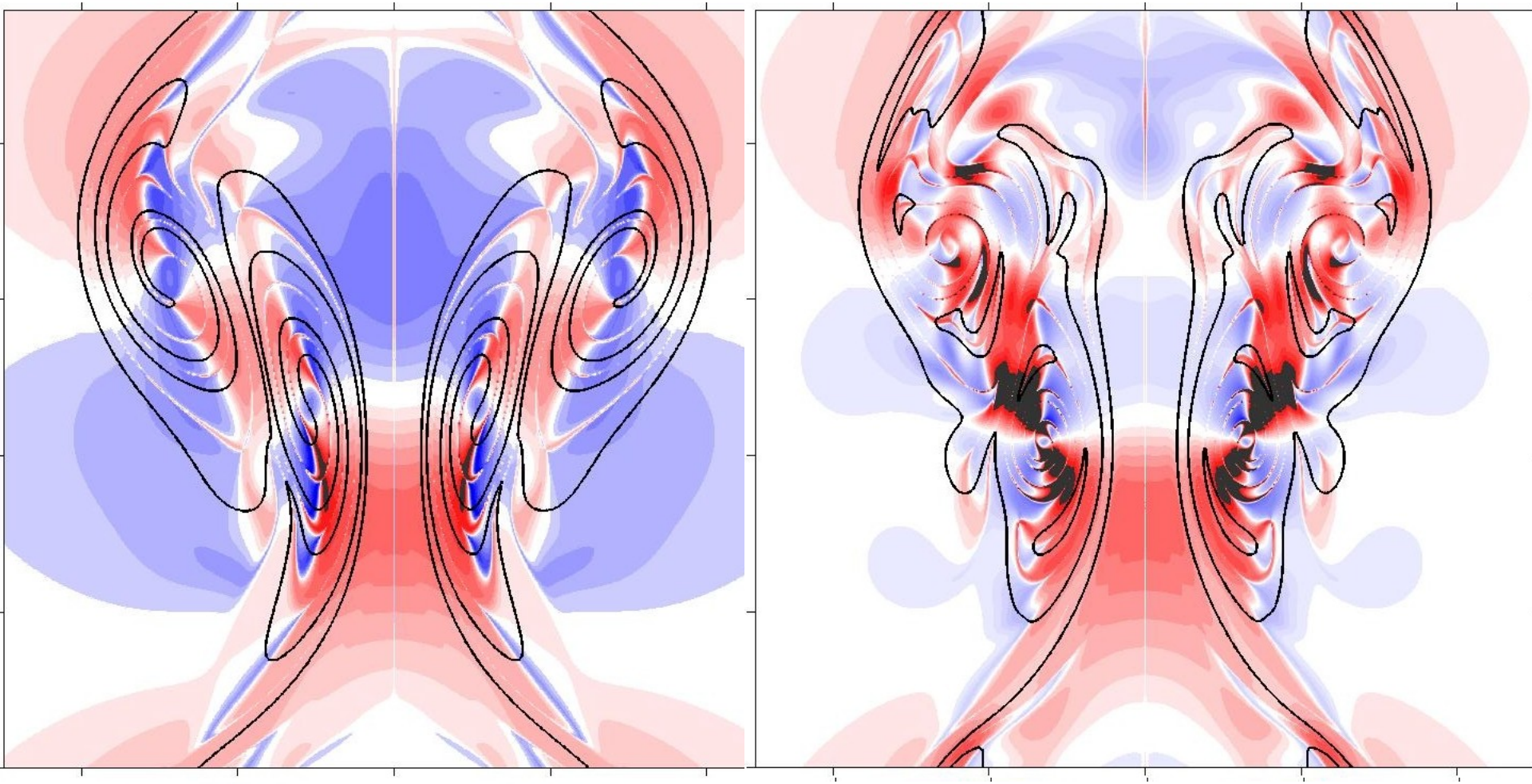

Passive scalar **t = 12** *Light jet*

The strain field according to the Caulfield and Kerswell's analysis

Temporal jet s=1/3, Re = UD/ν = 2500

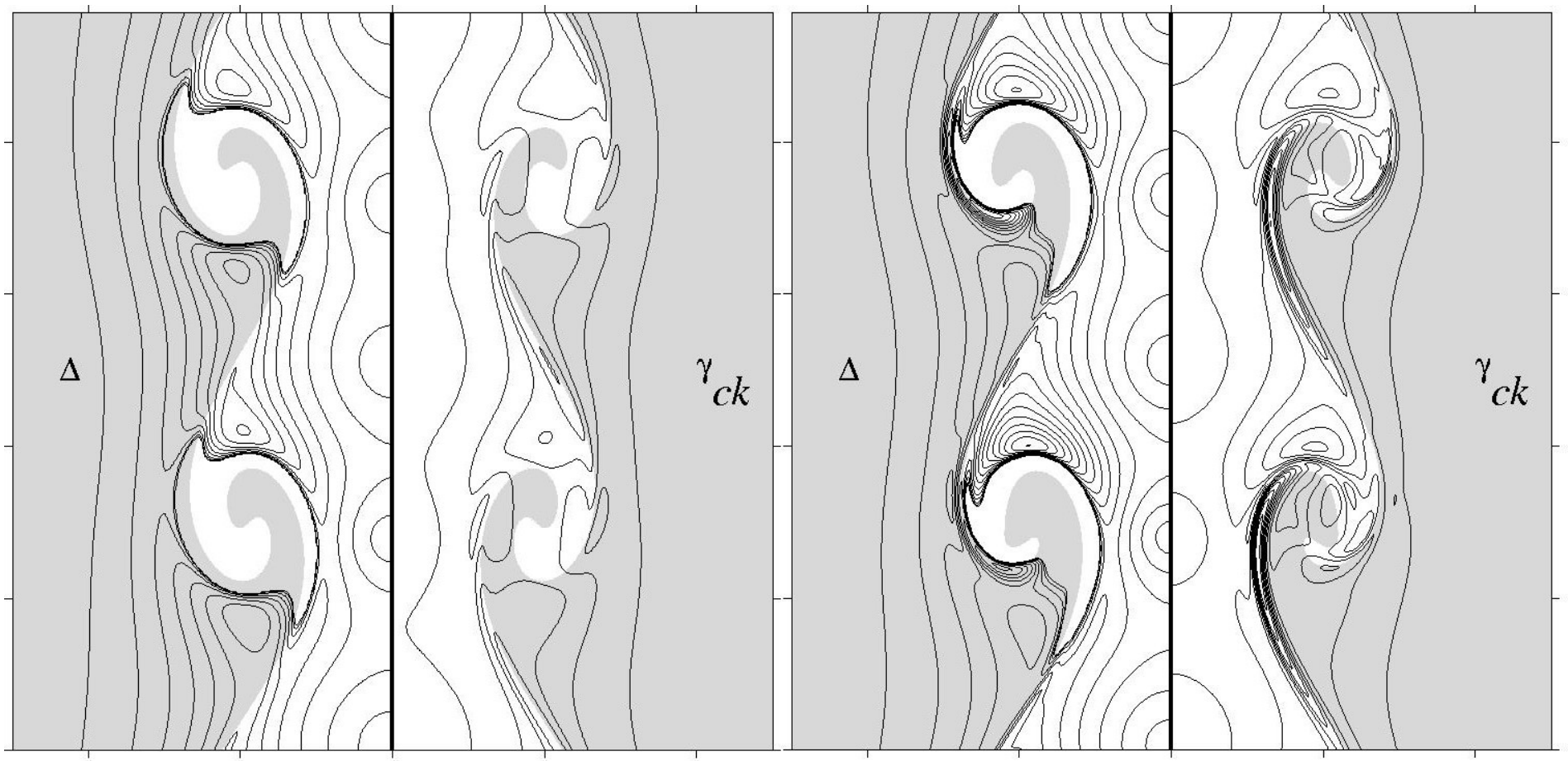

Passive scalar **t = 4,5** *Light jet*

The strain field according to the Caulfield and Kerswell's analysis

Temporal jet s=1/3, Re = UD/ν = 2500

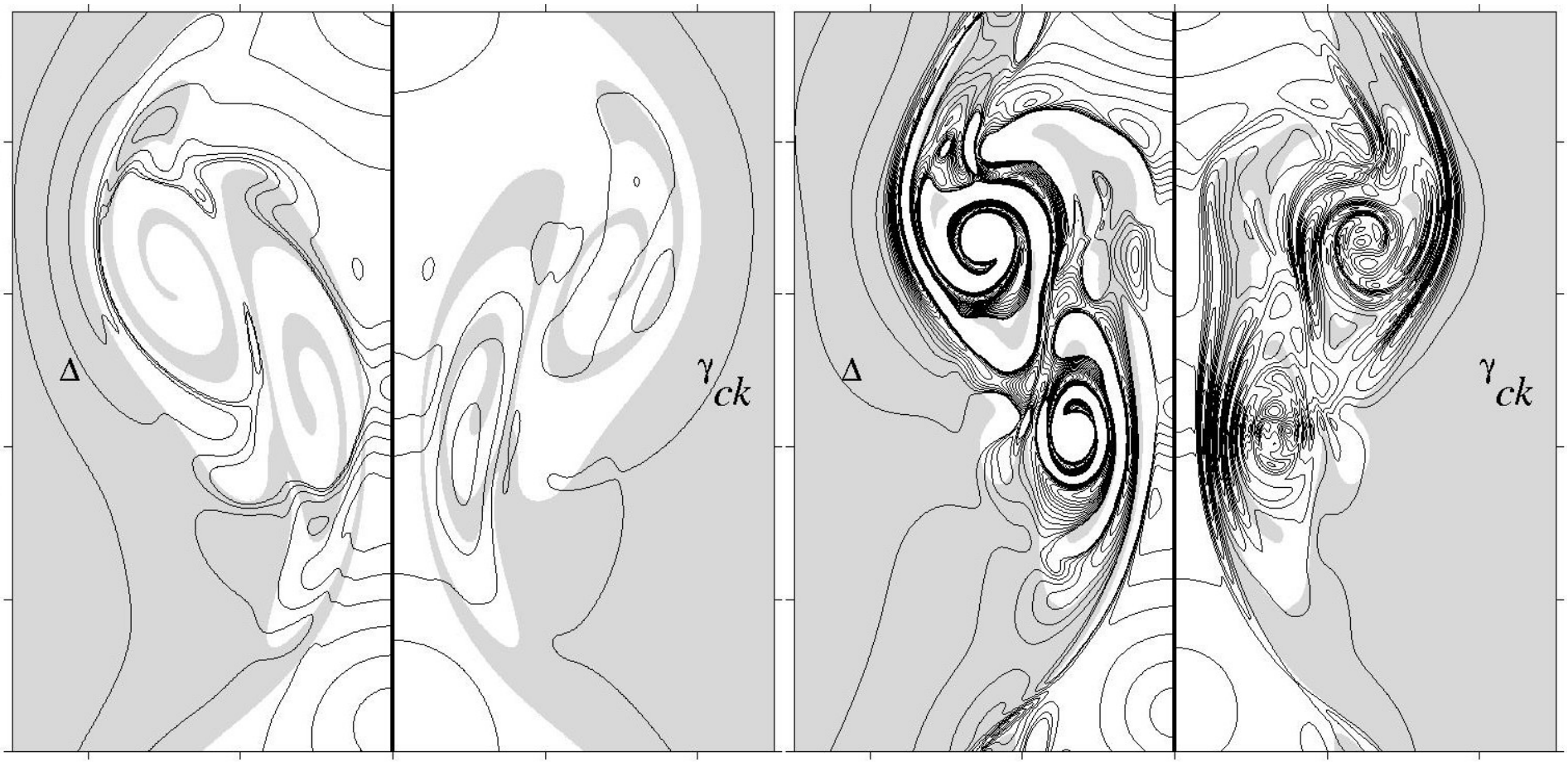

Passive scalar **t = 12** *Light jet*

Strain rates in the light jet

	Before the pairing - t = 4.5τ			During the pairing - t = 12.0τ		
	γ_{ck}	$r = \frac{\omega}{2}$	Δ	γ_{ck}	$r = \frac{\omega}{2}$	Δ
	Homogeneous Jet					
Elliptic	0.52	1.33	<0	0.57	1.37	<0
Hyperbolic	1.22	0.96	0.75	0.27	0.11	0.25
	Light Jet					
Elliptic	0.71	1.53	<0	0.34	3.83	<0
Hyperbolic	1.00 to 2.47	1.04	0.51 to 0.73	0.49	0.45	0.18

Outline of the talk

1. *The 2D mixing-layer in the nonlinear regime and the secondary baroclinic instability*
2. *The strain field of 2D light jets*

- *The strain fields of light jets present a folded layered structure,*
- *Much higher strain rates may be produced in the baroclinically modified roll-up,*
- *High strain rates are to be expected « inside » the light jet and close to favored leg of the vorticity braid.*

- *Transition to three-dimensionality in light jets and the question of side-jets*
- *Baroclinic instability of heavy vortices and some elements on vortex interaction in inhomogeneous 2D turbulence*

More on side jets

Fisrt observation by Monkewitz & Bechert (Album of Fluid Motion - 1988)

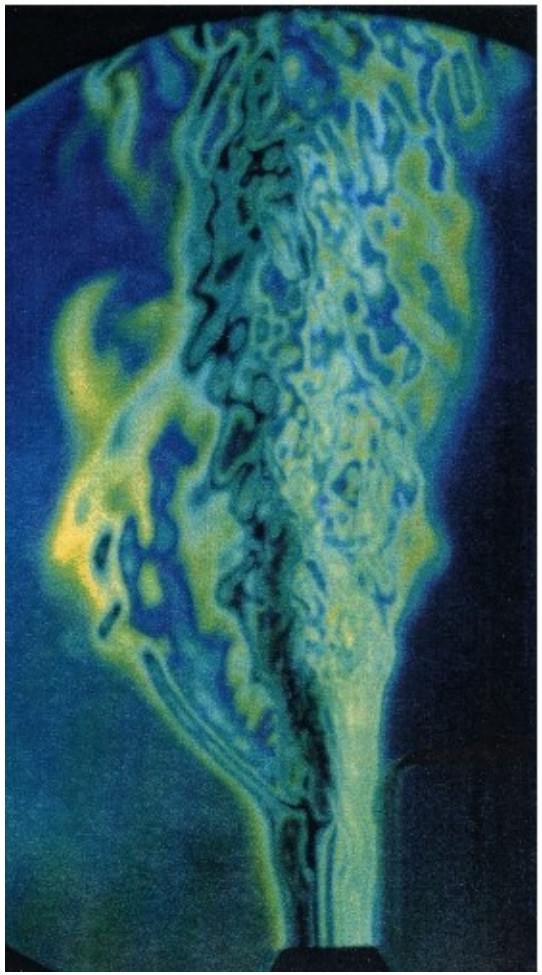

Side ejections on Re = 1000 helium jets from Hermouche, *Imft* (1996)

1. Side jets occur when the jet is absolutely unstable,
2. The jet is absolutely unstable under a critical density ratio s<0.7,
3. Side jets aknowledged within some range of Reynolds number,
4. Side Jets induced by counter-rotative streamwise vortices lying in the braid region between successive vortex rings (Brancher et al. Phys Fluids 1994)
5. A shorter route to the mixing transition and a large increase of the mixing rate,
6. Side Jets recovered in a pulsed homogeneous jet by Monkewitz and Pfizenmaier (1991) leading these authors to conclude that the strength and synchronization of the primary mode in the absolutely unstable light jets is the sufficient conditions for spontaneous lateral ejections of fluids.
7. Additionnal facts from Hermouche experiments :
    i. Intemmittent ejection,
    ii. Unsteady number and azymuthal positon,
    iii. Quasi-steady streamwise position,
    iv. Life time of several PM periods

9. Remaining questions

Paradigm of secondary 3D mode yielding counter-rotative vortices lying between adjacent distorted rings

Side jets induced by pairs of counter-rotative streamwise aligned vortices

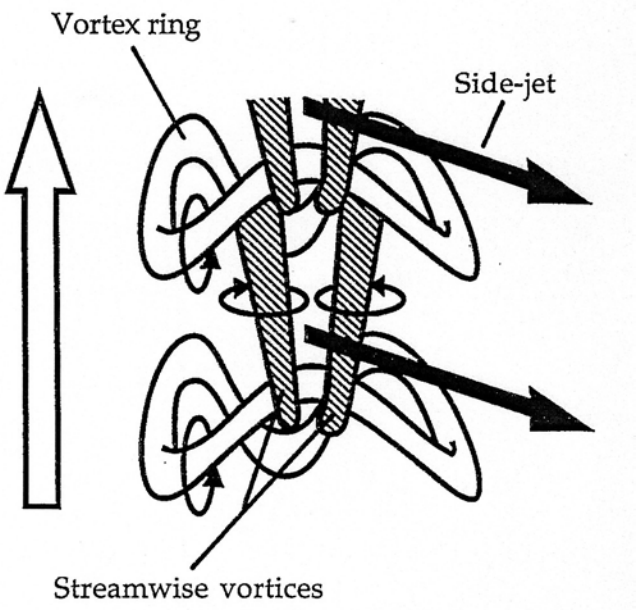

FIG. 6. Vortical structures involved in the side-jet generation process. Only a single streamwise pair is represented (hatched structures) while two consecutive vortex rings are sketched (white structures). The radial ejection of fluid is symbolized by the two black arrows emerging from the streamwise pair.

Brancher, Chomaz & Huerre (1994)

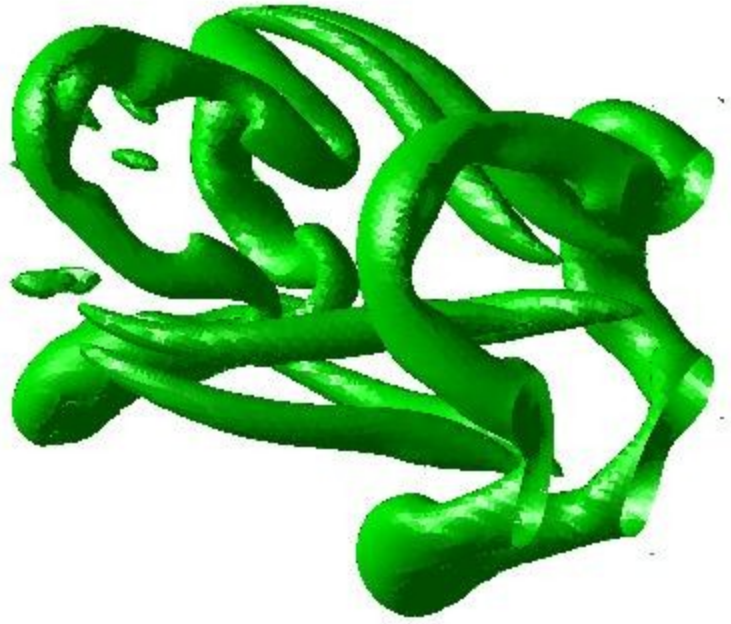

Lambda2 probe of coherent structures in a DNS of a homogeneous 3D temporal jet with a 3-lobe corrugation of the initial vorticity tube.

No side jets in planes light jets

Two-dimensionnal Heated jets from Yu and Monkewitz JFM 255 (1993)

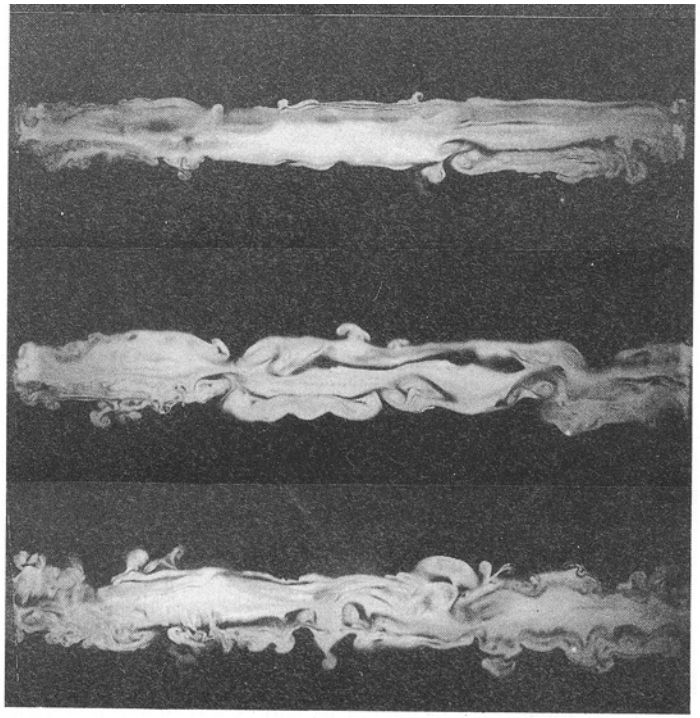

RE 20. Cross-sectional views of the cold jet with $q_j = 1.25$ mmH_2O, at $x = 1, 2, 3, 4, 5, 6, 7$ (from top to bottom).

Cold (homogeneous) jet

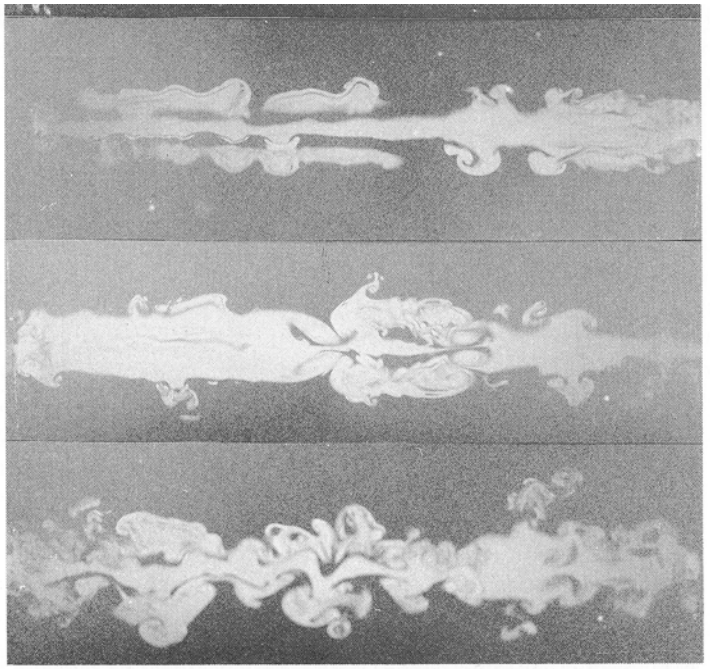

FIGURE 21. Cross-sectional views of the hot jet with $S = 0.76$ and $q_j = 1.25$ mmH_2O, at $x = 1, 2, 3, 4, 5, 6, 7$ (from top to bottom).

Hot (light) jet

A first guess : the strain rate in the 2D light jet and predicted growth rates

	Before the pairing - t = 4.5τ		During the pairing - t = 12.0τ	
	Homogeneous Jet			
Elliptic	$\sigma \sim \gamma_{ck}$ 0.52		$\sigma \sim$ 0.57	
Hyperbolic	$\sigma_{tr} \leqslant 2\gamma_{ck}$ **2.44**	$\sigma_{as} \sim 2\Delta$ **1.5**	$\sigma_{tr} \leqslant$ **0.54**	$\sigma_{as} \sim$ **0.5**
	Light Jet			
Elliptic	$\sigma \sim$ 0.71		$\sigma \sim$ 0.34	
Hyperbolic	$\sigma_{tr} \leqslant$ **2. to 5.**	$\sigma_{as} \sim$ **1. to 1.46**	$\sigma_{tr} \leqslant$ **0.98**	$\sigma_{as} \sim$ **0.36**

Scheme of the vorticity generation on the model flow of unstrained counter-rotating vortices

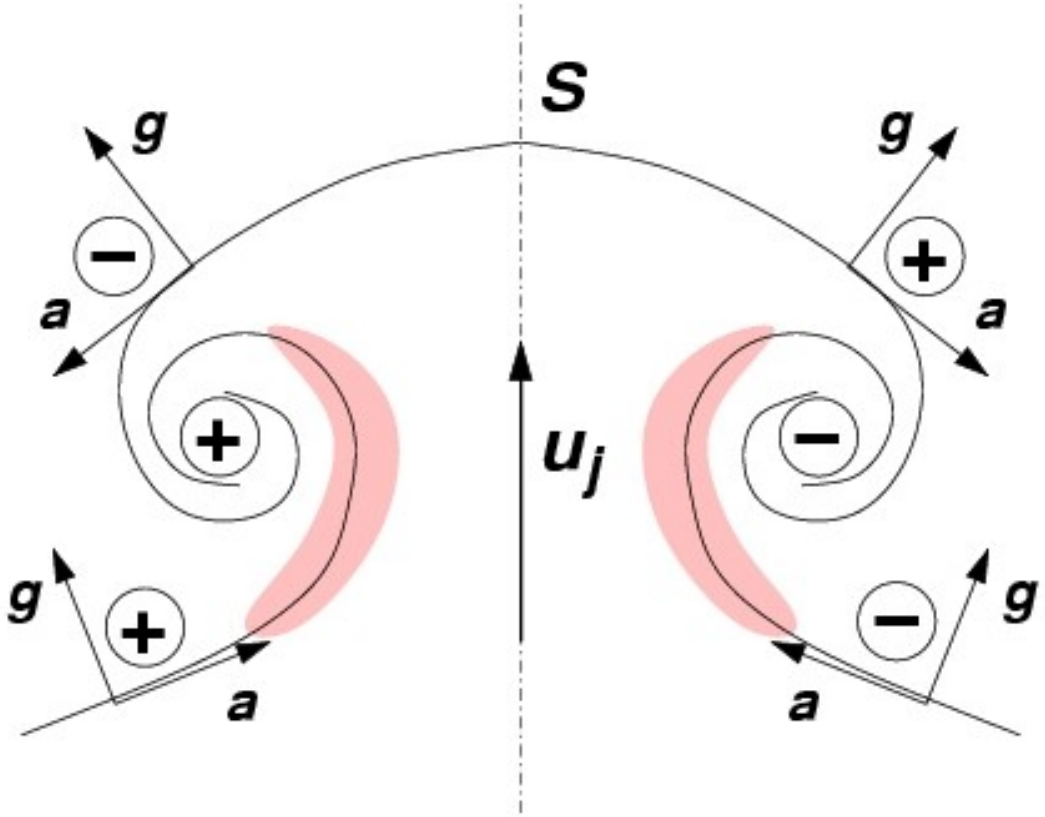

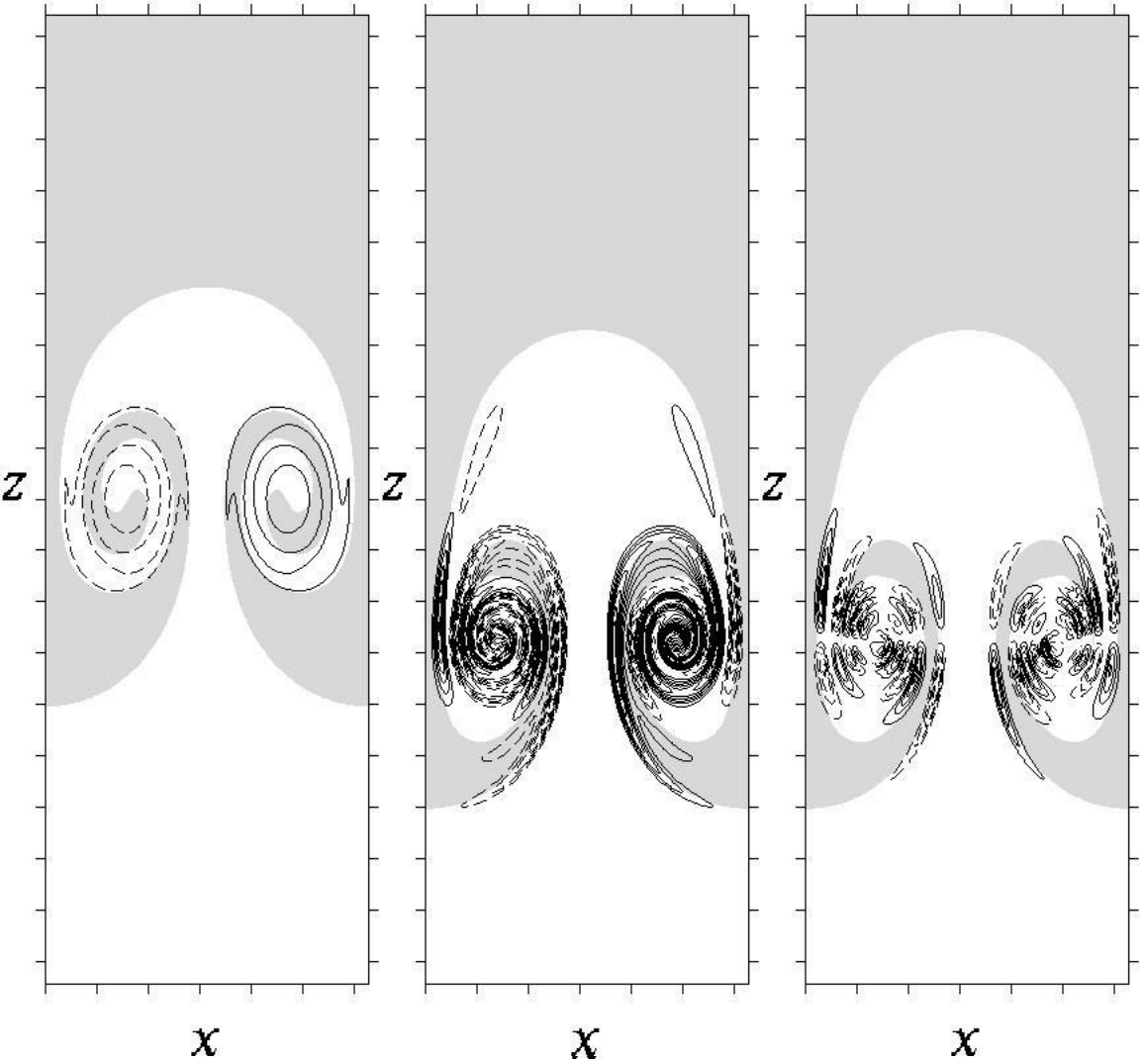

vorticité vorticité couple barocline

- Shift of the vortex centers toward the light side
- Asymmetric entrainment
- A trend expected to be enhanced by the underlynig stretching in full configuration

Corrugated temporal jet, Re = 1900 et $Re_\theta = 170$

- primary mode perturbation resulting from 2D stability
- no result in 3D stability : $k\theta$?

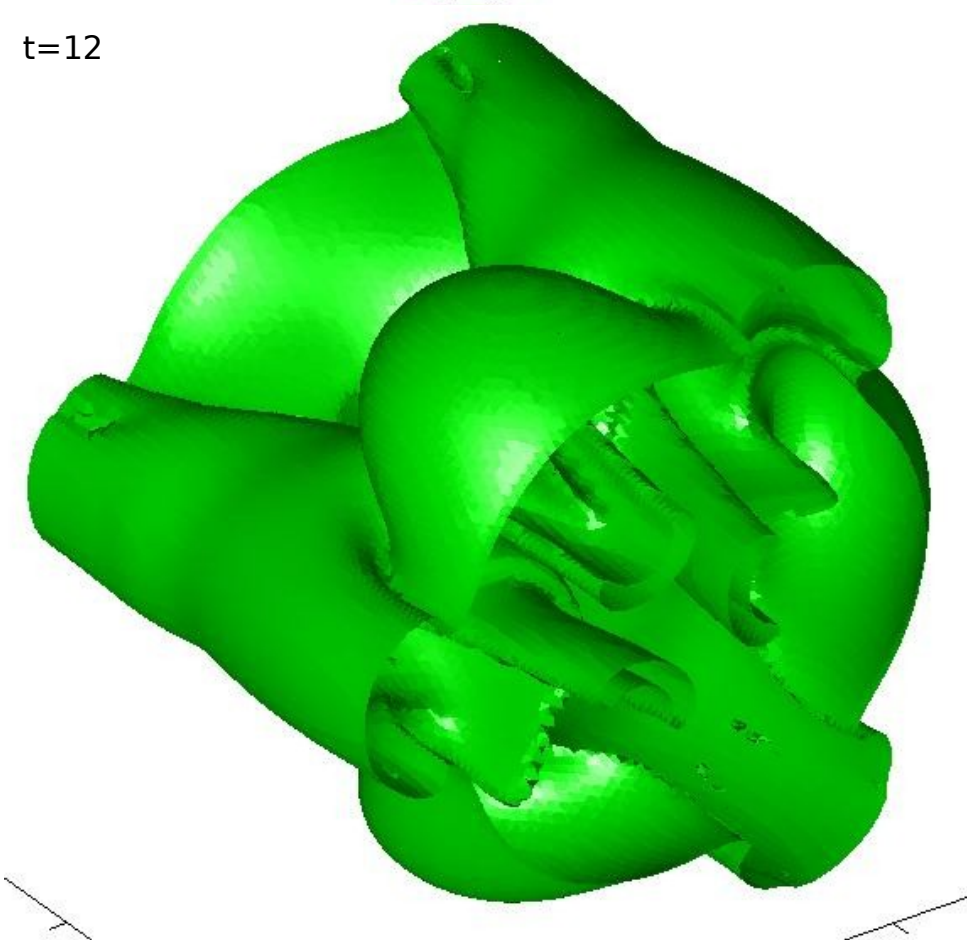

Crosswise cuts through the ring and braid of simulated 3D jets

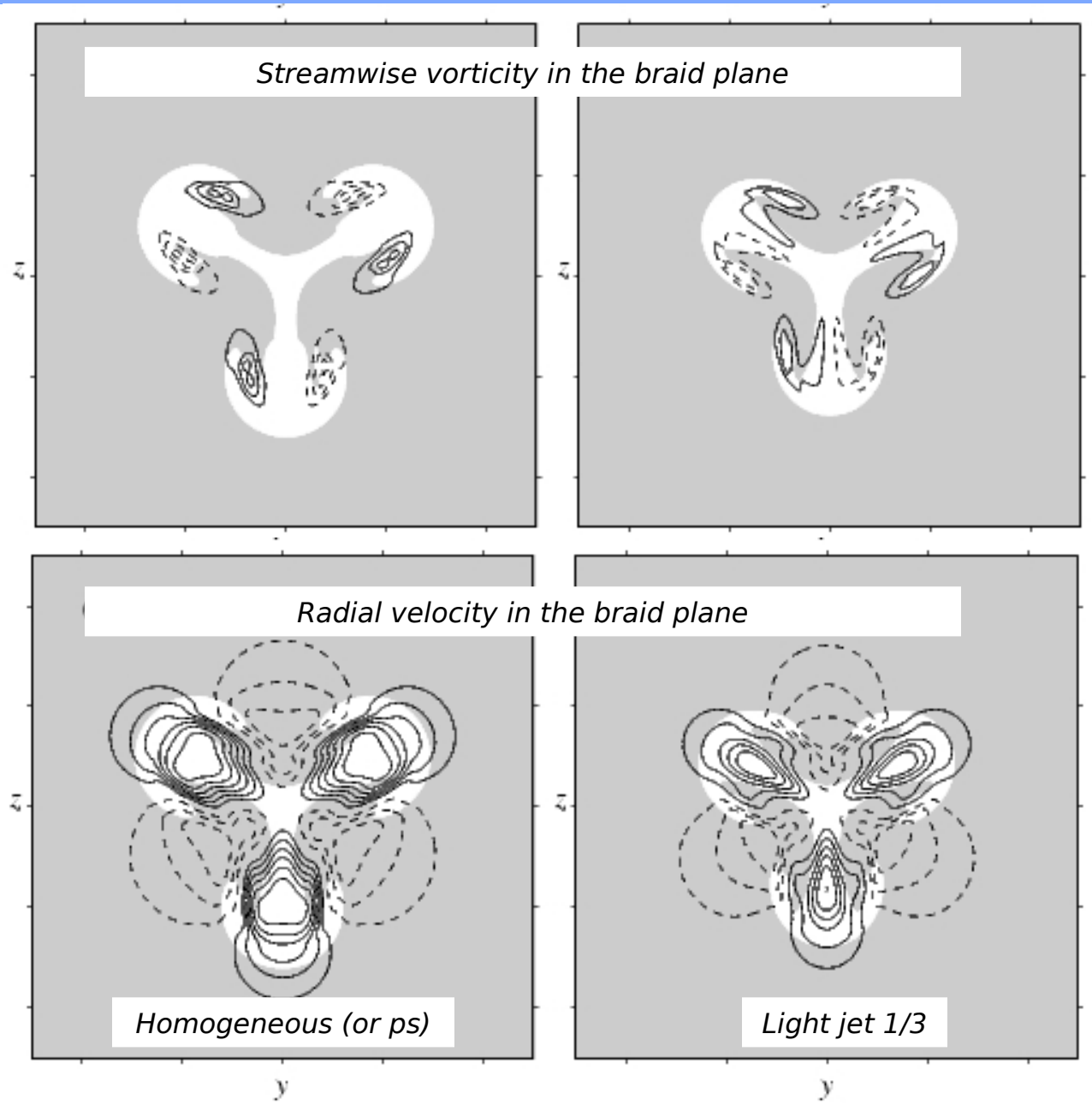

Growth of the energy (enstrophy) of three-dimensionnal motion

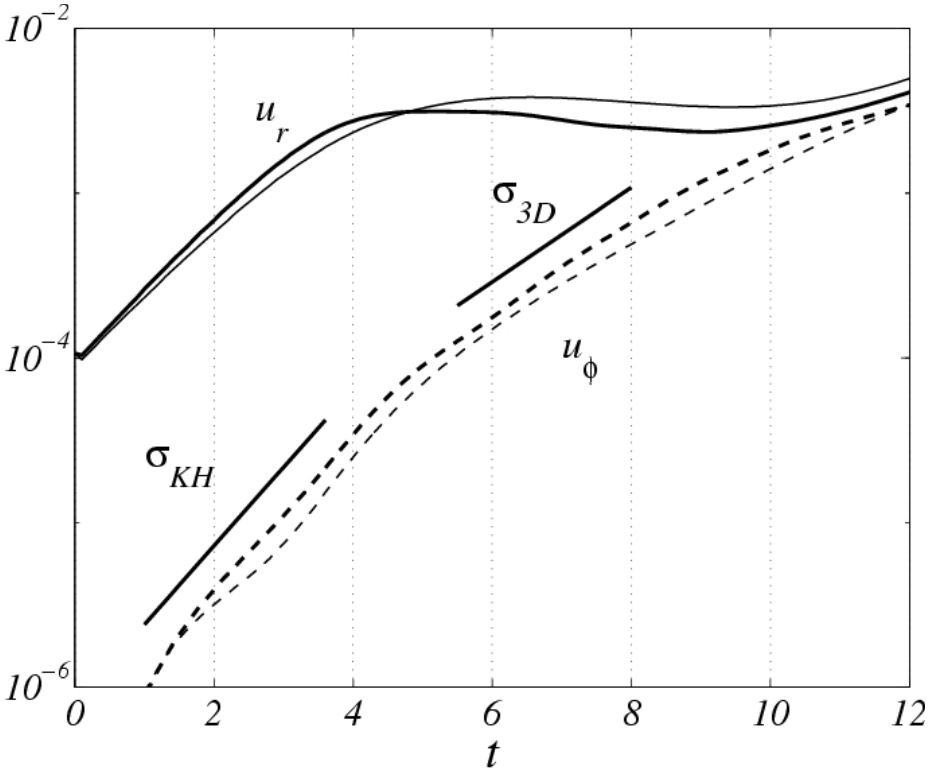

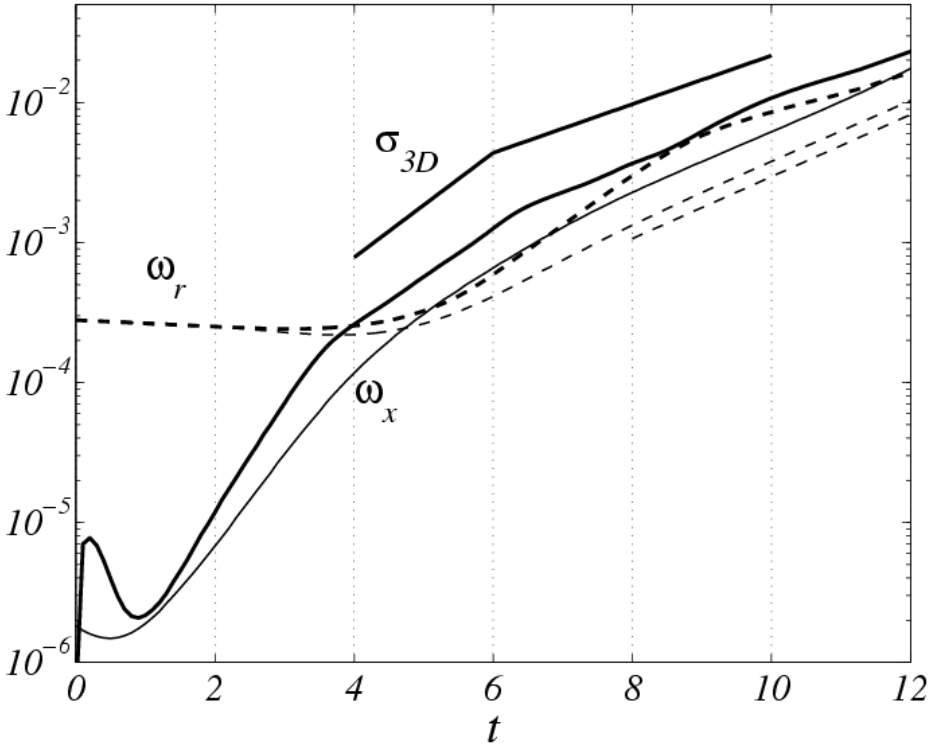

- Influence of density ratio Reynolds number and R/θ on the characteristics of the azimuthal mode;
- Higher Re_θ simulations to get the full baroclniic effect on 2D primary mode

Influence of the Reynolds number

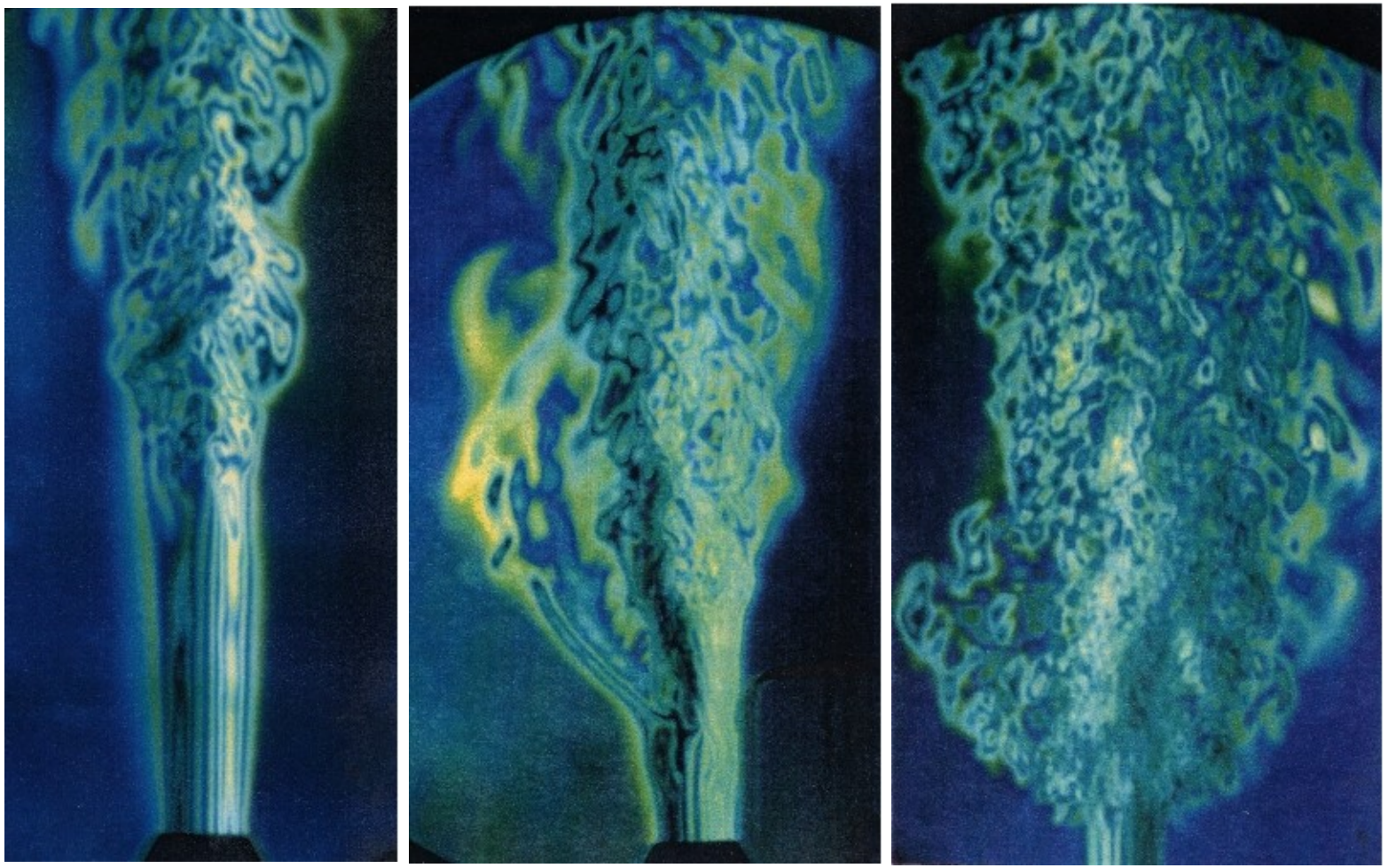

Re = 750 Re = 1000 Re = 2600

Conjecture on the transition sensitivity to the exit Reynolds number

- Viscous regime : no spontaneous side jets;
- Side jets regime;
- Secondary 2D instability regime.

Structure of the laminar helium jet

- PIV vorticity mapping (Hermouche's test bank and Jérôme Fontane PhD);
- Primary structure of the light jet;
- 3D perturbation on the azimuthal wave number given by the 3D stability analysis:
- Impact on the mixing efficiency.

The end …

Floquet analysis of the axisymmetric jet

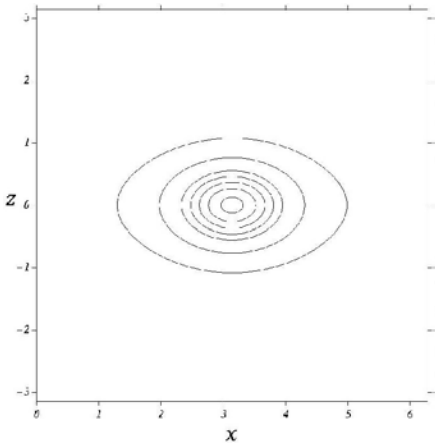

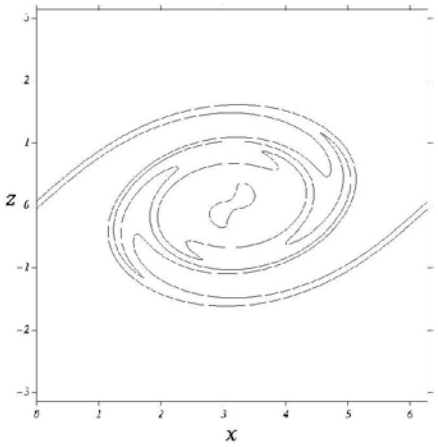

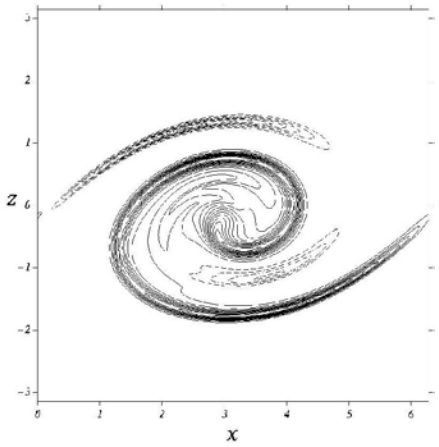

Vortex de Stuart, r=0,5 Rouleau KH homogène, Re=1500 Rouleau KH s=3, Re=1500

Pierrehumbert et Widnall JFM 114 (1982) : $\lambda_z = 0{,}6\ \lambda_x$ – Klaassen et Peltier JFM 227 (1991)

$$
\begin{aligned}
\mathrm{D}_t\hat{\rho} + \mathbf{G}\cdot\hat{\mathbf{v}} &= 0 \\
R\mathrm{D}_t\hat{\mathbf{v}} + RM\hat{\mathbf{v}} + \hat{\rho}M\mathbf{U} &= -\boldsymbol{\nabla}\hat{p} \\
R\mathrm{D}_t\hat{w} &= -\partial_z\hat{p} \\
\boldsymbol{\nabla}\cdot\hat{\mathbf{v}} + \partial_z\hat{w} &= 0
\end{aligned}
$$

$$\hat{\mathbf{q}} = (\hat{\rho}, \hat{\mathbf{v}}, \hat{p}) \qquad \hat{\mathbf{q}}(\mathbf{x}, t) = \mathbf{e}^{ikz}\mathbf{q}(x, y, t)$$

$$\partial_t\, \mathcal{L}_1(R, \mathbf{U}, k)\ \mathbf{q}(x, y, t) = \mathcal{L}_2(R, \mathbf{U}, k)\ \mathbf{q}(x, y, t)$$

$$\mathbf{q}(x, y, t) = \mathbf{e}^{\sigma t}\mathbf{e}^{i\mu x}\tilde{\mathbf{q}}(x, y)$$

$$\sigma\mathcal{L}_1(R, \mathbf{U}, k)\ \tilde{\mathbf{q}}(x, y) = \mathcal{L}_2(R, \mathbf{U}, k)\ \tilde{\mathbf{q}}(x, y)$$

Recherche déductive des modes propres transverses de la cdm et azimuthaux du jet léger

Outline of the talk

- *The 2D mixing-layer in the nonlinear regime and the secondary baroclinic instability*
- *The strain field of 2D light jets*
- *Transition to three-dimensionality in light jets and the question of side-jets*

  - *Spontaneous side jets in absolutely unstable light jets,*
  - *If understood may help mixing,*
  - *Experimental, Floquet analysis and DNS approach to get relevant data*

- *Baroclinic instability of heavy vortices and some elements on vortex interaction in inhomogeneous 2D turbulence*

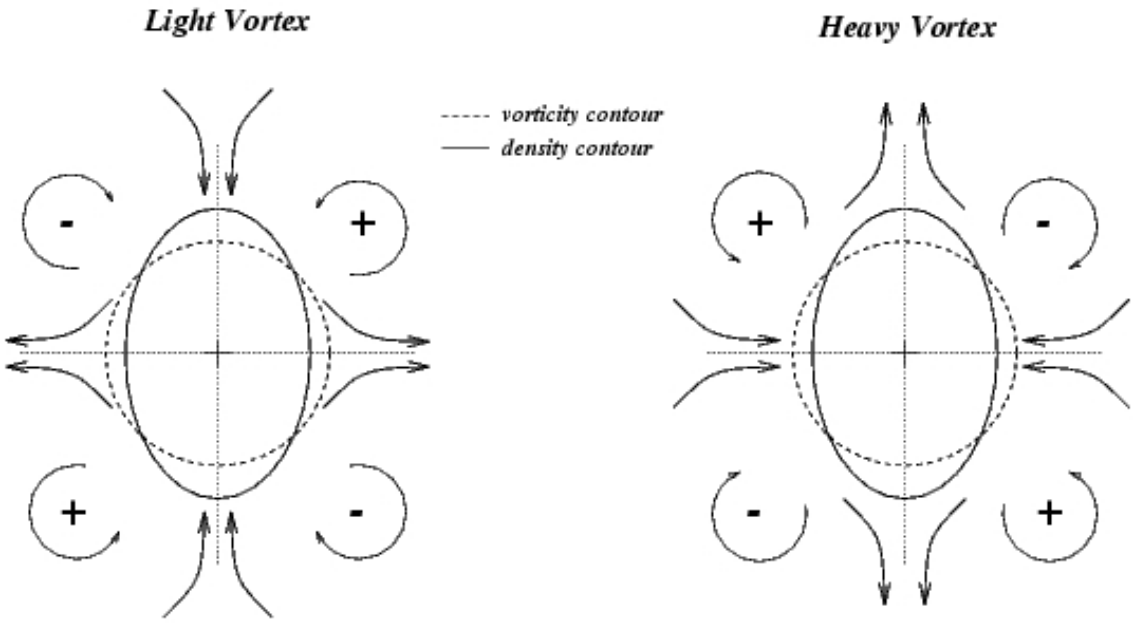

Figure 4.4: Sketch of the baroclinic effects on heavy and light vortices.

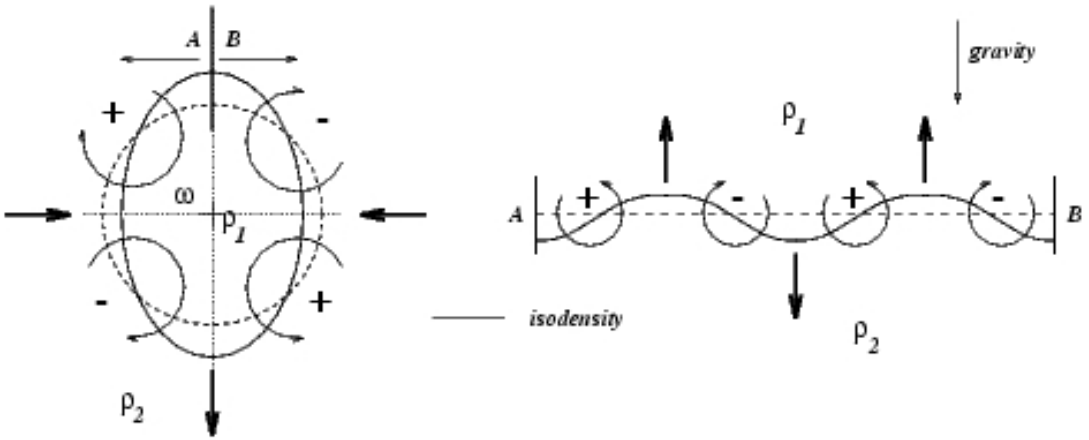

Figure 4.5: Analogy between the heavy vortex and the equivalent unrolled density stratification submitted to a downward gravity field ($\rho_1 > \rho_2$).

- *Vorticity of the gaussian vortex :* $$\omega(r,\theta) = \frac{\Gamma}{\pi\delta^2}\exp(-r^2/\delta^2)$$

- *Orthoradial velocity and centripetal acceleration :* $$u_\theta = [1-\exp(-\frac{r^2}{\delta^2})]\frac{\Gamma}{2\pi\, r}$$ $$a_r = -u_\theta^2/r$$

- *Density field on an elleptic patch :* $$r_\rho^2(\theta) = r^2[1+(e^{-2}-1)\sin^2\theta]$$

- *Density gradient vector :* $$\rho(r,\theta) = \rho_e + (\rho_i - \rho_e)\exp(-\frac{r_\rho^2(\theta)}{\delta^2})$$

- *Baroclinic torque :* $$\mathbf{g} = \boldsymbol{\nabla}(\ln\rho) = \begin{cases} g_r = -(1-\frac{\rho_e}{\rho})\frac{2r}{\delta^2}[1+(e^{-2}-1)\sin^2\theta] \\ g_\theta = (1-\frac{\rho_e}{\rho})\frac{r}{\delta^2}(1-e^{-2})\sin(2\theta) \end{cases}$$

$$b = a_r\, g_\theta = [1-\exp(-\frac{r^2}{\delta^2})]^2\frac{\Gamma^2}{4\pi^2\, r^2\delta^2}\,(1-e^{-2})\,\frac{\rho_e-\rho}{\rho}\,\sin(2\theta)$$

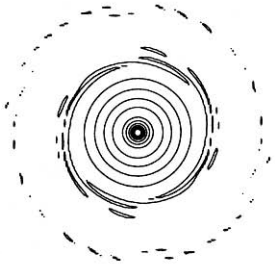

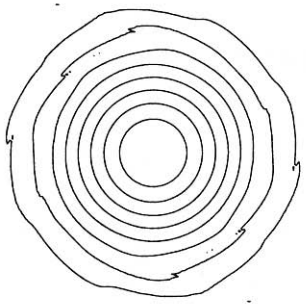

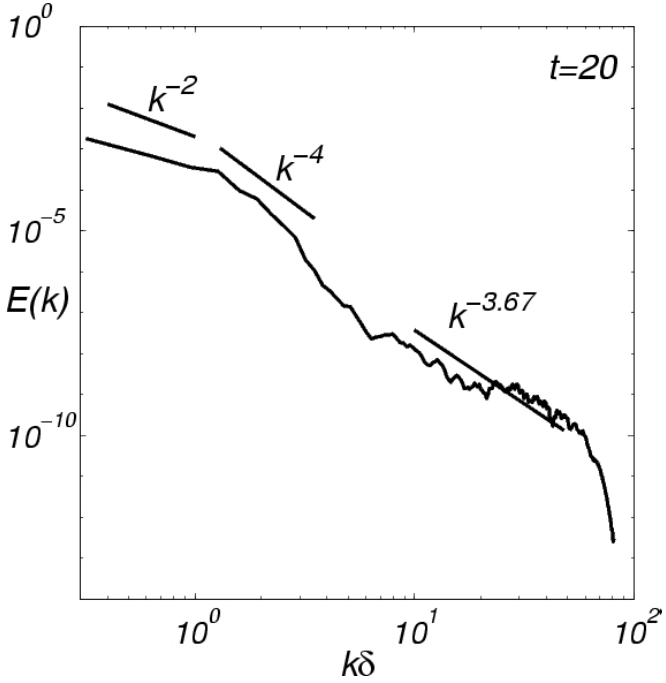
10^0
10^{-5}
10^{-10}
E(k)
t=20
k^{-2}
k^{-4}
$k^{-3.67}$
10^0
10^1
10^2
kδ

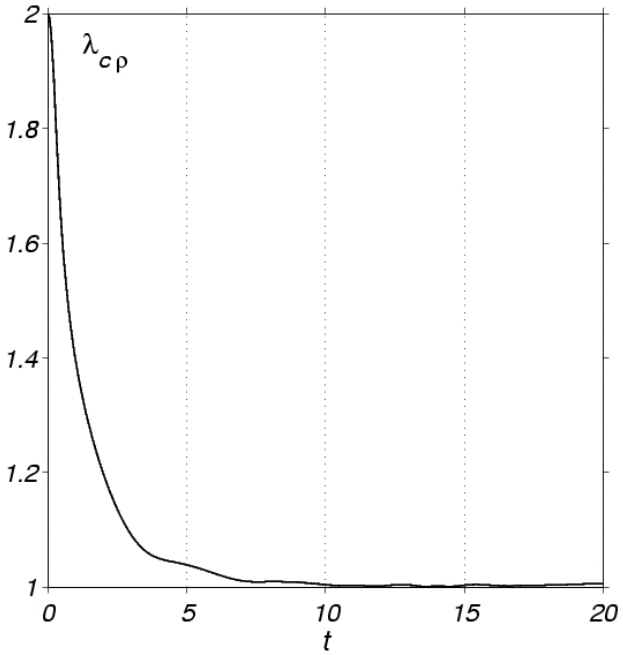
$\lambda_{c\rho}$
2
1.8
1.6
1.4
1.2
1
0
5
10
15
20
t

The breakdown of an heavy vortex

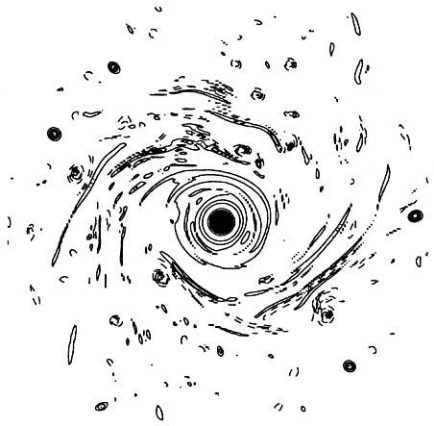

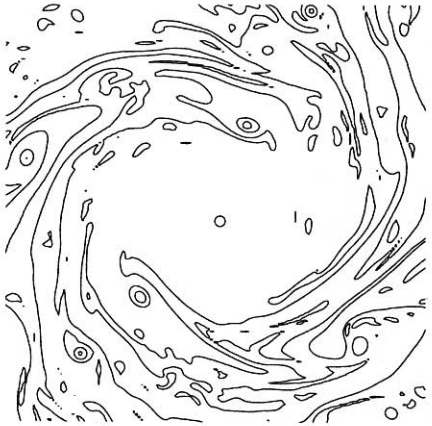

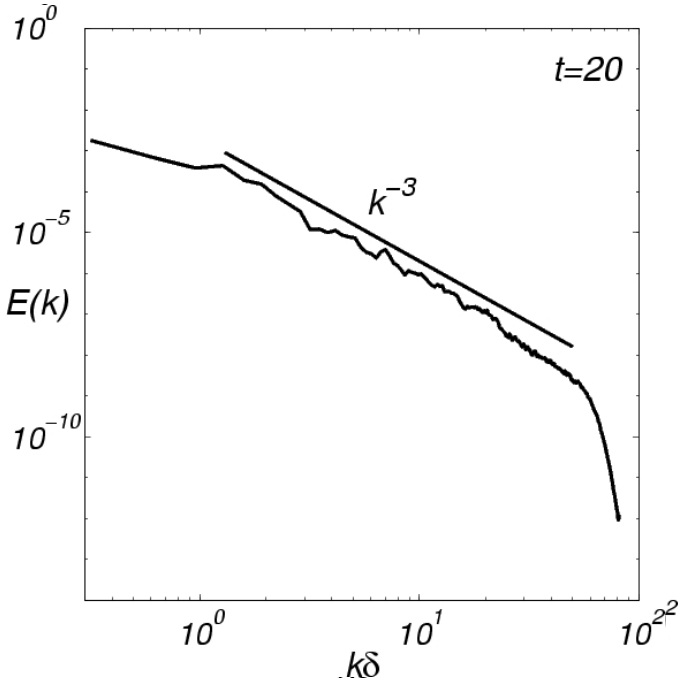

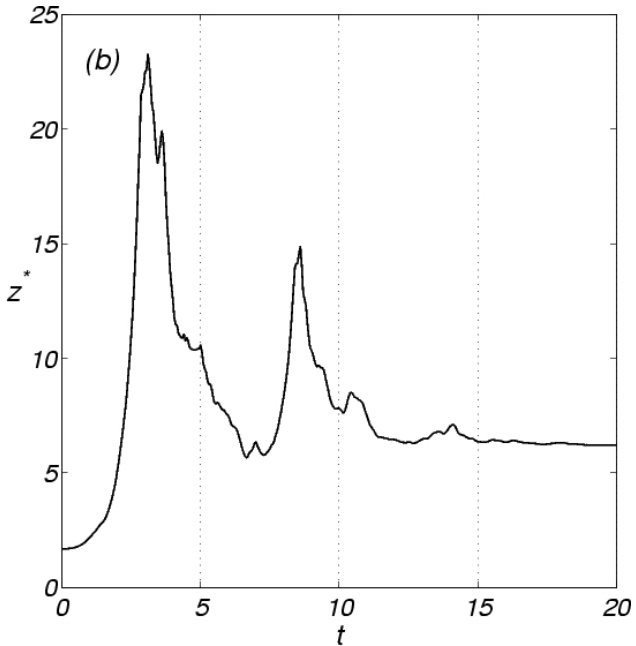

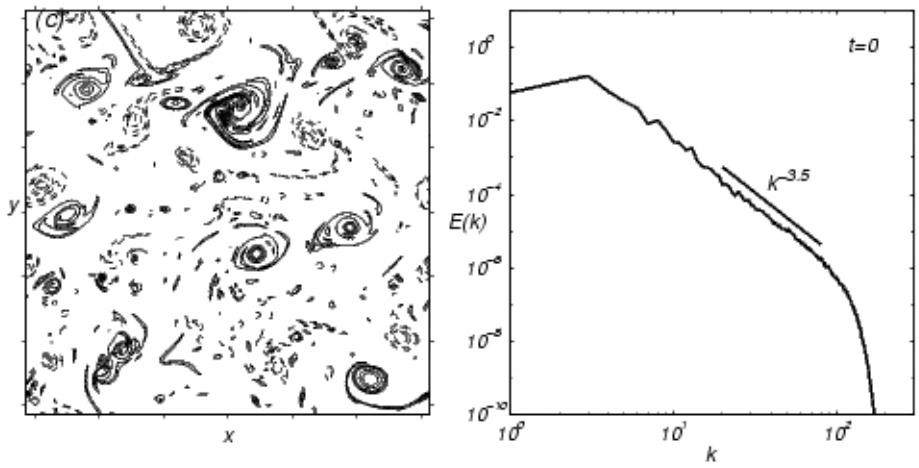

Figure 4.13: Initial vorticity field with solid positive contours and dashed negative ones, increment between contour is $\max(\omega)/2\pi$ and the zero contour is omitted (left); the corresponding energy spectrum (right).

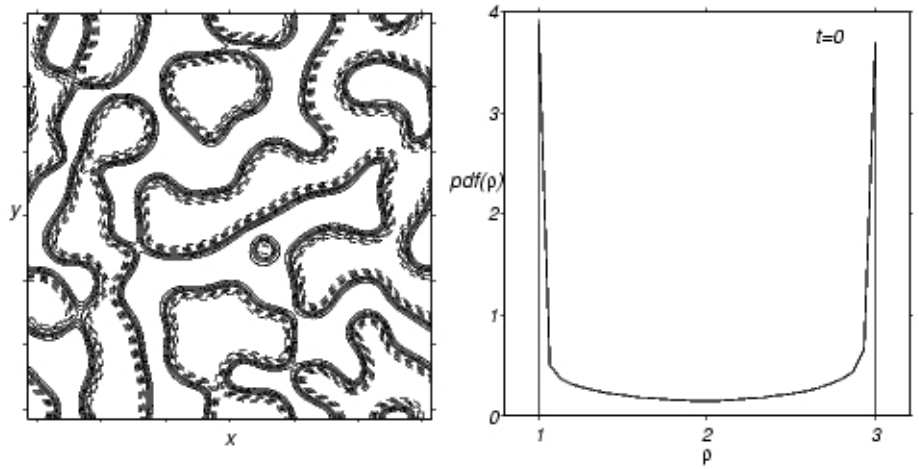

Figure 4.14: Initial density field with solid contours above mean and dashed contours beneath, increment between contour is $\Delta\rho/10$ (left); the corresponding probability density function (right).

Mass segregation in 2D turbulence

Passive scalar 2D turbulence

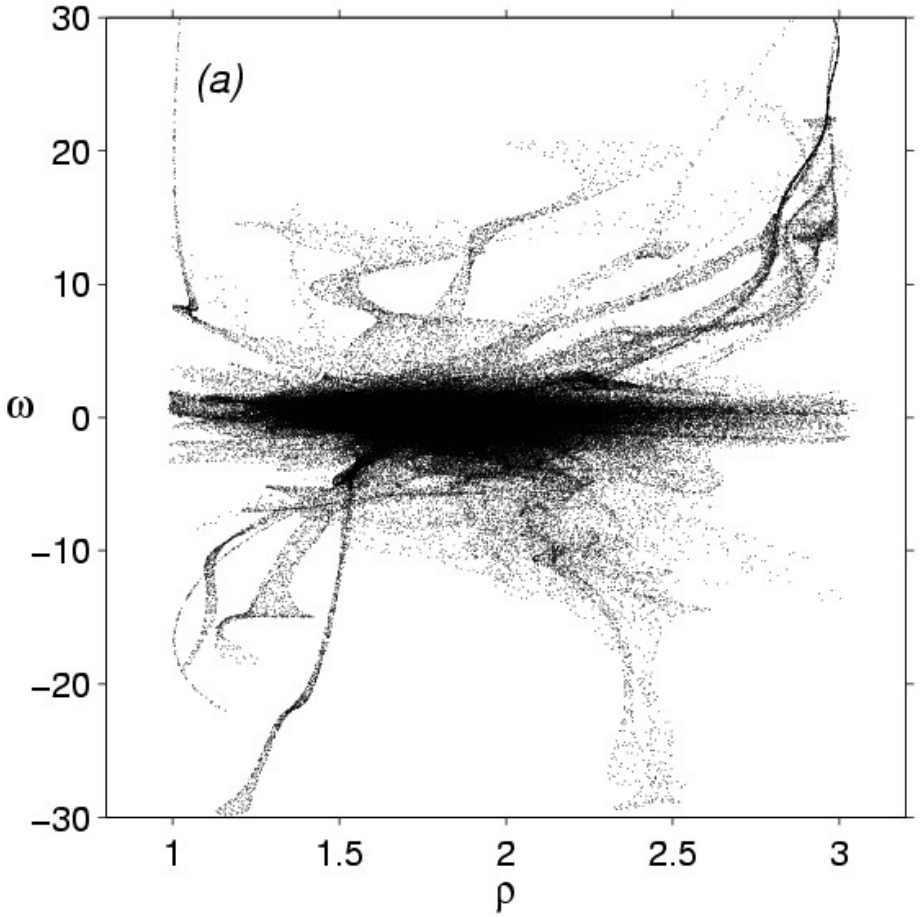

Inhomogeneous 2D turbulence

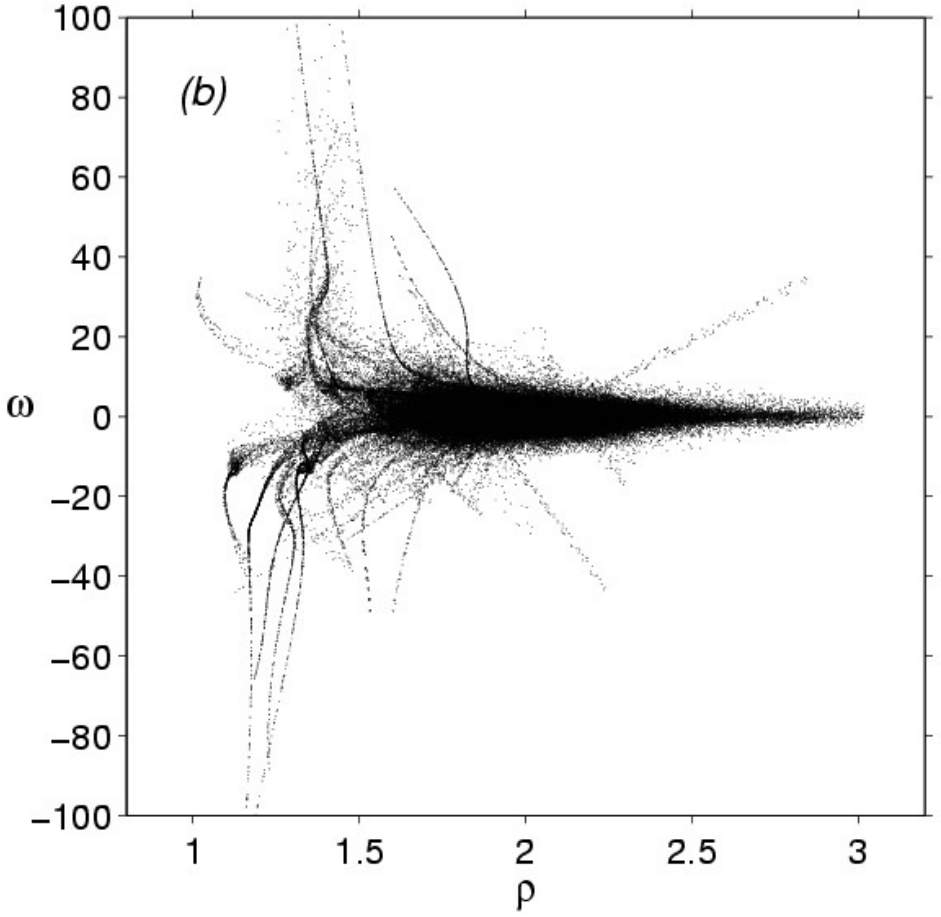

Outline of the talk

1. *The 2D mixing-layer in the nonlinear regime and the secondary baroclinic instability*
2. *The strain field of 2D light jets*
3. *Transition to three-dimensionality in light jets and the question of side-jets*
4. *Baroclinic instability of heavy vortices and some elements on vortex interaction in inhomogeneous 2D turbulence*

- *Light vortex stable, heavy vortex unstable,*
- *Mass segregation by vorticity in 2D inhomogeneous turbulence,*
- *Enstrophy (hence dissipation) generation.*

Thank you …